Development of the Modular Extracorporeal Lung Assist System (ModELAS): $ECCO_2R$ and Pediatric Applications

by

Alexandra G. May

B.S. in Chemical Engineering, Florida State University, 2014

Submitted to the Graduate Faculty of the

Swanson School of Engineering in partial fulfillment

of the requirements for the degree of

Doctor of Philosophy

University of Pittsburgh

2019

UNIVERSITY OF PITTSBURGH

SWANSON SCHOOL OF ENGINEERING

This dissertation was presented

by

Alexandra G. May

It was defended on

October 11, 2019

and approved by

Harvey S. Borovetz, PhD,
Distinguished Professor, Department of Bioengineering and Chemical Engineering

William R. Wagner, PhD,
Director, McGowan Institute for Regenerative Medicine, and Professor, Department of Surgery, Bioengineering and Chemical Engineering

Peter D. Wearden, MD, PhD,
Chair, Nemours Division of Cardiothoracic Services, McGowan Institute for Regenerative Medicine

Dissertation Director: William J. Federspiel, PhD,
William Kepler Whiteford Professor, Department of Bioengineering, Chemical Engineering, and Critical Care Medicine

Development of the Modular Extracorporeal Lung Assist System: $ECCO_2R$ and Pediatric Applications

Alexandra G. May, PhD

University of Pittsburgh, 2019

Acute and chronic respiratory diseases continue to be a leading cause of death in the United States.[1] Mechanical ventilation has been used to treat these patients, however this can further damage the lungs.[2] Patients with acute hypercapnic respiratory failure have benefited from extracorporeal CO_2 removal ($ECCO_2R$) in conjunction with non-invasive or lung-protective ventilation. For patients with end-stage lung disease extracorporeal membrane oxygenation has been used as a bridge-to-transplant. Active rehabilitation while on these devices has shown improved outcomes, however is limited by current, cumbersome systems.

We are developing the Modular Extracorporeal Lung Assist System (ModELAS) as a compact, wearable, platform artificial lung. The ModELAS may be configured for adult low-flow $ECCO_2R$, and pediatric or adult full respiratory support through an exchange of the fiber bundle. The platform nature of this technology allows the pediatric application to leverage the larger adult markets and is likely the most feasible pathway to market for a pediatric device.

This dissertation investigates the $ECCO_2R$ and pediatric applications of the ModELAS. A mathematical model was used to define the $ECCO_2R$ bundle geometry, and benchtop performance was evaluated followed by in vivo testing. The minimum CO_2 removal target of 70 mL/min CO_2 removal was met at a blood flow rate of ~250 mL/min. Benchtop studies determined a significant relationship between hematocrit and artificial lung CO_2 removal. In vivo plasma-free hemoglobin remained below 25 mg/dL and no thrombus formed within the device under normal operation.

The P-ModELAS was evaluated in 6-hr and 7-day animal studies to validate benchtop performance and optimize cannulation and post-surgical recovery strategies, respectively. The P-ModELAS fully saturated blood while generating less than 20 mg/dL plasma-free hemoglobin. From these studies, an RA to PA cannulation via a right thoracotomy and maintaining a post-surgical 25 IU/kg/hr heparin infusion until the chest tube output stabilizes will be used in upcoming 30-day studies.

In vitro methods were developed to evaluate the effect that the ModELAS impeller design modifications have on thrombus formation at the bottom pivot-bearing. Smoother, zirconium pivots did not appear to decrease thrombus formation compared to ceramic pivots. Washout holes did not further improve thrombus formation.

Table of Contents

List of Tables

List of Figures

Acknowledgements

I would like to thank my advisor Dr. William Federspiel for his continual mentorship and guidance. The support I have received while in the Medical Devices Lab has enabled me to develop my skills as an engineer, critically evaluate my work and conduct translational research. His mentorship has also greatly improved my abilities as a scientific communicator.

I would like to thank the members of my dissertation committee, Dr. Harvey Borovetz, Dr. William Wagner and Dr. Peter Wearden. The knowledge and guidance each member has generously provided has helped shape the direction of this research. I am also grateful for the training and experiences I have gained through the Artificial Heart Program. This program has provided me the opportunity to interact with patients who rely on medical devices every day and provided me a practical appreciation for what our projects are trying to achieve.

A special thanks to the members of the Medical Devices Lab and the undergraduate students who I have the opportunity to work with. This work would not have been possible without their collaboration and input. I also greatly appreciate the involvement and dedication of the McGowan Center for Preclinical Studies personnel provided during the in vivo studies. I would especially like to thank Brian Frankowski. His mentorship has provided me with a wealth of practical medical device and fabrication knowledge. He also constantly reminded me: If you start with junk, you end with junk. Finally, a special thank you to my family and friends for supporting me during graduate school.

I would also like to acknowledge and thank the sources that funded this research. This research would not have been possible without the support of the NIH NHLBI (R01HL117637 &

R01HL135482), the University of Pittsburgh CBTP training grant, the McGowan Institute for Regenerative Medicine and the Coulter Translational Research Partners II Program.

Nomenclature

ACT	Activated Clotting Time
ae-COPD	Acute Exacerbations of COPD
ARDS	Acute Respiratory Distress Syndrome
$AVCO_2R$	Arterio-Venous CO_2 Removal
CA	Carbonic Anhydrase
CF	Cystic Fibrosis
COPD	Chronic Obstructive Pulmonary Disease
CVP	Central Venous Pressure
DLC	Dual Lumen Catheter
$ECCO_2R$	Extracorporeal CO_2 Removal
ECMO	Extracorporeal Membrane Oxygenation
HCT	Hematocrit
HFM	Hollow Fiber Membrane
Hgb	Hemoglobin
HR	Heart Rate
IMV	Invasive Mechanical Ventilation
IVC	Inferior Vena Cava
LF- PAL	Low-Flow Pittsburgh Artificial Lung
LPV	Lung Protective Ventilation
MAP	Mean Arterial Pressure
ModELAS	Modular Extracorporeal Lung Assist System

MV	Mechanical Ventilation
NIH	Normalized Index of Hemolysis
P-PAL	Pittsburgh Pediatric Artificial Lung
PA	Pulmonary Artery
PAF	Platelet Activating Factor
PAP	Pulmonary Artery Pressure
pCO_2	Partial Pressure of CO_2
pfHb	Plasma Free Hemoglobin
PH	Pulmonary Hypertension
RA	Right Atrium
RPM	Rotations Per Minute
SVC	Superior Vena Cava
TIH	Therapeutic Index of Hemolysis
vCO_2	CO_2 Removal Rate
VILI	Ventilator-Induced Lung Injury
VV-$ECCO_2R$	Veno-Venous Extracorporeal CO_2 Removal

1.0 Introduction

1.1 Adult Respiratory Failure

Chronic lung disease in adults, including chronic obstructive pulmonary disease (COPD), continue to be the 3rd leading cause of death in the US and 5th worldwide.[1,3] Annually, COPD results in over 800,000 hospitalizations and is projected to continue to increase due to an aging population and increased tobacco use in developing countries.[4,5] COPD is characterized by a chronic cough, dyspnea, and diminished lung function.[6] It encompasses multiple respiratory conditions including chronic bronchitis (mucus over secretion) and emphysema (alveoli destruction).[5] The primary cause of COPD is smoking, however environmental/occupational pollutants and genetic factors may also increase one's risk of developing COPD.[6] COPD symptoms may be managed pharmacologically to improve quality of life and reduce the frequency and severity of acute exacerbations, however the lung damage associated with COPD is irreversible.[6]

Acute exacerbations of COPD (ae-COPD) are defined by worsening dyspnea and hypercapnia, hypoxemia and an increased amount of mucus.[7] Acute exacerbations are commonly due to viral or bacterial infections, but are also attributable to environmental factors and smoking. COPD patients typically experience 2 – 3 acute exacerbations per year, and account for approximately 63% of COPD hospitalizations.[4,5] One study reported a 43% one-year mortality rate for COPD patients requiring hospitalization for an acute exacerbation.[8] The current standard of care for moderate to severe ae-COPD is mechanical ventilation to correct blood gas tensions while the cause of the exacerbation is addressed.

Acute respiratory distress syndrome (ARDS) is an acute form of respiratory disease which accounts for 200,000 hospitalizations in the US per year and is associated with a 30 – 50% mortality rate.[9] ARDS develops secondary to a direct (pneumonia, aspiration, air emboli) or indirect (sepsis, drug overdose, trauma with transfusions) lung injury.[10,11] The Berlin Definition is commonly used to identify ARDS and requires noncardiogenic bilateral opacities on radiographic chest imaging, symptomatic within 7 days of injury and a minimum positive end-expiratory pressure of 5 cm of water (measure of the degree of hypoxemia).[12] The intensity and invasiveness of ARDS treatment is dependent upon the severity of the lung injury as indicated by the PaO_2/FiO_2 ratio and ranges from non-invasive ventilation to extracorporeal membrane oxygenation.[13]

1.1.1 Treatments

Carbon dioxide removal is the primary challenge in patients with ae-COPD and moderate ARDS. These patients maintain adequate lung function to oxygenate blood via minimally invasive, or non-invasive methods, however they are unable to utilize the lung volume required for CO_2 removal.

1.1.1.1 Mechanical Ventilation

Invasive mechanical ventilation (IMV) has conventionally been used to provide the necessary respiratory support for moderate ARDS and ae-COPD patients. The high tidal volumes (10 – 15 mL/kg) required to effectively ventilate these patients can result in ventilator-induced lung injury (VILI) thereby exacerbating the initial lung injury. VILI encompasses both barotrauma and volutrauma caused by the over distension of the lungs as well as potential biotrauma resulting from the release of bacteria into the circulation.[2] Prolonged failure to wean patients form IMV

places patients at an increased risk for developing respiratory muscle fatigue[14] and can lead to extended IMV use[15] which is associated with increased mortality.[16]

Lung protective ventilation (LPV) and ultra-LPV (<6 mL/kg or 3mL/kg, respectively)[17,18] utilize lower tidal volumes to prevent VILI. These strategies are able to adequately oxygenate the blood in moderate ARDS and ae-COPD patients, however 15 – 26% of patients will fail LPV strategies due to CO_2 retention.[19,20] The resulting hypercapnia, acidosis, and dyspnea often necessitates placing the patient on IMV.[21,22] Mortality rates are higher for patients who fail LPV and are subsequently placed on IMV compared to patients who were initially supported with IMV.[23]

1.1.1.2 Extracorporeal CO_2 Removal

Extracorporeal CO_2 removal ($ECCO_2R$) devices have been used in conjunction with LPV to reduce the hypercapnia by providing partial CO_2 removal independent of the lungs. The partial CO_2 removal has also allowed some ae-COPD patients to be extubated while on $ECCO_2R$. Although initially plagued by high complication rates, $ECCO_2R$ has gained traction as advancements in fiber technology, biocompatible coatings, and simplified circuits have made extracorporeal support safer.

$ECCO_2R$ utilizes analogous gas exchange principles as extracorporeal membrane oxygenation (ECMO). Targeting CO_2 removal rather than oxygenation, however allows $ECCO_2R$ devices to be operated at much lower extracorporeal blood flow rates than ECMO devices while still removing clinically relevant amounts of CO_2 (60 – 100 mL/min at normocapnia). This is due to the high solubility of CO_2 within plasma and the nearly linear slope of the CO_2 dissociation curve within the physiologically relevant range.[24,25] The high solubility of CO_2 is primarily due to the majority of CO_2 being carried as bicarbonate (>95%).[26] Bicarbonate is rapidly converted to

dissolved CO_2 as it is eliminated thereby an unsaturated, linear dissociation curve within the physiologic range is maintained. The resting, normocapnic CO_2 production in an adult (~200 mL/min) is equivalent to the CO_2 carried in ~400 mL of blood.[27] Thus, even when resistances to gas transfer within an artificial lung are taken into account[28], clinically relevant CO_2 removal can be achieved at blood flow rates below 1 L/min. Comparatively, typical blood flow rates for adult ECMO are 4 – 8 L/min (50 – 100 mL/kg/min).[29] The lower extracorporeal blood flow rates associated with $ECCO_2R$ allow smaller cannulas to be used, and is generally considered less invasive than ECMO.

1.1.1.2.1 Arteriovenous $ECCO_2R$ (AV-$ECCO_2R$)

Low resistance, polymethylpentene (PMP) hollow fiber membrane bundles (5 mmHg/L/min) permit the use of the arterio-venous pressure gradient to generate flow through the hollow fiber membrane (HFM) lung. This eliminates the need for a pump and consequently reduces the trauma to the blood. The iLA Membrane Venilator (Novalung, Xenios AG, Heilbronn, Germany) is the most widely used AV-$ECCO_2R$ device and was first introduced in 2002.[30] The iLA utilizes a 1.3 m^2 heparin coated PMP bundle and has a blood flow specification of 0.5 – 4.5 L/min.[31] Complications associated with arterial cannulation and specific patient selection criteria have limited the clinical appeal of AV-$ECCO_2R$. The most serious complication is limb ischemia due to the large bore arterial cannula. Zimmerman, et al. report lower limb ischemia in 6% of patients even with the use of ≤17 Fr arterial cannula, a two physician insertion process and ultrasound assessment of the vessel.[32] AV-$ECCO_2R$ is also contraindicated in patients with heart failure or peripheral vascular disease due to its reliance on the cardiac function to drive

extracorporeal blood flow. The fraction of the cardiac output flowing through the membrane lung bypasses the peripheral vascular, thereby essentially reducing the patient's cardiac output.[30]

1.1.1.2.2 Veno-venous $ECCO_2R$ (VV-$ECCO_2R$)

Early forms of VV-$ECCO_2R$ were first explored in the 1970s, however these circuits essentially operated ECMO devices at lower blood flow rates.[33] These early devices utilized large surface area (1.6 – 3.5 m^2) silicone membranes, required two venous access cannulas and operated at blood flows between 2 and 4 L/min.[27,34] A 1994 randomized clinical trial, however did not show improved survival for patients treated with low frequency positive pressure ventilation in conjunction with $ECCO_2R$.[34]

Recently, clinical interest has returned to VV-$ECCO_2R$. Modern VV devices utilize PMP HFM bundles, operate at blood flow rates below 1 L/min and vascular access can be gained via a percutaneously placed dual lumen catheter. The complexity of these systems is increased compared to AV-$ECCO_2R$ due to the need for a blood pump. Pump-driven extracorporeal blood flow removes the reliance on the heart to generate the pressure gradient and obviate the need to arterial cannulation. Multiple companies are actively pursuing artificial lungs specifically designed for VV-$ECCO_2R$. These systems remove 20 – 40 % of the basal metabolic CO_2 production and operate at blood flows ranging from 250 mL/min to 4.5 L/min.[35–37]

The Hemolung RAS (ALung Technologies, Pittsburgh, PA) utilizes an integrated spinning core to enhance gas exchange efficiency within the 0.59 m^2 annular HFM bundle.[38,39] This allows the Hemolung to remove 30 – 50% of the metabolic CO_2 production at blood flow rates below 500 mL/min. Multiple small case reports have utilized the Hemolung in conjunction with NIV to avoid

intubation, allow extubation or aid in weaning patients from MV in ae-COPD patients.[40–44] In ARDS patients the Hemolung has been used in addition to lung-protective ventilation strategies to manage hypercapnia.[45–47] In the SUPERNOVA Trial (ClinicalTrials.gov Identifier: NCT02282657) the Hemolung facilitated MV tidal volumes below 4 mL/kg in ARDS patients.[48]

The iLA Activve (Xenios, AG, Heilbronn, Germany) product line provides low-, mid- and high-flow to provide $ECCO_2R$ to ECMO support through three different membrane lung options.[31] In the ECLAIR clinical trial, the mid-flow iLA Activve device (1.3 m^2) prevented intubation in 56% of the acute hypercanic respiratory failure patients compared patients initially started on NIV therapy. Major bleeding, however occurred in 9 of the 25 $ECCO_2R$ patients compared to 2 patients in the control MV group.[49] Clinical and benchtop evaluations of the low-flow, partial CO_2 removal iLA Activve device, the MiniLing Petite (0.32 m^2 and blood flows up to 0.8 L/min) have not been published.

The low blood flow rates required for $ECCO_2R$ has resulted in several systems leveraging the capabilities of renal replacement therapy platforms, already widely used in intensive care units, to drive blood flow. The 0.32 m^2 PrismaLung (Gambro-Baxter, Meyzieu, France) is integrated into the Gambro Prismaflex system.[50] In a feasibility and safety study of 20 mild to moderate ARDS patients an average CO_2 removal of 51 mL/min was achieved at a blood flow of ~420 mL/min. Although the 28-day mortality was 15%, in 50% of the cases the membrane lung had clotted within 20 hours.[51] The Abylcap (Bellco, Mirandola, Italy) couples the Lilliput 2 oxygenator (0.67 m^2, LivaNova) and the Bellco renal replacement systems to provide CO_2 removal at blood flow rates below 500 mL/min.[52] A 4 patient study utilizing the Abylcap in ARDS patients showed up to 98 mL/min CO_2 removal at a blood flow rate of 400 mL/min.[53] Neither device however has gained significant clinical use.

Evidence supporting the use of $ECCO_2R$ in ARDS and ae-COPD patients continues to grow, however is primarily limited to case reports, and prospective and retrospective studies. This has led some to caution referring to $ECCO_2R$ as less invasive and safer than ECMO,[49,54] and limited the commercial use of $ECCO_2R$ to outside of the United States. Pivotal clinical trials currently underway are required to gauge the safety and efficacy of $ECCO_2R$ over traditional therapies. The VENT-AVOID trial in the US (ClinicalTrials.gov Identifier: NCT03255057) is evaluating the safety and efficacy of the Hemolung RAS plus standard of care MV compared to standard of care MV alone in COPD patients. The REST trial in the UK (ClinicalTrials.gov Identifier: NCT02654327) is comparing outcomes of ARDS patients treated with VV-$ECCO_2R$ plus low tidal volume MV to those treated with standard of care MV.

1.2 Pediatric Respiratory Failure

Chronic and acute respiratory failure continue to be prominent sources of pediatric morbidity and mortality. Acute respiratory infections in pediatric patients account for 17% of reported pediatric deaths.[55] Cystic fibrosis (CF) and pulmonary hypertension (PH) are the primary chronic lung diseases which affect children. CF affects approximately 70,000 people worldwide and has a mean survival of 37.4 years.[6,56] The genetic mutation responsible for CF results in the thickening of the lung mucus which causes clearing the mucus from the airways to be challenging. The result is difficulty breathing and an elevated risk for lung infections. CF is not curable and treatment focuses on preventing lung infections, and techniques and medicines to clear mucus from the lungs.[6] Lung transplantation is currently used as a life-extending treatment for those patients with advanced CF.[57]

PH in children is primarily idiopathic pulmonary artery hypertension (PAH), inherited PAH or PAH associated with congenital heart disease, however it can also be secondary to developmental lung diseases.[58] PH is defined as a mean pulmonary artery pressure ≥25 mmHg after 3 months of age and is a result of thickening of the muscle within the walls of the pulmonary blood vessels.[59] The increased pulmonary resistance requires additional work by the right heart which leads to right heart failure. Although there is no cure for PH, pharmacological agents are used to treat symptoms and slow disease progression. Pulmonary vasodilators have increased the 5-year survival from PAH diagnosis to 74%.[60] Lung and heart-lung transplantation are options for end-stage PH, however outcomes and survival are poor. Median survival for transplanted IPAH patients is 5.8 years, with a 61% 5-year survival rate.[61]

1.2.1 Treatments

Early stages of CF and PAF can be managed non-invasively via non-invasive ventilation and pharmacological methods. As these diseases progress patients ultimately require lung transplantation. CF and PH are the most common indicators for lung transplantation in pediatric patients[62] with patients typically waiting 1 – 6 months for donor lungs to become available.[63] Mechanical ventilation and ECMO are used to bridge these lung failure patients to transplant.

Invasive mechanical ventilation in pediatric respiratory failure patients, however has similar drawbacks to its use in adults. The potential for VILI is increased in end stage pediatric lung failure due to the long lung transplant waitlist times. A single center study evaluating post-transplant outcomes of pediatric CF patients demonstrated significantly more graft failures (55.6% vs 11%) and longer mean post-transplant hospital stays in patients who had been ventilated pre-transplant.[64] Lung protective ventilation techniques used in adult ae-COPD and ARDS patients are

not appropriate for these pediatric patients due to their need for both oxygenation and CO_2 removal support.

ECMO provides full respiratory support (oxygenation and CO_2 removal) independent of the lungs and can be used as an alternative therapy to IMV. Significant progress has been made in adult ECMO technology, however the pediatric population has not seen similar advances. This is primarily due to the small pediatric patient population, and subsequent small financial returns, and the wide range of patient sizes (< 2kg in neonates to >70 kg in older children).[65] Clinicians are able to use adult devices off-label in large children, however off-label use is not feasible in smaller children and neonates.

Devices available for pediatric ECMO are limited and commonly require piecing together pumps and oxygenators from multiple manufacturers. The Quadrox iD neonatal and pediatric oxygenators (Getinge Group, Germany) and the NovaLung iLA (Xenios, Germany) provide pediatric specific support with maximum blood flow rates of 1.5, 2.8, or 4.5 L/min, respectively.[31,66] In pulmonary hypertension patients, blood flow through low resistance oxygenators, such as the Quadrox Neonatal and Novalung, is able to be driven via the pressure gradient between the pulmonary artery and typically either the pulmonary vein or left atrium, essentially bypassing the lungs.[67,68] In a VV configuration these oxygenators would need to be paired with a pump, such as the Pedimag.

The literature has also suggested that devices marketed for $ECCO_2R$ could also be operated as pediatric ECMO devices.[65] The blood flow rates and HFM bundle surface area of $ECCO_2R$ devices are well suited for pediatric ECMO. Jeffries, et al. demonstrated in a preclinical animal study that the Hemolung was able to provide the required oxygen transfer for 3 – 10 kg children.[69] This, however, is the only study evaluating the application of an $ECCO_2R$ device for pediatric

ECMO. A significant drawback to using either an adult ECMO or $ECCO_2R$ device off-label for pediatric ECMO is that the devices have not been optimized for pediatric needs (i.e. larger than necessary HFM surface area).

ECMO, and MV, are typically deemed contraindications for lung transplant by some centers due to poor post-transplant outcomes. In one retrospective study survival to discharge was 66% for patients weaned from ECMO prior to transplant and 22% for those patients unable to be weaned.[70] Neither current ECMO circuits nor MV is well-suited for long-term pediatric respiratory support due to the required immobilization and sedation of the patient, and resultant muscle deconditioning. Post-transplant outcomes, however, have been improved in ECMO patients who participated in active rehabilitation, including ambulation, pre-transplant.[71] Pre-transplant active rehabilitation of ECMO patients has been used to counter muscle deconditioning.[72–75] A small study from Duke Children's Hospital, demonstrated patients involved in pre-transplant rehabilitation had significantly fewer post-transplant days on MV, and fewer post-transplant days in the ICU and hospital compared to patients not participating in pre-transplant rehabilitation.[75] The majority of reported "awake ECMO" however has been in adult and adolescent patients rather than younger children.[71,76–79] This is partly due to limited availability of appropriately sized dual lumen catheters for children and, hence reliance on multisite VV-cannulation which increases circuit complexity.[80]

Current research efforts are focused on devices specific to pediatric gas transfer requirements and that also allow safe, and simplified patients ambulation. The University of Michigan group is pursuing a pediatric pump-less, low resistance oxygenator. The Pediatric MLung (0.13 m^2) uses concentric gating to create secondary flow and increase gas transfer. Animal studies have demonstrated an oxygenation rate of 45 mL/min and pressure drop of 25 mmHg at

the rated flow (1 L/min).[81] The University of Maryland group and Breethe Inc. are developing the Pediatric Pump Lung (PediPL) which combines a centrifugal pump and HFM bundle (0.3 m^2) into a single, wearable unit. The PediPL has demonstrated positive performance in 30-day sheep studies.[82]

1.3 The Modular Extracorporeal Lung Assist System (ModELAS)

This thesis presents work contributing to the development of the Modular Extracorporeal Lung Assist System (ModELAS). The ModeLAS is being designed as a platform artificial lung capable of meeting the needs of three respiratory assist applications. Full adult or pediatric respiratory support (oxygenation and CO_2 removal) and adult low-flow CO_2 removal may be achieved by the ModELAS. All three applications utilize the same centrifugal pump and a simple exchange of the HFM bundle permits the ModELAS to be configured for either pediatric or adult use.

The ModELAS was developed from the Paracorporeal Ambulatory Assist Lung (PAAL)[83] and the Pittsburgh-Pediatric Ambulatory Lung (P-PAL)[84]. All three devices utilize the same centrifugal pump, and the pediatric and adult versions of the ModELAS utilize the identical HFM bundles as the P-PAL and PAAL, respectively. The blood flow channel leading from the pumping compartment to the HFM bundle in the ModELAS is identical to that in the PAAL. Due to the commonalities in the internal geometries and the design evolution from the PAAL and P-PAL to the ModELAS some work presented in this thesis was conducted in the PAAL and P-PAL.

1.3.1 Benefits of a Platform Technology

Commercialization and innovation of pediatric specific medical devices is often hindered by the small pediatric patient population. The cost of developing and conducting clinical trials on pediatric specific devices typically exceeds their future profitability, and thus these devices attain little interest from industry.[85] To combat this issue Pediatric Medical Device Safety Improvement Act (PMDSIA) established in 2007 the Pediatric Device Consortia to fund pediatric device development and provided fiscal incentives for devices approved under the Humanitarian Device Exemption.[86] Since its enactment the PMDSIA has increased the percentage of PMA and HDE approved devices indicated for pediatric patients per year from 6.9% in 2008 to 18.3% in 2016.[87] The majority of these devices in 2016, however were approved for patients 18 years and older, or for pediatric and adult use. Thus, despite the PMDSIA incentives, there does not appear to be an industry shift towards developing pediatric medical devices unless there is also an adult application.

The ModELAS, being a platform technology, follows this trend by having both a pediatric as well as adult applications. The adult $ECCO_2R$ ModELAS patient population is nearly two orders of magnitude larger than the pediatric population (Table 1). By targeting a combined adult and pediatric population, the ModELAS presents a more viable pathway to bringing a pediatric device to market.

Table 1 Patient Populations of the ModELAS

Application	Intended Function	Typical Blood Flow Rate [L/min]	Patients Supported Annually[88]
Pediatric Support	O_2 supply and CO_2 removal	1 – 2.5	~500
Adult Support	O_2 supply and CO_2 removal	1 – 5	~2,000
$ECCO_2R$	CO_2 removal	< 1	~200,000

1.3.2 Objective for the ModELAS

This dissertation focuses on the development of the $ECCO_2R$ and pediatric respiratory support applications of the ModELAS. Performance targets were established based upon devices which are clinically available as well as those under development. The design targets for the $ECCO_2R$ ModELAS configuration are removal of 35 – 50% of the metabolic CO_2 produced at a blood flow rate less than 700 mL/min (approximately 70 – 100 mL CO_2/min at normocapnia), compatibility with the Hemolung 15.5 Fr dual lumen catheter, non-clinically significant hemolysis, and capable of providing 7 days of continuous support. The design targets for the pediatric ModELAS configuration are 30 – 105 mL/min oxygenation at a blood flow rate of 1.0 – 2.5 L/min, compatibility with a right atrium to pulmonary artery cannulation (including a 50 mmHg pulmonary hypertension assumption), a normalized index of hemolysis below 0.05 g/100L, and the capability of providing 1 – 3 months of continuous support.

This thesis describes the development, in vitro and in vivo characterization of the $ECCO_2R$ and pediatric applications of the ModELAS. Chapter 2 focuses on the in vitro evaluation of the $ECCO_2R$ configuration of the device. A mathematical model was developed and used to drive the

geometric design of the HFM bundle. The proposed design from Chapter 2 was evaluated in 7-day animal studies in Chapter 4. Chapters 5 and 6 focus on the in vivo characterization of the pediatric ModELAS in 6-hour and 7-day animal studies. The 6-hour, acute animal studies developed the pediatric cannulation strategy and evaluated short-term, in vivo device performance. Chapter 6 builds upon the acute animal studies and developed the post-operative anticoagulation and recovery strategies in a series of 7-day studies. Finally, Chapter 7 aims to develop in vitro methods to evaluate the effect impeller washout holes have on the thrombogenicity of the ModELAS.

2.0 In Vitro Characterization of the Low-Flow PAAL

The following chapter presents work peer-reviewed and published in the Intensive Care Medicine Experimental Journal. Computation fluid dynamics analysis presented within this chapter was completed by Greg Burgreen, PhD.

2.1 Introduction

Mechanical ventilation is commonly used to help normalize arterial blood gases in patients with acute hypercapnia but can also contribute to ventilator-induced lung injury (VILI). VILI results from over-distension of the lung, barotrauma and alveolar damage caused by high volume ventilation.[2,89] Extracorporeal CO_2 removal ($ECCO_2R$) provides a minimally invasive option to remove CO_2 independently of the lungs and allow lung rest. $ECCO_2R$ has been used in patients with acute exacerbations of chronic obstructive pulmonary disease (ae-COPD) to avoid invasive mechanical ventilation, avoid intubation or assist in extubation and in ventilator weaning.[40,90,91] In patients with moderate acute respiratory distress syndrome (ARDS), $ECCO_2R$ has been used in conjunction with lung protective or ultra-protective ventilator settings (tidal volume less than 6 ml/kg[17] or 3 mL/kg[18], respectively) to reduce VILI and correct acidosis.[18,32]

Contemporary $ECCO_2R$ devices use simplified designs, biocompatible coatings and polymethylpentene fibers to reduce adverse events.[25] Dual lumen catheters permit single site veno-venous (VV) cannulation and obviate the need for, and risks of, arterio-venous (AV) cannulation. A 2016 epidemiological study showed that the trend is toward VV cannulation.[92] The recent focus

has been on improving the gas exchange efficiency of $ECCO_2R$ devices. Active mixing, blood acidification, electrodialysis and carbonic anhydrase immobilization to the fiber surface are being explored in an effort to reduce fiber surface area and further lower blood flow rates.[69,93–95]

$ECCO_2R$ utilizes similar principles as extracorporeal membrane oxygenation (ECMO), but with the main goal of removing CO_2 in patients with otherwise sufficient oxygenation and at a fraction of ECMO blood flow rates. Lower blood flow rates are usable in $ECCO_2R$ due to the linear slope of the CO_2 dissociation curve within the physiological pCO_2 range. Thus, the amount of CO_2 available per volume of blood decreases linearly with decreasing pCO_2. Comparatively, the sigmoidal oxy-hemoglobin dissociation curve plateaus at pO_2 values above 100 mmHg thereby limiting the amount of O_2 that can be transferred to the blood.[25] Clinically used $ECCO_2R$ blood flow rates vary from 180 to 1700 mL/min[96] and are classified as either low-flow (< 1 L/min) or mid-flow (1 – 2 L/min) with ECMO considered high flow.

Proponents of mid-flow $ECCO_2R$ contend that higher blood flow rates are required to decrease the likelihood of thrombus formation and to attain the required CO_2 removal rates. Both of these concerns stem from the velocity of the blood through the device. Research has shown that regions of a device with low blood velocity are prone to thrombus formations,[97] and that increasing the velocity of the blood past the fibers increases the gas exchange efficiency.[98] There are ways, however, to engineer an $ECCO_2R$ device with increased blood velocity independent of bulk blood flow and permit low-flow $ECCO_2R$. The Hemolung RAS and the Ultra-Low Flow $ECCO_2R$ Device (ULFED) each use active mixing technology to increase the blood velocity at the fiber surface while still removing a clinically significant amount of CO_2.[38,69] The Hemolung RAS device has been successfully used at blood flow rates below 500 mL/min to correct hypercapnia in patients.[41,45,46] The Low Flow Pittsburgh Ambulatory Lung (LF-PAL) evaluated in this manuscript

operates in the low-flow region and uses a narrow bundle cross sectional area to increase blood velocity past the fibers.[98]

Here the performance of the LF-PAL as a low-flow $ECCO_2R$ device is evaluated through bench studies. The LF-PAL utilizes a 0.65 m^2 bundle integrated with a centrifugal pump into a highly compact device aimed at increasing patient mobility. The CO_2 removal performance of the LF-PAL was modeled and then measured in vitro at blood flow rates up to 700 mL/min. Additionally, the hydrodynamic performance of the LF-PAL and the resistance of the Hemolung 15.5 Fr catheter were measured and used to determine the anticipated operating conditions. Lastly, in vitro hemolysis was evaluated in the 0.65 m^2 LF-PAL and compared to two control circuits.

2.2 Methods

2.2.1 Device Description

The LF-PAL incorporates the HFM bundle into a highly compact integrated pump-lung. The centrifugal pump drives blood flow from the patient, through the HFM bundle and back to the patient via a dual lumen catheter located in the jugular vein. The impeller is magnetically coupled to, and driven by, an external motor. The device utilizes a 0.65 m^2 cylindrical, stacked-type HFM bundle with a diameter of 1.75 in. The bundle is manufactured from polymethypentene fiber sheets (OXYPLUS, Membrana, Wuppertal, Germany).[98] This prototype device weighs 1850 g and is intended to have the option to be worn by the patient. The specific design and manufacturing details of the LF-PAL devices have been previously published.[83] The device has previously been evaluated for high flow adult oxygenation,[83] but not for low-flow CO_2 removal.

2.2.2 CO_2 Removal Model

The CO_2 removal model was based on a previously published mass transfer correlation and assumes radially uniform flow through the bundle.[98,99] Briefly, the overall CO_2 mass balance is

$$Q_b \frac{dC_{CO_2}}{dz} = \pi R^2 k a_v \Delta P_{CO_2} \tag{2-1}$$

where Q_b is the blood flow rate, C_{CO_2} is the total concentration of CO_2, *z* is the axial coordinate, R is the bundle radius, k is the mass transfer coefficient, a_v is the surface area by volume ratio, and ΔP_{CO2} is the CO_2 pressure gradient between the sweep gas and blood. The average P_{CO2} in the sweep gas is assumed to be 4 mmHg and is based on a previously calculated average of the inlet and outlet sweep gas P_{CO2}.[99]

A fit of the CO_2 dissociation curve allows for C_{CO_2} to be written as a function of partial pressure.[99]

$$C_{CO_2} = q P_{CO_2}^t \tag{2-2}$$

where q and t are regression parameters equal to 0.128 and 0.369, respectively. A previously developed mass transfer correlation[99] relating the Sherwood (Sh), Reynolds (Re), and the Schmidt (Sc), numbers was used:

$$Sh = 0.54 Re^{0.42} Sc^{1/3} \tag{2-3}$$

The Sherwood number is defined as $Sh=\frac{k_{CO_2} d_f}{\alpha_{CO_2} D_f}$, where k_{CO2} is the mass transfer coefficient, d_f is fiber diameter, α_{CO_2} is the solubility of CO_2 in blood, and D_f is the facilitated diffusivity. The Reynolds number is defined as $Re = \frac{\rho v}{\varphi a \mu}$,[100] where ρ is the fluid density, v is the superficial fluid velocity, φ is the cylindrical particle correction factor, a is the surface area per volume of the fiber bundle, and μ is fluid viscosity. The Schmidt number is defined as $Sc=\frac{v_b}{D_{eff}}$ where v_b is kinematic viscosity, and D_{eff} is the effective diffusivity which takes into account chemically bound CO_2. The importance of including facilitated diffusion in the calculation and details on the development of these equations have been previously described.[99] An ordinary differential equation solver built into MATLAB (MathWorks, Natick, MA) and based on the Runge-Kutta method was used to solve the differential equation formed by equations 1-3.

2.2.3 Pump Performance

The hydrodynamic performance of the 0.65 m^2 LF-PAL was evaluated using an 8.5 g/L solution of carboxymethylcelluose sodium salt (CMC) (Sigma Aldrich, St. Louis, MO) as the working fluid. The viscosity of the CMC solution at 37 °C was 3.5 cP and verified using a capillary viscometer (Cannon Instrument Company, State College, PA). The LF-PAL was connected to a reservoir submerged in a 37 °C water bath. The rotation rate of the impeller was varied between 800 and 2000 RPM. Hoffman clamps placed at the inlet and outlet to the LF-PAL were used to vary the flow rate between 0 and 1.4 L/min. Pressure was measured at the inlet and outlet to the device using a differential fluid pressure transducer (PX771-025DI; Omega Engineering, Inc., Stamford, CT).

The anticipated catheter for use with the LF-PAL is the Hemolung 15.5 Fr dual lumen catheter. The catheter was inserted into a 1600-mL reservoir bag, and pressure was measured at the inflow and outflow ports of the catheter using a differential fluid pressure transducer. Pressure within the reservoir was assumed to be spatially uniform so that the resistance of the catheter may be calculated as the pressure difference between the inflow and outflow tubing connection ports of the catheter. Flow was driven by a Biomedicus BP-80 pump (Medtronic, Minneapolis, MN) and ranged between 100 and 900 mL/min.

2.2.4 In Vitro Gas Exchange

Gas exchange was performed in bovine blood collected from a local slaughterhouse and adhered to the ISO7199 standard.[101] The blood was filtered (40 μm Pall Biomedical, Inc., Fajardo, PR), heparinized (30 U/mL), and treated with Gentamicin (0.1 mg/mL). Blood was diluted to a hemoglobin of 12 ± 1 g/dL with phosphate buffered saline. The test circuit (Figure 1) consisted of a LF-PAL device, two 6-L compliant blood reservoirs, and an Affinity oxygenator (Medtronic, Minneapolis, MN). The reservoir bags were submerged in a water bath to maintain blood temperature at 37 ± 1 °C. The blood was recirculated through a single reservoir while the Affinity oxygenator was used to balance the blood gases to venous conditions. Once the blood was conditioned, clamps were used to divert blood flow through the LF-PAL and into the empty, second reservoir. Blood gas measurements were taken before and after the LF-PAL, and analyzed by a Rapidpoint 405 blood gas analyzer (Siemens, Deerfield, IL).

Blood flow rates ranged from 250 to 700 mL/min and were measured by an ultrasonic flow probe (Transonic Systems Inc., Ithaca, NY). Hoffman clamps were used to simulate the resistance of the Hemolung 15.5 Fr dual lumen catheter (ALung Technologies, Pittsburgh, PA). The pressure

across the device was monitored with a differential fluid pressure transducer (PX771-025DI; Omega Engineering, Inc., Stamford, CT). The normocapnic condition was tested at an inlet pCO_2 of 45 ± 5 mmHg and sO_2 of 65 ± 5%. The gas exchange rate at each flow rate was measured in triplicate.

The oxygen sweep gas flow rate was controlled by a gas flow controller (Fathom Technologies, Georgetown, TX) and ranged from 9 to 19.5 L/min. A WMA-4 CO_2 analyzer (PP Systems, Amesbury, MA) measured the CO_2 concentration in the sweep gas (F_{CO2}) exiting the LF-PAL. Steady state was achieved when the CO_2 concentration in the sweep gas changed by less than 10 ppm. CO_2 removal rate (vCO_2) was calculated according to equation 4, and normalized to an inlet pCO_2 of 45 mmHg (vCO_2^*) according to equation 5.[102]

$$\mathrm{vCO_2} = \mathrm{Q_{SG}F_{CO2}} \tag{2-4}$$

$$\mathrm{vCO_2^*} = \mathrm{vCO_2}\,\frac{45\ \mathrm{mmHg}}{\mathrm{P_{CO2}^{Inlet}}} \tag{2-5}$$

where Q_{SG} is sweep gas flow rate, F_{co2} is the concentration of CO_2 in the sweep gas, and P_{CO2}^{Inlet} is the inlet blood pCO_2.

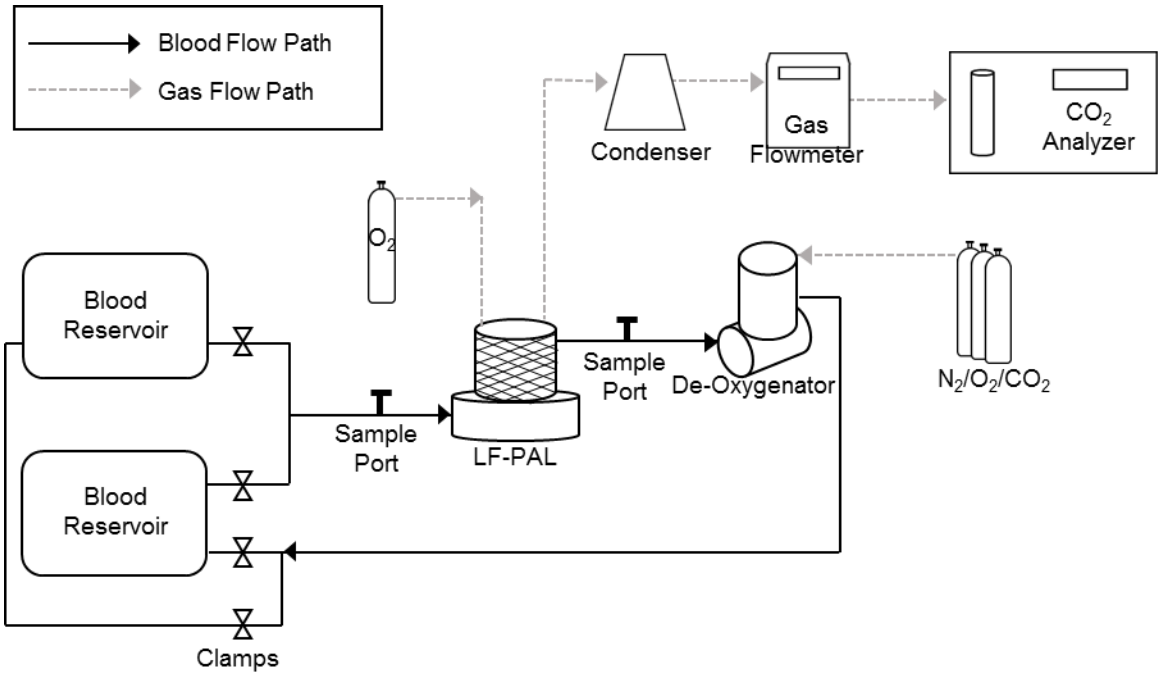

Figure 1 Schematic of the Single Pass In Vitro CO_2 Removal Loop

2.2.5 In Vitro Hemolysis

Bovine blood was collected and prepared as in the gas exchange experiments. The hemolysis test circuit consisted of the LF-PAL and the Hemolung 15.5 Fr dual lumen femoral catheter in order to reflect clinical use. The LF-PAL was tested at 500 mL/min. The control circuit replaced the LF-PAL with a PediMag pump (Thoratec, Pleasanton, CA) and Minimax PLUS Hollow Fiber Oxygenator (Medtronic, Minneapolis, MN) and was run in parallel with the test circuit. The control circuit was operated at 1500 mL/min (3750-3800 rpm) to match the CO_2 removal rates of the LF-PAL operated at 500 mL/min.[103] Hoffman clamps were used to simulate inclusion of a 12 Fr arterial cannula (Medtronic Bio-Medicus Cannula #96820-012) and 14 Fr venous cannula (Medtronic Bio-Medicus Cannula #96830-014).[104,105] Both circuits contained an

800-mL compliant blood reservoir (Medtronic; Minneapolis, MN) submerged in a water bath to maintain blood temperature at 37 ± 2 °C.

Blood samples from each circuit were taken every 30 minutes over a 6-hour period to measure plasma free hemoglobin (pfHb), hematocrit and hemoglobin. Details of the sampling and pfHb measurement methods, calculation of the normalized index of hemolysis (NIH) and therapeutic index of hemolysis (TIH) have been previously published.[69,98] Three independent trials were conducted for each circuit. The results of a second control (Medtronic Biomedicus BP-50, Minimax, and Medtronic Bio-Medicus Cannulas) are also included and methods have been previously described by our group.[69] This second control, BP-50 control, was operated at the blood flow rate required for the Minimax to meet our 70 mL/min CO_2 removal target.

2.3 Results

2.3.1 Model and In Vitro CO_2 Removal

In vitro gas transfer results and model predictions 0.65-m^2 bundle are shown in Figure 2. The CO_2 removal rate increased with increasing blood flow rate. The maximum CO_2 removal rate of the LF-PAL was 105 ± 9.2 mL/min at a blood flow rate of 703 mL/min. The model predicted CO_2 removal rates were within 7.7 – 15.4% of the experimental values.

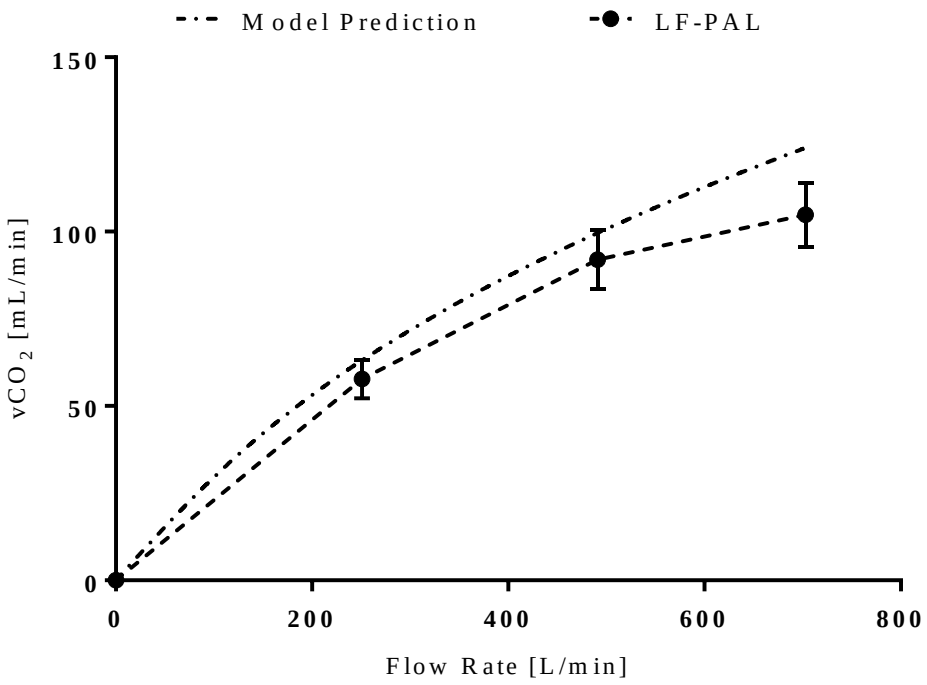

Figure 2 LF-PAL In Vitro and Model Predicted CO_2 Removal Rate

The maximum CO_2 removal rate for the LF-PAL was 105 mL/min. The model predicted the performance between 7.7 – 15.4% of the in vitro results

2.3.2 Pump Performance

The pressure generated by the 0.65 m^2 LF-PAL device is shown in Figure 3. The pressure requirements for operation with the 15.5 Fr dual lumen catheter are also shown in Figure 3. The 0.65 m^2 LF-PAL reached the required flow rate range of 250 to 700 mL/min at impeller rotation rates between 800 and 1800 RPM.

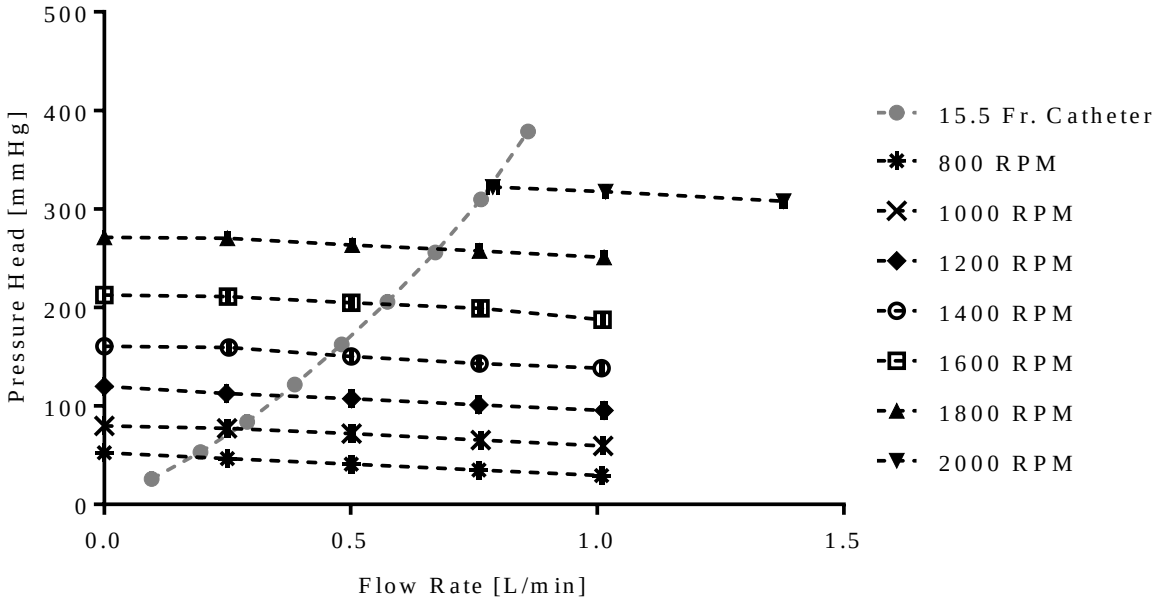

Figure 3 Pump Performance of the LF-PAL

The pressure generated by the LF-PAL at impeller rotation rates of 800, 1000, 1200, 1400, 1600, 1800 and 2000 RPM between 0 and 1 L/min. The pressure requirements of the 15.5 Fr dual lumen catheter are also shown

Typical CFD results shown in Figure 4 for the 0.65 m^2 LF-PAL demonstrate adequate pressure generation and uniform flow distribution throughout the bundle. Generated pressure heads predicted by CFD were 51 mmHg for 850 RPM, 0.25 L/min and 265 mmHg for 1870 RPM, 0.70 L/min. The maximum shear stress predicted by CFD in the device for these operating conditions was located on the rotor surfaces and was less than 200 Pa. Flow through the fiber bundle was shown to have a very uniform distribution and exhibited no flow separation. For both operating conditions, the LF-PAL was shown to have the slowest flow occurring in the inflow elbow and the bundle inlet and outlet plenums.

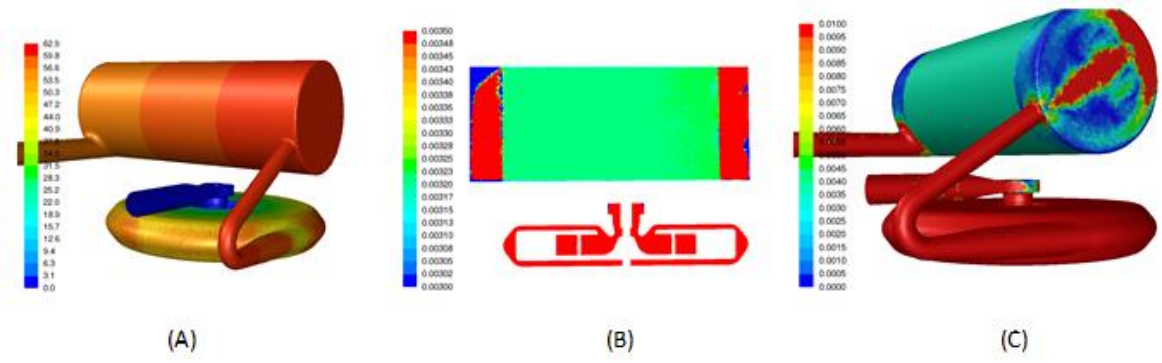

Figure 4 CFD Analysis of the LF-PAL

CFD analysis results for 850 RPM and 0.25 L/min showing (A) predicted pressure (mmHg) throughout the device, (B) fluid velocity (m/s) thorugh the fiber bundle, and (C) near wall velocity magnitudes (m/s) on the device surfaces

2.3.3 In Vitro Hemolysis

Table 2 provides the TIH and NIH values for the 0.65 m^2 LF-PAL and control circuits. The rate of pfHb increase over time was linear ($R^2 > 0.90$) for the LF-PAL and control circuit. The TIH of the LF-PAL (0.08 ± 0.017 g/100min), the Pedimag control (0.043 ± 0.0004 g/100 min) and the BP-50 control (0.123 ± 0.013 g/100min) all significantly differed from one another ($p<0.05$). The NIH of the LF-PAL (0.158 ± 0.034 g/100 L), the Pedimag control (0.029 ± 0.003 g/100 L) and the BP-50 control (0.105 ± 0.012 g/100 L) all significantly differed from one another ($p<0.05$).

Table 2 In Vitro Hemolysis of the LF-PAL

Device	Flow Rate [mL/min]	NIH [g/100 L]	TIH [g/100 min]
LF-PAL (0.65 m^2)	500	$0.158 \pm 0.034^{\dagger}$	$0.080 \pm 0.017^{\ddagger}$
Pedimag Control	1500	$0.029 \pm 0.003^{\dagger}$	$0.043 \pm 0.004^{\ddagger}$
BP-50 Control	1250	$0.105 \pm 0.012^{\dagger}$	$0.123 \pm 0.013^{\ddagger}$

$^{\dagger},^{\ddagger}$ Statistically significant ($p < 0.05$) compared to other devices

2.4 Discussion

Clinical evidence demonstrates that $ECCO_2R$ can prevent the need for intubation, allow for protective and ultra-protective lung ventilation, and aid in weaning patients from mechanical ventilation.[17,106] Low-flow $ECCO_2R$ devices aim to provide minimally invasive, complementary treatment options for ae-COPD patients and patients with moderate ARDS requiring mechanical ventilation. This manuscript details the in vitro and computational characterization of the LF-PAL for $ECCO_2R$. The LF-PAL is an integrated pump-lung designed to allow simplified patient ambulation while on $ECCO_2R$. The LF-PAL removed up to 105 mL/min of CO_2 thereby exceeding the 70 mL/min target and had acceptable hemolysis.

$ECCO_2R$ has been applied to a variety of clinical applications including weaning patients from mechanical ventilation, avoiding intubation and permitting lung protective ventilation.[18,32,40,90,91] As a result of the range of clinical applications, the CO_2 removal rate required for $ECCO_2R$ is not well defined. Additionally, CO_2 removal is dependent on the total CO_2 content of the blood. Hence, the degree of hypercapnia will affect the CO_2 removal rate at a

given blood flow rate. The CO_2 removal rate, however, will proportionally increase with increases in pCO_2. The CO_2 removal target must therefore be reported as a percentage of the rate of metabolically produced CO_2 or the pCO_2 of the blood entering the device must be specified. Trahanas et al. provide a review of studies since 2009 of $ECCO_2R$ used in hypercapnic COPD patients and CO_2 removal rates ranged from 80-160 mL/min.[44] From this the authors proposed that an ambulatory $ECCO_2R$ device must remove at least half of the metabolic CO_2. Under normocapnic conditions this would be approximately 100 mL/min. Commercial $ECCO_2R$ devices report removal rates of 20 – 40% of the metabolically produced CO_2.[35–37] Under normocapnic conditions these rates are equal to 40 – 80 mL/min. Based on this data we set 70 mL/min as the minimum target CO_2 removal rate for the LF-PAL at normocapnia. The LF-PAL exceeded this target at low-flow $ECCO_2R$ blood flow rates. Recent, on-going and upcoming $ECCO_2R$ clinical trials (XTRAVENT[18], REST (ClinicalTrials.gov Identifier: NCT02654327), SUPERNOVA (ClinicalTrials.gov Identifier: NCT02282657), and VENT-AVOID (ClinicalTrials.gov Identifier: NCT03255057)) should provide a more defined CO_2 removal target for devices in development.

Concerns with low-flow $ECCO_2R$, compared to mid-flow, include inadequate CO_2 removal and thrombus formation resulting from low velocity regions within the device.[97] To mitigate both of these effects the LF-PAL uses a fiber bundle with a narrow cross sectional area to increase local blood velocities and achieve clinically significant CO_2 removal. In addition, CFD results of the LF-PAL demonstrate uniform blood velocity through the bundle. Other low-flow devices use active mixing technology to increase local blood velocity in an effort to achieve the required CO_2 removal rates. The Hemolung incorporates a rotating core[38] and the ULFED uses rotating impellers.[69] The drawback is that too high of an increase in blood velocity may detrimentally

increase hemolysis. The Hemolung, however, has been used in humans without causing clinically significant hemolysis, though no in vitro hemolysis data are available for comparison.[41]

At least one center has begun ambulating $ECCO_2R$ patients to reduce muscle deconditioning and allow for greater physical therapy.[90] A compact device which does not require a saline infusion or vacuum pump, such as the LF-PAL, that could also be worn would simplify ambulation. Current, clinically used $ECCO_2R$ devices are portable, but are not designed to be worn by the patient.[39,107,108,31,109] The jugular cannulation and cartridge design of the Hemolung RAS permits ambulation. The device however must reside on the roller cart, which houses the required saline infusion and gas side vacuum pump, and does not provide the option to be worn by the patient. The Arterio-Venous CO_2 Removal ($AVCO_2R$) device is also under development as a wearable $ECCO_2R$ device.[110(p2)] The AV-cannulation of the $AVCO_2R$, however, relies on the patient's cardiovascular system to drive blood flow. The CO_2 removal rate is therefore dependent on the cardiac function of the patient.[30] The VV-cannulation and pump-driven blood flow of the LF-PAL allows the clinician greater control of the extracorporeal blood flow and, in turn, the CO_2 removal rate. The compact design and dual lumen cannulation of the LF-PAL lends itself to ambulation.

In this study the hemolysis of the LF-PAL was only evaluated at 500 mL/min. Shear stress within the circuit will increase as blood flow increases and likely result in elevated hemolysis at higher blood flow rates. Thus, when the LF-PAL is operated at the maximum blood flow rate, 700 mL/min, the TIH of the LF-PAL will likely increase, as would the TIH of the control circuit when operated at a higher blood flow rate. A limitation to the TIH is the lack of an established threshold value correlated to clinically significant hemolysis in vivo. Thus, in vitro studies are limited to a comparative assessment between two circuits. Future in vivo studies will thoroughly evaluate if

the hemolysis generated by the LF-PAL is clinically significant in addition to any effect the device may have on platelet activation or end organ function.

2.5 Conclusion

Evidence demonstrating the benefits of partial CO_2 removal by $ECCO_2R$ systems in conjunction with non-invasive ventilation or lung protective ventilation continues to grow. The LF-PAL provides the CO_2 removal benefits of low-flow $ECCO_2R$ in a compact design. Future work will focus on 7-day in vivo studies to further characterize the LF-PAL performance and the effect of the device on the cardiopulmonary system.

3.0 The Effect of Hematocrit on the CO_2 Removal Rate of Artificial Lungs

The following chapter has been submitted for peer-review in the American Society for Artificial Internal Organs Journal

3.1 Introduction

Patients with moderate acute respiratory distress syndrome (ARDS) and acute exacerbations of COPD (ae-COPD) can benefit from lower tidal volume, lung protective ventilation or non-invasive ventilation strategies.[17,18,40,90,91] These ventilation strategies can prevent ventilator-induced lung injury, however failure is commonly due to hypercapnia and the resulting acidosis and dyspnea.[25] Low-flow extracorporeal CO_2 removal ($ECCO_2R$) devices have been utilized in this patient population to remove the excess CO_2 while maintaining lung protective or non-invasive ventilation.[18,32] $ECCO_2R$ devices operate on analogous principles to extracorporeal membrane oxygenation. Due to the primary objective of removing CO_2 rather than oxygenation, $ECCO_2R$ devices can operate at blood flow rates below 1 L/min.[96] The potential benefits of $ECCO_2R$ are currently being evaluated in the VENT-AVOID and REST clinical trials. $ECCO_2R$ device selection and operating parameters dictate the CO_2 removal rate (vCO_2) but the nuances of CO_2 removal can make interpreting changes in vCO_2 challenging. Correct interpretation is especially important as vCO_2 is the most sensitive indicator of intrabundle thrombosis.[111]

The vCO_2 of a specific artificial lung geometry is a known function of blood flow rate, inlet pCO_2, and sweep gas flow rate. The effect of extracorporeal blood flow rate and inlet pCO_2 on vCO_2 can be taken into account by normalizing the vCO_2 to these parameters.[112] The effect of sweep gas flow rate on vCO_2 and the importance of a sweep gas independent regime has also been well established.[113] Diminished vCO_2 performance, however, has also been noted in animal studies during periods of anemia.[114,115,116] The relationship between vCO_2 and hematocrit (HCT) seen in artificial lungs has been attributed to mechanisms analogous to those within the native lungs. Bidani and Crandall used computational modeling to demonstrate that a decrease in HCT from 45% to 15% results in a 50% decrease in vCO_2 within the native lungs.[116] A similar vCO_2-HCT relationship has been noted in animal studies,[114] however the complexities of animal studies makes isolating the artificial lung vCO_2-HCT relationship challenging.

In this study we evaluated the relationship between HCT and the vCO_2 of a low-flow $ECCO_2R$ device in an in vitro setting. Blood was hemodiluted with saline and plasma to reach the targeted HCT in order to evaluate any effect plasma proteins may have on vCO_2. The in vitro setting allowed the effect of HCT and plasma proteins on vCO_2 to be isolated. The results of this study will aid in predicting vCO_2 in $ECCO_2R$ devices and interpreting changes in vCO_2 related to hematocrit.

3.2 Methods

3.2.1 In Vitro Gas Exchange

Bovine blood was collected from a local slaughterhouse and was heparinized (30 IU/mL), filtered (40 μm Pall Biomedical, Inc., Fajardo, PR), and treated with gentamicin (0.1 mg/mL). Blood was diluted to HCT levels of 8, 15, 25, and 33 ± 2 % with either isotonic saline (0.9% (w/v) Aqueous, Isotonic Saline, Fisher Scientific) or plasma. Plasma was obtained by centrifuging the whole bovine blood (2819 g for 15 min) and removing the plasma layer.

Gas exchange testing followed the ISO7199 standard[101] with the exception of the intentional alterations in HCT levels. The test circuit (Figure 1) included the ModELAS artificial pump-lung (0.65 m^2 HFM bundle)[112], two 6-L blood reservoir bags, and an Affinity oxygenator (Medtronic, Minneapolis, MN). The reservoir bags were submerged in a water bath to maintain a blood temperature of 37 ± 1 °C. The Affinity oxygenator was used to condition the blood to venous blood gas tensions (sO_2 = 65 ± 5%, pCO_2 = 45 ± 5 mmHg). Once the blood reached venous conditions, tubing clamps were manipulated so that blood was drawn from the venous conditioned reservoir, through the device, and returned to the second reservoir. Samples for blood gas measurements were taken immediately before and after the ModELAS. A RapidLab 405 blood gas analyzer was used to measure gas tensions (Siemens, Deerfield, IL). The CO_2 removal rate, hemoglobin concentration and plasma protein concentration were measured at each HCT level in triplicate.

The pump speed was adjusted to achieve 500 mL/min of blood flow through the ModELAS device. Blood flow rate was measured using an ultrasonic flow probe (Transonic Systems Inc., Ithaca, NY). The pure oxygen sweep gas flow rate (Q_{SG}) was set to 14 L/min using a gas flow

controller (Fathom Technologies, Georgetown, TX). From preliminary experiments this sweep gas flow rate is within the sweep gas independent regime. CO_2 concentration (F_{CO_2}) was measured in the exhaust sweep gas using a WMA-4 gas analyzer (PP Systems, Amesbury, MA). The CO_2 removal rate was calculated and normalized (vCO_2^*) to an inlet pCO_2 of 45 mmHg according to equation 1.

$$vCO_2^* = Q_{SG} F_{CO_2} \frac{45 \text{ mmHg}}{P_{CO2}^{Inlet}} \tag{3-1}$$

An additional 4 mL blood sample was drawn from the device inlet to measure HCT and plasma protein each time a CO_2 removal measurement was taken. HCT was measured using a capillary tube which was spun down for 3 minutes in a micro-centrifuge (International Equipment Co., IEC MB, Needham Hts, MA). The remaining blood was centrifuged for 15 minutes at 0.8 g, the supernatant plasma was removed and centrifuged again at 7.2 g for 10 minutes. The plasma protein concentration was measured using a refractometer (TS 400, Reichert, Depew, NY) from this purified plasma.

3.2.2 Statistical Analysis

Data is reported as the mean ± standard deviation. Statistical analysis was completed in SPSS (IBM, Armonk, NY). A two-way repeated measures ANOVA was used to evaluate the effect of dilution method and HCT level on measured vCO_2 and plasma protein concentration. Pairwise comparisons were made using Bonferroni post-hoc analysis. Statistical significance was determined at $p < 0.05$.

3.3 Results

In vitro vCO_2 for plasma and saline diluted blood are shown in Figure 5. There was no significant effect of dilution method (plasma dilution or saline dilution) on vCO_2 ($p = 0.427$). The CO_2 significantly decreased with decreasing hemoglobin concentration in a nearly linear fashion for both saline dilution ($R^2 = 0.998$) and plasma dilution ($R^2 = 0.984$). Decreasing the HCT from 33% to 8% resulted in a 32% and 42% decrease in vCO_2 when diluted with plasma and saline, respectively. The plasma protein concentration (Figure 6) decreased significantly after each hemodilution with saline ($p = 0.00$) and was significantly different between plasma and saline dilution ($p<0.05$).

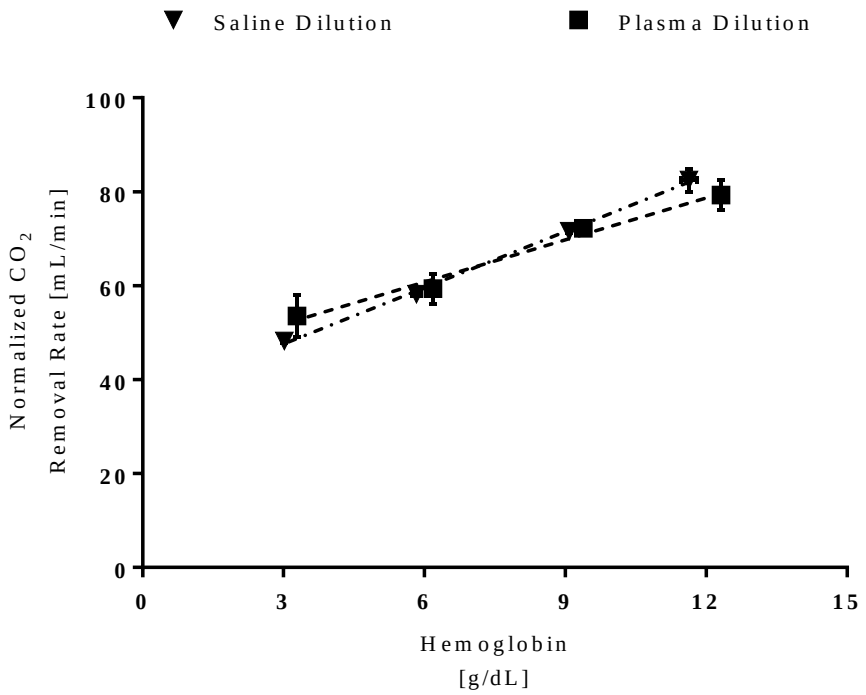

Figure 5 CO_2 Removal Rate of Blood Diluted With Saline or Plasma

The CO_2 removal rates were measured at hematocrit increments of 8, 15, 25, and 32 ± 2 % in blood diluted with saline or plasma. The blood flow rate through the device was held constant at 0.5 L/min.

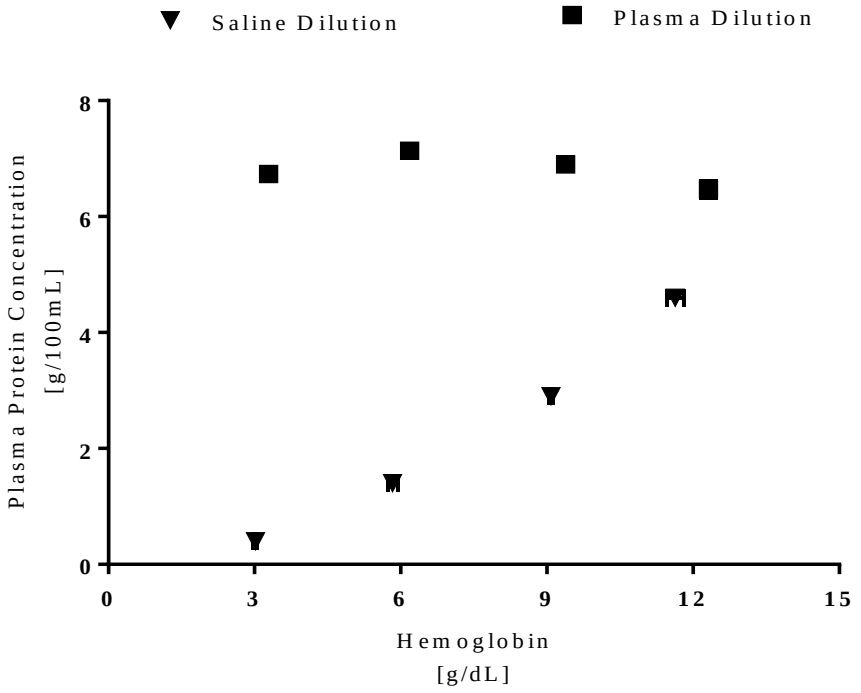

Figure 6 Plasma Protein Concentration after Dilution with Saline or Plasma

Hemodilution with saline significantly decreased the plasma protein concentration at all hematocrit levels ($p<0.05$).

3.4 Discussion

The evidence supporting the use of $ECCO_2R$ to permit non-invasive or lung protective ventilation strategies in moderate ARDS and ae-COPD patients continues to increase. With this comes a need to identify variables which influence the vCO_2 of artificial lungs, especially since a decrease in vCO_2 can be indicative of intrabundle thrombosis.[111] The vCO_2 of an artificial lung can be affected by blood and sweep gas flow rates, and the inlet pCO_2 of the blood.[112,113] The effect of HCT on CO_2 transfer has been documented in computational studies within the native lungs but

only observationally noted in artificial lungs during in vivo studies.[114] This in vitro study evaluated the vCO_2 within an $ECCO_2R$ device in blood diluted to multiple HCT levels using plasma and saline. In vitro testing demonstrated that the vCO_2 linearly and significantly decreased with decreasing HCT level. CO_2 removal rate was not affected by the method of hemodilution.

CO_2 transfer decreases with decreases in HCT within artificial lungs, as demonstrated here, as well as within the native lungs.[115–118] The vCO_2-HCT relationship within the native lungs has been attributed to 1) decreased buffering capacity provided by hemoglobin, 2) reduced flux of HCO_3^- across the red blood cell (RBC) membrane, and 3) the release of fewer Bohr protons.[116] The first two mechanisms are a direct result of fewer RBCs. Carbonic anhydrase (CA) within the RBC plays an integral role in rapidly hydrating CO_2 via the catalysis of $CO_2 + H_2O \overset{CA}{\Leftrightarrow} HCO_3^- + H^+$. Hemoglobin present within the RBC acts as a buffer by binding to H^+. Additionally, the Cl^-/HCO_3^- RBC membrane-bound exchanger rapidly exchanges HCO_3^- for Cl^-, the chloride shift, to prevent the rate-limiting accumulation of HCO_3^- within the RBC. These two mechanisms prevent the accumulation of $H^+$and HCO_3^- within the RBC which shifts equilibrium to the right. Reductions in hemoglobin and RBC concentration diminishes the buffering capacity and the surface area available for the chloride shift to occur. Thus, the reaction reaches equilibrium sooner and less CO_2 is combined with blood per increase in pCO_2. The third mechanism is the classic Haldane effect whereby the uptake of oxygen by hemoglobin in the lungs decreases the affinity of hemoglobin for CO_2 and results in the release of H^+ and bound CO_2. The released H^+ drives the equilibrium of the reaction to the left, towards dissolved CO_2. Although less than 5% of the total CO_2 content within blood is transported bound to hemoglobin, this source accounts for 30% of exhaled CO_2.[26] Bidani and Crandall utilized a computational model to isolate each of these mechanisms and demonstrated that 50 – 60% of the decrease in vCO_2 due to decreased HCT is

attributable to the third mechanism.[116] Thus, even moderate decreases in HCT will result in decreased CO_2 removal. These three factors result in anemic blood dissociating with less CO_2 per decrease in pCO_2. This essentially results in a flattening of the CO_2 dissociation curve as the HCT level decreases.[115] The above three mechanisms are inherent to properties of the blood, and not of the native lungs. Thus, these mechanisms are likely identical to those influencing the vCO_2-HCT relationship within the artificial lung.

The effects of anemia on CO_2 exchange within the native lungs is often masked by compensatory mechanisms within the body. In this study, however, a 25% decrease in HCT led to a 13% decrease in vCO_2. Normal gas exchange within the body is primarily maintained during periods of anemia by increases in cardiac output and ventilation rate, and changes to the microcirculation and metabolism.[117] Within an artificial lung, decreases in HCT will result in increased extracorporeal blood flow rate if the pump speed is held constant, and would be analogous to increased cardiac output. In the present study, however, the pump speed was adjusted to maintain an extracorporeal blood flow rate of 500 mL/min as the HCT level was decreased. The other three compensatory mechanisms would not be mimicked within an artificial lung. Hence, even small changes to the HCT level impacted the vCO_2 of the artificial lung during this study.

The effect of plasma proteins was evaluated in the present study by comparing the vCO_2 of blood diluted with plasma versus that diluted with normal saline. Plasma proteins, mainly albumin and phosphates, typically contribute minimally to CO_2 transport and CO_2 removal. This is due to the ability of normal levels of hemoglobin to buffer approximately 6 times more H^+ than plasma proteins are capable of.[119] In anemic blood, however, the role of the buffering action of plasma proteins has been postulated to be more significant due to the reduced amount of hemoglobin.[115] There was not a significant effect of dilution method (saline versus plasma) on

vCO_2, even though there was a significant difference in plasma protein concentration at each HCT level between the two dilution methods. Arazawa, et al. report a similar in vitro result, whereby a miniature artificial lung only removed 13 mL/min/m^2 more CO_2 in a PBS+albumin solution than in a PBS solution.[93] The results of the present study, and that of Arazawa, et al., demonstrate that the buffering capacity of plasma proteins is not significant enough to accommodate for the reduction, or absence, of HCT within an artificial lung. This is due to the CO_2 carrying capacity of plasma being substantially due to the Cl^- shift which requires the presence of the RBC to occur.[119] Thus, regardless of the nature of anemia (hemodilution versus diminished RBC production) an equivalent decrease in artificial lung vCO_2 should be anticipated as HCT level decreases.

In this study, as the blood was diluted the viscosity of the blood consequently also decreased. Extracorporeal blood flow rate was maintained at 500 mL/min by reducing the pump speed after each dilution. In an artificial lung**,** fluid viscosity (v) affects the fluid boundary layer thickness at the fiber surface by $v^{1/6}$. The fluid side boundary layer provides the majority of the diffusional resistance to gas transfer within the artificial lung. Thus, with all else held constant, the gas transfer rate will increase as fluid viscosity decreases within an artificial lung.[28] The results described within this manuscript do not make a distinction between increases in vCO_2 due to a lower viscosity fluid and diminished vCO_2 due to lowered HCT level.

The interpretation of changes in vCO_2 is only reliable if all factors influencing vCO_2 are accurately accounted for. The results of this in vitro study provide evidence demonstrating that decreases in HCT result in decreased artificial lung CO_2 transfer regardless of the nature of the anemia. Changes in the HCT must therefore be taken into account when determining the cause of changes in vCO_2 within an artificial lung.

4.0 Chronic In Vivo Performance of the Low-Flow ModELAS

The following chapter presents work submitted for peer-review in the Intensive Care Medicine Experimental Journal. Platelet activation studies were conducted by Sang-Ho Ye, PhD

4.1 Introduction

Mechanical ventilation (MV) has conventionally been used to normalize blood gas tensions in patients with acute respiratory distress syndrome (ARDS) or acute exacerbations of chronic obstructive pulmonary disease (ae-COPD). MV can further injure the lungs via ventilator-induced lung injury (VILI).[2,89] VILI encompasses the resulting barotrauma, biotrauma and volutrauma from the high-volume ventilation, 10 – 15 mL/kg.[120] Reducing the airway pressures through non-invasive ventilation (NIV) or lung protective ventilation techniques can improve patient outcomes, however up to 25% of ae-COPD patients will fail NIV due to hypercapnia.[19,20] The subsequent hypercapnia and acidosis require invasive MV to normalize blood gases.[21,22]

Extracorporeal CO_2 removal ($ECCO_2R$) devices provide a means to manage CO_2 levels in ARDS and ae-COPD patients while the source of the acute exacerbation is resolved. Protective and ultra-protective lung ventilation (tidal volumes of <6 mL/kg or 3 mL/kg, respectively) in conjunction with $ECCO_2R$ has been used in the treatment of moderate ARDS.[17,18] $ECCO_2R$ has been utilized to allow ae-COPD patients to avoid invasive MV or intubation.[40,90,91] Typical $ECCO_2R$ duration for ae-COPD patients is 7 days or less.[44] The on-going VENT-AVOID (ClinicalTrials.gov Identifier: NCT03255057) and REST (ClinicalTrials.gov Identifier:

NCT02654327) randomized clinical trials evaluate the application of VV-ECCO$_2$R in ae-COPD and ARDS patients, respectively.

We are developing the Modular Extracorporeal Lung Assist System (ModELAS) as a multi-functional respiratory assist technology designed to accommodate three levels of respiratory assist. The ModELAS is a highly compact, integrated pump-lung capable of being worn, or integrated on to a wheeled console. The device can be configured to provide pediatric or adult complete respiratory assist (oxygenation and CO_2 removal), or adult low-flow ECCO$_2$R. Selection of the cannula and HFM bundle size permits configuration for either pediatric or adult respiratory applications. The pediatric ModELAS utilizes a central cannulation and has been evaluated in 7-day animals studies[84,121] The adult complete respiratory assist application uses a dual lumen cannulation and is currently being evaluated in 30-day animal studies.[83,122]

In the present study, we evaluated the 7-day in vivo performance of the low-flow ECCO$_2$R ModELAS in an awake ovine model. The ECCO$_2$R ModELAS utilizes a 0.65 m^2 cylindrical, stacked, uncoated polymethylpentene HFM bundle. Our previously reported ECCO$_2$R device utilized an identical bundle.[112] The primary difference between the previous and current version of the device are washout holes within the impeller. The targeted CO_2 removal for this device is at least 35% of the metabolically produced CO_2 (70 mL/min at normocapnia) at a blood flow of 500 mL/min. Characterization of sustained device CO_2 removal, thrombogenicity, and hemocompatibility were the primary focus of the present study.

4.2 Methods

The ModELAS was evaluated for 7 days in healthy, 41.2 – 54 kg Suffolk sheep (n = 6) at the McGowan Institute for Regenerative Medicine's Center for Preclinical Studies. The animal care and surgical protocol was approved by the University of Pittsburgh's Institutional Animal Care and Use Committee. All animals received humane care.

Venous and arterial pressure lines were placed in the left external jugular vein and carotid artery, respectively. These lines were secured at the vessel and tunneled underneath the skin. The right external jugular vein was exposed via a surgical cut down. The target pre-catheterization activated clotting time (ACT) was above 300 s (ACT-II, Medtronic, Minneapolis, MN) and was achieved with a 180 IU/kg heparin bolus. Additional 1000 – 2000 IU heparin boluses were administered to increase the ACT above 300 s if necessary. The right external jugular vein was cannulated with a 15.5 Fr dual-lumen catheter (ALung Technologies, Pittsburgh, PA). The catheter was advanced to the right atrial-superior vena cava junction. Catheter position was confirmed via fluoroscopy. The catheter was secured to the neck via sutures and further protected with a neck wrap.

The primed ModELAS (4 IU/mL heparinized saline) was connected to the catheter and extracorporeal blood flow was initiated at 0.5 L/min. Pure oxygen sweep gas was initially set to 4 L/min. The animal was recovered in the intensive care unit and wore the device in a modified backpack (Figure 7). The animal was tethered within a pen and able to freely stand, lay and move its head during the study. Prophylactic antibiotics were given every 8 hours (25 mg/kg cephazolin) and an analgesic (1 mg/kg flunixin megulmin) was administered as needed. Mean arterial pressure (MAP), central venous pressure (CVP) and heart rate were recorded hourly. ACT was measured at least every 8 hours post-operatively, and more frequently when heparin titration was required.

Figure 7 Study Animal Wearing the ModELAS

CO_2 removal rate (vCO_2) was measured daily and is reported as the average of 10 minutes of data collected at a sampling frequency of 2 Hz. Reported vCO_2 was collected at a sufficiently high sweep gas flow rate (Q_{SG}) that the vCO_2 was not a function of sweep gas flow rate. The vCO_2 was measured as the fraction of CO_2 in the outlet sweep gas (F_{co2}) (WMA-4 Analyzer, PP Systems, Amesbury, MA). The CO_2 removal rate (vCO_2) was calculated according to equation 4-1 and normalized to an inlet pCO_2 of 45 mmHg according to equation 4-2:[112]

$$vCO_2 = Q_{SG}F_{CO2} \tag{4-1}$$

$$vCO_2^* = vCO_2 \frac{45\ \text{mmHg}}{P_{CO2}^{Inlet}} \tag{4-2}$$

The inlet pCO_2 (P_{CO2}^{Inlet}) used to normalize the vCO_2 is the average of the device inlet pCO_2 taken immediately before and after data collection (P_{CO2}^{Inlet}). During periods of low HCT (below 18%) device inlet pCO_2 was only taken prior to data collection.

Plasma free hemoglobin (pfHb), blood chemistry and complete blood count (CBC) were measured pre-operatively and post-operatively on pre-operative days 6 and 1, and on POD 0, 1, 3, 6, and 7. The blood sampling schedule was modified if HCT was below 18% in order to reduce the number of blood draws. The reported pre-operative measurements are an average of data from both pre-operative days. POD 0 data is an average of samples taken when the arterial line was placed, initiation of extracorporeal blood flow and 4 hours post-operatively. PfHb and platelet activation were measured using previously described methods.[102,123,124] Blood chemistry, manual platelet count and CBC were measured by an external lab (IDEXX Laboratories, Inc., Westbrook, ME). Liver and kidney function and tissue injury were monitored by aspartate transferase (AST), alanine transferase (ALT), alkaline phosphatase (ALP), blood urea nitrogen (BUN), creatinine, and creatine kinase (CK). Platelet activation was measured via flow cytometry as previously reported.[123,124] Platelet function was quantified by activating platelets with platelet activating factor (PAF).

Blood chemistry, platelet count and CBC samples were not drawn on POD 6 for Trials 3 and 6 due to low hematocrit. The blood chemistry for Trial 4, pre-operative day 6 and manual platelet count for Trial 6, preoperative day 1 and POD 1 and 3 were not measured due to a technical oversight.

4.2.1 Statistical Analysis

Data points were averaged across studies for each POD and are reported as the average ± standard deviation. Statistical analysis was completed using IBM SPSS (IBM Corporation, North Castle, NY). Due to instances of missing data previously described, the statistical analysis was completed using a mixed linear model analysis of variance and the restricted maximum likelihood estimation method.[125] Raw extracorporeal blood flow rate, motor torque, heart rate, CD62P expression, creatinine, CK, ALT and BUN data violated the assumption of normality based on the Kolmogorov–Smirnov test and were normalized[126] prior to statistical evaluation. For those comparisons in which time had a significant effect, pairwise comparisons were conducted using least significant difference analysis. Statistical significance was considered at $p<0.05$.

4.3 Results

All animals were successfully recovered post-implant and five studies were electively terminated on POD 7. Trial 4 was terminated early on POD 4 due to low MAP and an elevated lactate level. The necropsy showed significant pulmonary emboli within both lungs. Histopathological examination of the pulmonary emboli demonstrated that the initial emboli likely occurred several days prior to the end of study. On POD 1 of Trial 4 the extracorporeal blood flow rate was 0.0 L/min for approximately 1 hour. The device inflow tubing was clamped off while saline was forced through the device outflow tubing and this returned blood flow to 0.5 L/min. Significant anemia was observed during Trial 3 due to a non-study related hematoma within the right scapular/axillary region. No thrombus or free fluid was evident within the chest or

pericardium, thus the scapular hematoma was likely due to accidental trauma to the shoulder. Trial 5 was terminated approximately 3 hours prior to the planned end of study due to a fractured positive pressure port on the device used to measure bundle inlet pressure on the prototype device. Significant blood loss through the fractured port necessitated rapid euthanasia and POD 7 bloodwork and gas exchange data was not collected.

Figure 8 provides average extracorporeal blood flow rate and vCO_2. Average blood flow rate across all trials was 0.48 ± 0.01 L/min and did not vary significantly over the course of the 7 days ($p = 0.338$). Average CO_2 removal (normalized to an inlet of 45 mmHg) across all trials and time points was 75.6 ± 4.7 mL/min. Daily average vCO_2 did not vary significantly from POD 0 ($p = 0.233$). The average device inlet pCO_2 was 43.6 ± 1.1 mmHg. The device inlet pCO_2 values measured before and after the vCO_2 data collection did not deviate by greater than 15%. MAP, CVP, and heart rate did not significantly change from POD 0 (Table 3). Table 4 provides pre-operative and post-operative animal hematologic parameters used to evaluate end organ function and hemocompatibility. Platelet function and activation did not statistically change from pre-operative values. BUN statistically increased on POD 6 prior to returning to pre-operative values on POD 7. HCT post-operatively was statistically less than pre-operative measurements. Post-operative pfHb remained below 25 mg/dL with the exception of POD 3 - 5 of Trial 2 prior to returning to a normal level on POD 7 (Figure 9). This animal showed signs of an acute kidney injury on POD 4 which resolved on POD 6. Macroscopic and microscopic examination showed no abnormalities or damage to the heart, lungs, liver, kidneys or spleen, except Trial 4 which exhibited signs of a pulmonary embolism.

The explanted device from Trial 2 had thrombus at the bottom pivot of the impeller and within the bundle (Figure 10). During this trial the ACTs were below the target range for a quarter of the study. All other explanted devices were free of significant thrombus.

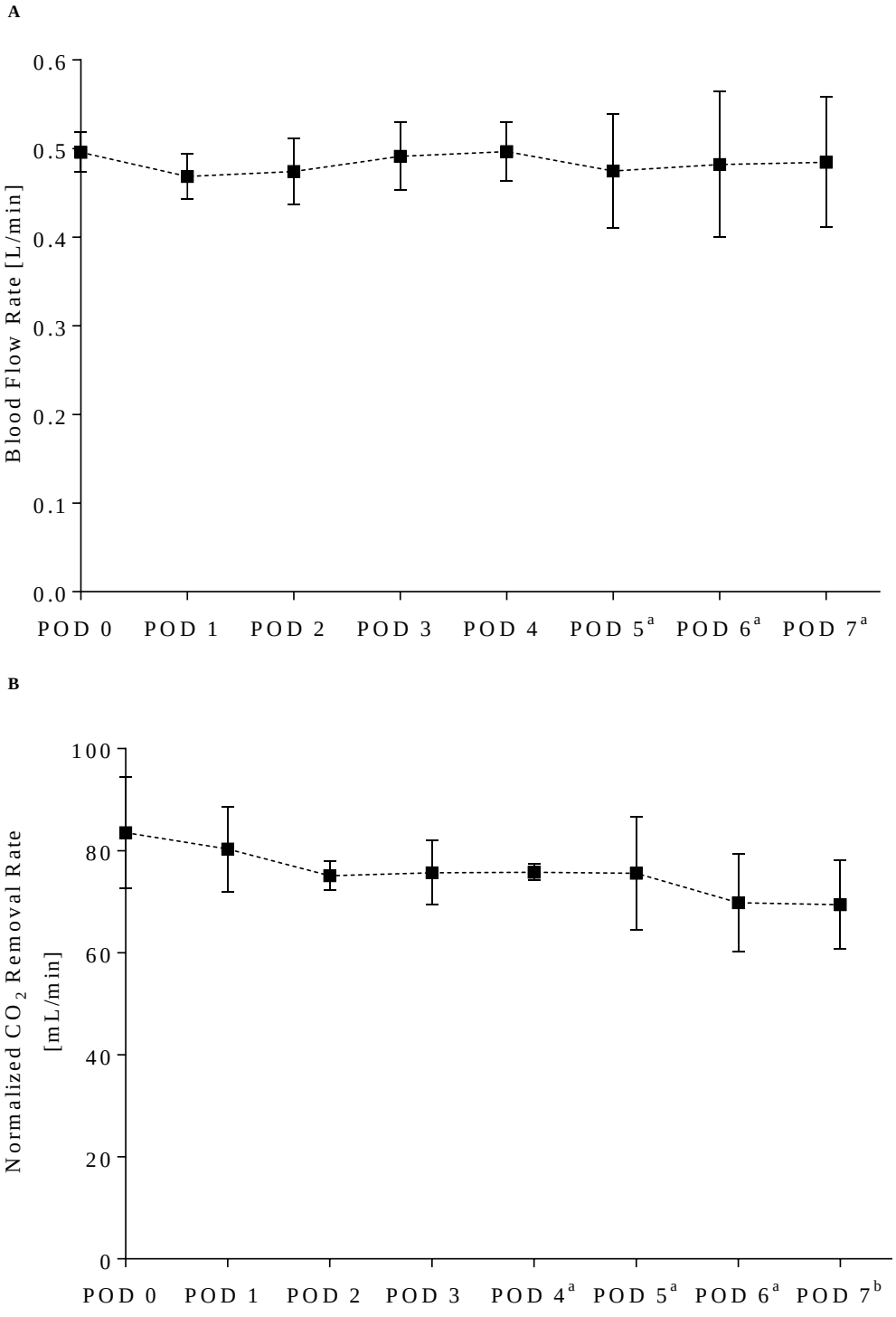

Figure 8 Extracorporeal Blood Flow Rate and CO_2 Removal Rate

Daily extracorporeal blood flow rate (A) and normalized CO_2 removal rate (B). When compared to POD 0 data neither parameter significantly changed over duration of the study ($p>0.05$). [a]n=5, [b] n=4.

Table 3 Hemodynamic and Device Parameters

	POD 0	POD 1	POD 2	POD 3	POD 4	POD 5 †	POD 6 †	POD 7 †
MAP[mmHg]	91 ± 5	91 ± 7	89 ± 7	93 ± 5	96 ± 8	104 ± 5*	100 ± 7*	96 ± 7
CVP [mmHg]	-1 ± 2	-2 ± 2	-2 ± 2	-2 ± 1	-1 ± 2	-3 ± 2	-1 ± 3	-2 ± 2
HR [BPM]	94 ± 2	85 ± 13	92 ± 23	107 ± 25	124 ± 31*	111 ± 19	119 ± 27	119 ± 44
Speed [RPM]	1208 ± 80	1212 ± 47	1223 ± 54	1231 ± 53	1225 ± 54	1228 ± 59	1227 ± 62	1227 ± 60
Torque[mN-m]	10 ± 1	10 ± 1	10 ± 1	10 ± 1	10 ± 1	10 ± 2	10 ± 2	11 ± 3

*Statistically significant compared to POD 0 ($p<0.05$), † Trial 4 data no collected due to early termination

Table 4 Hematologic and End Organ Parameters

	Pre-op	POD 0	POD 1†	POD 3‡	POD 6§	POD 7‖,**
PAF Activated [%]	71 ± 9	70 ± 10	77 ± 11	72 ± 11	75 ± 12	76 ± 3
CD62P [%]	3 ± 1	4 ± 2	2 ± 1	5 ± 5	5 ± 3	4 ± 2
Platelet Count [k/μL]	576 ± 252	397 ± 110	499 ± 186	703 ± 281	520 ± 115	552 ± 198
WBC [K/μL]	8.6 ± 3	6.7 ± 2	12.3 ± 4	11.5 ± 4	12.2 ± 5	11.9 ± 1.7*
HCT [%]	36 ± 3	24 ± 2*	29 ± 2*	27 ± 6*	24 ± 4*	27 ± 7*
End Organ Status						
Creatinine [mg/dL]	1 ± 0	1 ± 0	2 ± 1	3 ± 3	1 ± 0	1 ± 0
BUN [mg/dL]	11 ± 2	11 ± 3	11 ± 5	27 ± 21	26 ± 16*	14 ± 4
CK [U/L]	103 ± 23	155 ± 51	143 ± 72	71 ± 11	149 ± 88	126 ± 80
ALT [U/L]	12 ± 5	9 ± 3	9 ± 4	5 ± 3	5 ± 2	5 ± 5
AST [U/L]	71 ± 14	58 ± 11	73 ± 19	56 ± 10	53 ± 12	59 ± 9
ALP [U/L]	218 ± 56	165 ± 55	158 ± 41	141 ± 33	101 ± 26	128 ± 64

† Missing platelet count from Trial 6; ‡ Missing platelet count from Trials 2, 5, 6; § Missing all data, except HCT, for Trials 3, 4, 6; ‖ Missing all data, except HCT, for Trials 4, 5; ** Missing CD62P and PAF Activated for Trial 3;
*Statistically significant compared to pre-op value ($p<0.05$);

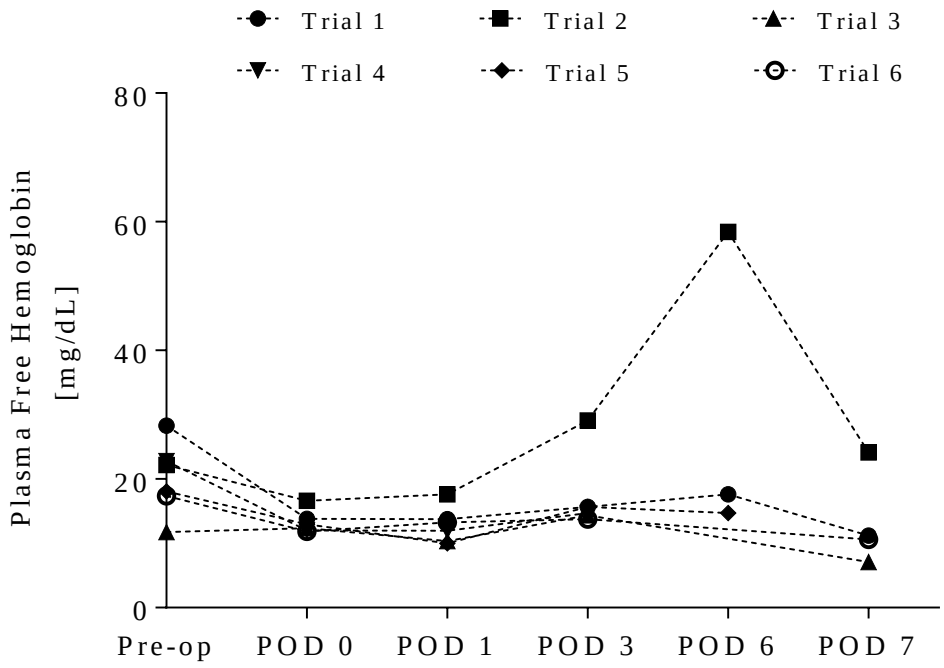

Figure 9 In Vivo Plasma Free Hemoglobin of the ECCO$_2$R ModELAS

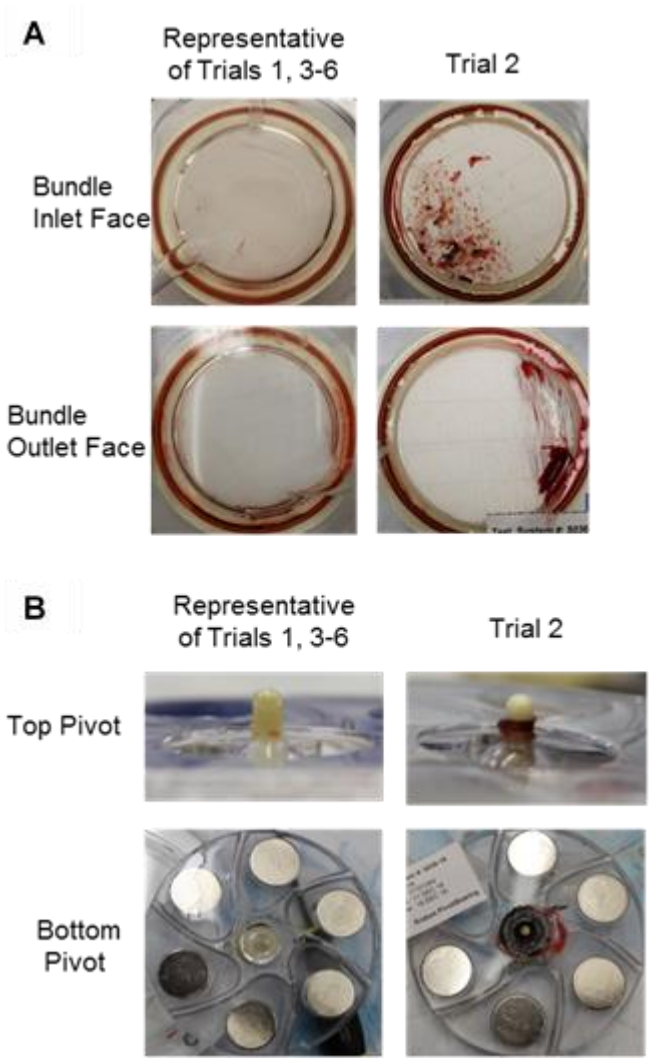

Figure 10 Explanted Bundle and Impeller

Images of the explanted hollow fiber membrane bundle inlet (top row) and outlet (bottom row) faces and the (B) impeller top (top row) and bottom (bottom row) pivots. The Trial 2 (right) bundle and pivots had significant thrombus formation due to low ACT. All other trials were free of significant thrombi (left).

4.4 Discussion

The Modular Extracorporeal Lung Assist System (ModELAS) is an integrated, modular pump-lung capable of providing three levels of respiratory assistance. Selection of the cannula and hollow fiber membrane bundle configures the ModELAS for pediatric complete respiratory assist, adult complete respiratory assist or adult low-flow CO_2 removal. The adult and pediatric complete respiratory assist applications have been evaluated in animals for up to 7-days, and are currently undergoing 30-day animal studies.[83,121,122] The present study evaluated the performance and hemocompatibility of the low-flow CO_2 removal ModELAS in a healthy ovine model for 7 days. All animals were successfully recovered from the surgery and a single trial required early termination on POD 4. No device exchanges were required.

Clinical evidence demonstrating the benefits of low-flow $ECCO_2R$ in ae-COPD and moderate ARDS patients continues to grow. The VENT-AVOID (ClinicalTrials.gov Identifier: NCT03255057) and REST (ClinicalTrials.gov Identifier: NCT02654327) randomized clinical trials aim to further expand the clinical evidence of using VV-$ECCO_2R$ as an alternative to invasive mechanical ventilation or in conjunction with low tidal volume ventilation, respectively. Lung protective ventilation, which utilizes low tidal volumes, can fail due to hypercapnia and require transitioning patients to invasive mechanical ventilation which is known to cause VILI. The CO_2 removal capabilities of $ECCO_2R$ can resolve the hypercapnia during lung protective ventilation, and in some instances allow extubation and NIV.[17,18,40,90,91] In addition, the low extracorporeal blood flow rate of $ECCO_2R$, typically less than 1 L/min, makes the technology less invasive compared to ECMO.

The ModELAS was generally well tolerated by the animals. These preclinical studies indicate that the low-flow $ECCO_2R$ configured ModELAS can operate for 7 days without

diminished CO_2R performance nor significant damage to blood or end organs. The average vCO_2 was 75.6 mL/min and the vCO_2 on POD 7 was 83% of that on POD 0. Platelet and organ function parameters used to evaluate device safety did not significantly change during the study (Table 1). Except Trial 4, macroscopic and histopathological evaluation of the end organs did not indicate any device related pathology. Low HCT resulting from a shoulder hematoma (Trial 3), pulmonary embolism (Trial 4) and subcutaneous bleeding (Trial 5) resulted in slightly diminished CO_2 removal rates [116] and increased blood flow rates during the latter half of the study. Pre-operative pfHb samples were drawn via a venous puncture, and are therefore slightly elevated. A single study (Trial 2) had elevated pfHb measurements greater than the 40 – 50 mg/dL clinically relevant threshold [114,127,128]. The maximum pfHb value occurred on POD 6 before decreasing on POD 7. The elevated pfHb was not associated with any hematuria. Trial 2 is also the sole trial in which the explanted device contained significant thrombus at the pivot bearing, likely caused by periods of improperly concentrated heparin infusion solutions. The thrombus and subsequent friction at the pivot bearing are a possible contributors to the elevated pfHb. In addition, just prior to this period of elevated pfHb the animal displayed symptoms of an acute kidney injury. The combination of the pivot thrombus and the kidney injury likely caused the sharp increase in pfHb in Trial 2. Elevated pfHb was isolated to one out of the six studies, rather than a trend, and is not indicative of significant safety concerns.

The most significant device related adverse event was a pulmonary embolism during Trial 4. This trial required early termination on POD 4 due to low MAP and elevated heart rate and blood lactate concentration. The root cause of these symptoms was an acute pulmonary embolism in both lungs. This thrombus initiated several days prior to the end of study based on histopatholigical examination of the thrombus organization. Thromboembolism is a known risk of

connecting any device to the vasculature including current artificial lungs[129,130] and ventricular assist devices [131,132]. In preclinical testing, the key is to differentiate whether the thromboembolism is inherent to the device design, or was independent of the device used. The densely packed hollow fiber membrane bundle of the ModELAS acts as a filter, hence it is unlikely that the thrombus was generated within the pump and migrated post-device. Thus, the precipitating thrombus likely originated between the outlet of the device and the cannula tip and was dislodged on POD 1 with the saline flush. The exact cause of the original thrombus remains unknown, however it does not appear to be characteristic of the device. The entire ModELAS circuit is also uncoated, whereas most commercial artificial lungs circuits are coated with a biocompatible coating.[39,108] Our laboratory is currently developing a tip-to-tip zwitterionic surface coating which will further improve hemocompatibility and further deter any thrombosis within the ModELAS circuit.[133]

The most relevant comparison to the $ECCO_2R$ ModELAS is the Hemolung RAS (ALung Technologies, Pittsburgh, PA) which is currently undergoing an FDA clinical trial (VENT-AVIOD) to evaluate the use of the Hemolung RAS as an alternative or supplement to invasive MV in ae-COPD patients. The Hemolung RAS is also a part of the REST trial in the UK which is assessing the use of VV-$ECCO_2R$ in conjunction with lung protective ventilation in ARDS patients. The Hemolung utilizes a rotating core to induce active mixing within the annular bundle (0.59 m^2). In pre-clinical healthy ovine studies, the Hemolung achieved 42 – 53 mL/min of CO_2 removal and blood flow rates between 350 and 450 mL/min.[114] The ModELAS CO_2 removal rate ranged from 69 - 84 mL/min at blood flow rates ranging between 430 – 590 mL/min. The improved vCO_2 in the ModELAS could be a result of slightly higher blood flow rates and bundle surface area (0.65 m^2). Neither the ModELAS nor the Hemolung had apparent adverse effects on hemodynamics or end organ function. The ModELAS performed comparatively to the Hemolung,

with the additional benefit of being designed as a wearable unit and capable of a wider range of therapies.

4.5 Conclusion

The ModELAS is a platform respiratory assist technology designed to provide adult or pediatric complete respiratory assist, or adult low-flow CO_2 removal. The device has been extensively tested in vitro at all three respiratory assist levels[83,84,112] and the complete respiratory assist applications have been evaluated in animals.[121,122] This series of 7-day studies in healthy, awake sheep provides in vivo evaluation of the low-flow CO_2 removal ModELAS. These studies demonstrated that the ModELAS can consistently remove a clinically relevant amount of CO_2 without causing detrimental effects on the animal. The ModELAS was well tolerated by the animals with only isolated device related events. In addition to developing a zwitterionic biocompatible coating to potentially afford reduction in the required anticoagulation[133], future work involves developing the controller into a compact, wearable unit with incorporated feedback controls and an intuitive user interface.

5.0 Acute In Vivo Performance of the Pediatric ModELAS

The following chapter presents work peer-reviewed and published in the American Society for Artificial Internal Organs Journal.

5.1 Introduction

Chronic lung diseases such as cystic fibrosis, pulmonary hypertension and pulmonary fibrosis continue to be sources of pediatric morbidity and mortality. These patients often require a heart or heart-lung transplant, however the waitlist duration is typically 1 – 6 months.[63] Mechanical ventilation (MV) and extracorporeal membrane oxygenation (ECMO) can be used to provide respiratory support to these patients as a bridge-to-transplant. Between 2009 and 2015, the number of pediatric extracorporeal respiratory support cases reported to the Extracorporeal Life Support Organization (ELSO) increased by 48% (569 cases in 2015).[134] Both MV and ECMO however are often considered contraindications pre-transplant. MV can result in ventilator induced lung injury[2] and the complex circuitry of current ECMO devices can lead to complications. In one study, up to 36% of the pediatric ECMO cases exhibited circuit complications.[135] Recent advancements in ECMO therapy including polymethylpentene fibers, heparin coatings, centrifugal pumps and portability has led to the reevaluation of ECMO pre-transplant.[136]

Recent efforts have focused on improving the portability of ECMO circuits in order to improve patient mobility. The immobilization of patients on MV or ECMO can lead to muscular deconditioning and poor post-transplant outcomes. Several centers have demonstrated improved

post-transplant outcomes in patients who were able to ambulate while on ECMO.[71,72,75] One of the current barriers to ambulatory ECMO is the complexity of the ECMO circuit and need for a specialized, highly coordinated team effort during patient ambulation. Thus, current efforts aim to design ECMO units specific to pediatric needs that also allow for simpler and less risky patient ambulation within the hospital.

We are currently developing the Pittsburgh Pediatric Ambulatory Lung (P-PAL) and its second generation device, the Pediatric ModELAS (P-ModELAS), as an ambulatory artificial lung for long-term respiratory support.[84] The P-PAL improves compactness and decreases complexity by integrating the oxygenator and pump into a single wearable unit. The device could be worn by either the patient or a caregiver. In the present study, we evaluated the in vivo performance of the P-PAL in an acute ovine model. In vivo gas transfer and hemolysis were measured in addition to animal hemodynamics. Additionally, we developed and refined our surgical and cannulation strategy in preparation for chronic, recovery studies.

5.2 Methods

5.2.1 Device Description

The P-PAL is an integrated pump-lung designed for respiratory support of pediatric patients and is ultimately intended to provide long-term (1 – 3 months) support. The device is intended to be operated at blood flow rates of 1 – 2.5 L/min and provide up to 90% of the respiratory support of 5 -25 kg children. This represents an oxygenation rate of 30 – 105 mL/min. Blood is drawn from the right atrium and pumped through a polymethylpentene HFM bundle (0.3

m^2) by an integrated centrifugal pump. Oxygenated blood is then returned to the pulmonary artery via an arterial cannula.

Two slightly different P-PAL design iterations were used during the acute trials. Trials 1 - 4 used the previously described P-PAL design (subsequently referred to as P-PAL).[84] Trials 5 and 6 were conducted with a second generation design (P-ModELAS and shown in Figure 11). The P-ModELAS centrifugal pump and HFM bundle are identical to that used in the P-PAL. The primary difference between the designs is a shortened blood flow channel leading from the pump compartment to the bundle compartment in the P-ModELAS. This change allows for easier priming and a more compact overall device. The priming volume of the P-ModELAS circuit was 270 mL. Excess acrylic was also removed from the device housing in the P-ModELAS. This reduced the mass of the device from 1157 g to 721 g. The in vitro pump performance, gas transfer and hemolysis results of the P-PAL have been previously published.[84] Benchtop pump and gas transfer performance were equivalent between the two versions.

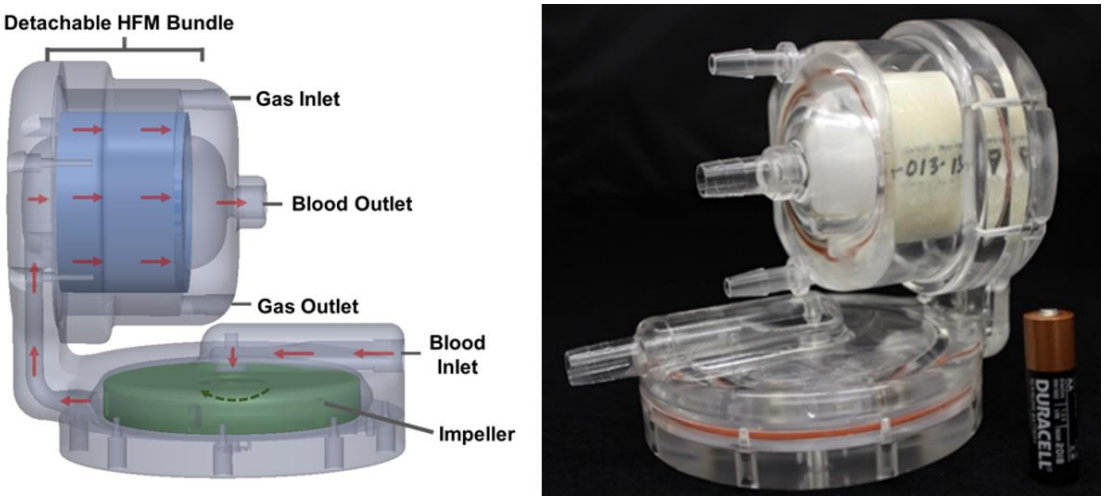

Figure 11 Schematic and Photograph of the P-ModELAS

5.2.2 Acute In Vivo Testing

Animal hemodynamics, gas exchange performance, and biocompatibility were evaluated in an acute (4 – 6 hours) ovine model. Sheep (n=6) weight ranged from 23.3 to 32.2 kg. All trials were completed in the Center for Preclinical Studies at the McGowan Institute and all animals received humane care. The University of Pittsburgh's Institutional Animal Care and Use Committee approved the protocol for animal care and surgery.

Anesthesia was induced by a subcutaneous injection of atropine (0.05 mg/kg) followed by intravenous administration of ketamine (3.9 – 5.3 mg/kg). Animals were directly intubated with a cuffed Magill endotracheal tube. Anesthesia was maintained throughout the study via isoflurane inhalation (1.5 – 3 %) to effect. An arterial line was placed in the carotid artery to monitor mean arterial pressure (MAP). A venous line was placed in the jugular vein to monitor central venous pressure (CVP) and provided access for maintenance drips. Access to the right atrium and pulmonary artery was made via a right (Trials 1 – 2) or left (Trials 3 – 6) thoracotomy. A pressure monitoring line was placed in the pulmonary artery (Trials 2 – 6) to monitor pulmonary artery pressure (PAP). Heart rate, MAP, CVP and PAP were recorded every 15 minutes. Prior to cannula placement a heparin bolus (300 IU/kg) was administered to increase the activated clotting time (ACT) to greater than twice baseline to prevent clot formation in the cannulas prior to starting the pump. The venous cannula was placed in the right atrium and the arterial cannula was placed in the pulmonary artery. The ACT target for the duration of the study was 1.5 – 2 times baseline. Heparin was continuously administered through the venous line and the infusion rate periodically altered to maintain the target ACT range.

The cannulas were connected to a primed (1 IU/mL heparinized saline) P-PAL device. After the P-PAL pump was started and flow initiated, a stabilization period of at least 10 minutes

was permitted prior to the commencement of gas exchange sampling. A 5% CO_2 95% O_2 sweep gas mixture was set to 3 – 5 L/min. The P-PAL impeller rotation rate was varied in order to attain each targeted blood flow rate (1.0, 1.5, 2.0, 2.5 L/min) during three repeated measurements. Blood gas tensions and hematocrit were measured from device inlet and outlet samples. Plasma free hemoglobin was measured from blood samples taken from the arterial line. Methods for spectrophotometrically measuring plasma free hemoglobin have been previously published.[102] Additional blood samples were routinely taken from the arterial line in order to monitor the animal's arterial blood gas tensions, electrolytes and hematocrit. Ventilator settings (FiO_2, PEEP and rate) were adjusted to maintain normal physiologic arterial blood gases. Pressure drop across the bundle was measured continuously (PCU-2000, Millar, Texas).

At the completion of the study, the heart and lungs were examined for gross abnormalities. The device was disconnected and saline was passively flowed through the device to wash away blood while preserving any intra-device thrombus. The device was disassembled, and any thrombus formation was noted. The inlet and outlet faces of the HFM bundle were photographed.

5.2.3 Statistical Analysis

Statistical analysis was conducted in SPSS (IBM, Armonk, NY). Results are reported as an average and standard deviation. The baseline and final MAP, CVP and heart rate were compared using a paired samples t-test per animal. The baseline MAP, CVP and heart rate are an average of vital signs recorded during the 30 minutes prior to initiation of device blood flow. The final MAP, CVP and heartrate are an average of the vital signs taken during the final hour of the study. Vital signs were recorded every 10 – 15 minutes. Statistical analysis was not performed on the PAP due to a lack of repeated measurements. A two-way ANOVA was used to evaluate the effect of device

type (P-PAL versus P-ModELAS). Differences were considered statistically significant for $p < 0.05$.

5.3 Results

All studies were electively terminated following the completion of data collection. Table 5 provides a comprehensive summary of each trial. The ACT range throughout the studies was 1.2 – 4.1 times baseline. The blood flow rate range for Trial 2 was limited to 1.0 – 1.4 L/min due to a venous cannula occlusion resulting in suction and limited blood flow at higher impeller rotation rates. The necropsy following Trial 2 revealed right atrium bruising indicative of cannula suction at the right atrium wall. Subsequent trials utilized a right thoracotomy to gain improved access to the heart and placement of the cannula at the main wall of the right atrium. In Trial 4, thrombus formed in the HFM bundle and subsequently led to decreased oxygen transfer and device blood flow rate. The bundle resistance increased from 11 mmHg/L/min to 120 mmHg/L/min by the end of the study. Visual inspection of the bundle showed thrombus formation within ~25% of the bundle (Figure 12). All other trials were completed without complication.

Table 5 Summary of Acute Pediatric Trials

Trial No.	Cannula Type	Implant Procedure	Device	Flow Rate [L/min]	Duration [hr]	Comment
1	18 Fr Straight (ven)[1] 16 Fr Straight (art)[2]	Left Thoracotomy	P-PAL	1.0-2.5	4.5	-
2	22 Fr Right Angle (ven)[3] 16 Fr Straight (art)[2]	Left Thoracotomy	P-PAL	1.0-1.4	4	Flow Limitation (ven cannula occlusion)
3	22 Fr Right Angle (ven)[3] 16 Fr Straight (art)[2]	Right Thoracotomy	P-PAL	1.0-2.5	6	-
4	22 Fr Right Angle (ven)[3] 16 Fr Straight (art)[2]	Right Thoracotomy	P-PAL	1.0-2.4	6	Device Failure (↑ bundle resistance)
5	22 Fr Right Angle Metal Tip (ven)[4] 18 Fr Straight (art)[5]	Right Thoracotomy	P-ModELAS	1.0-2.5	6	-
6	22 Fr Right Angle Metal Tip (ven)[4] 18 Fr Straight (art)[5]	Right Thoracotomy	P-ModELAS	1.0-2.5	6	-

[1]Medtroni DLP Single Stage Venous Cannula (#66118) [2]Medtronic DLP One-Piece Arterial Cannula (#77016) [3]Edwards Lifesciences Thin-Flex Single Stage Venous Drainage Cannula (VCS02290) [4]Medtronic DLP Single Stage Venous Cannula (#69322) [5]Medtronic Elongated One-Piece Arterial Cannula (EOPA) (#77518)

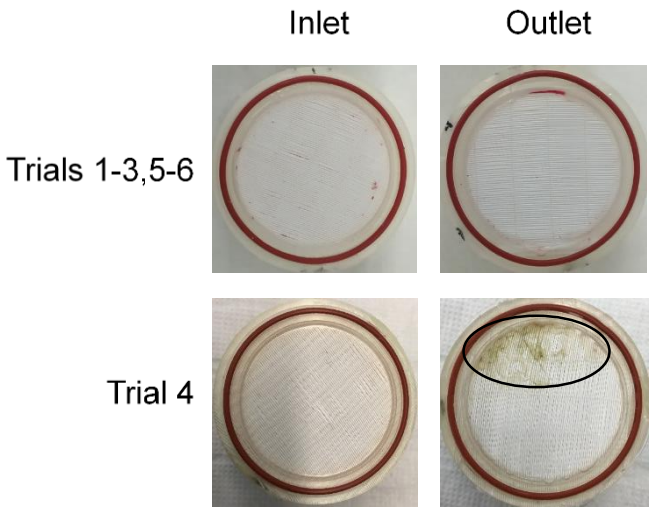

Figure 12 Photographs of a Explanted Bundle Faces

Typical inlet and outlet faces (*top row*) and that of Trial 4 (*bottom row*) at explant. Circle indicates area of clot formation.

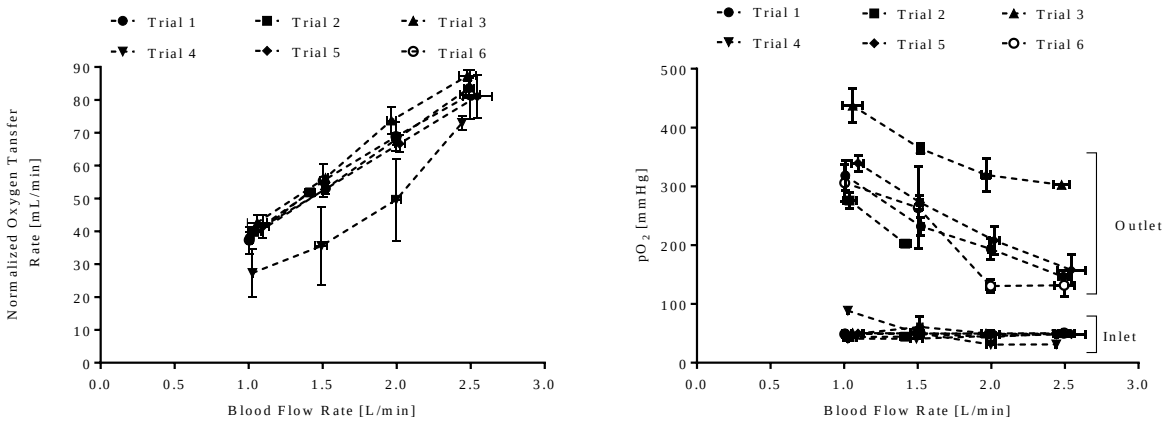

Figure 13 In Vivo Gas Transfer of the P-PAL

A maximum oxygen transfer rate of 83.7 ± 3.5 mL/min was achieved at 2.5 L/min (Figure 13). The average hemoglobin concentration across all trials was 6.2 ± 0.3 g/dL and the blood exiting the device was 100% saturated at all blood flow rates for all trials except Trial 4. There was no significant effect of device type (P-PAL versus P-ModELAS) on oxygenation rate ($p>0.05$).

Plasma free hemoglobin remained below 20 mg/dL for all trials (Figure 14). Post-study macroscopic inspection of the device flow paths, bearings and bundle revealed an absence of any significant thrombus for all trials except Trial 4. Figure 12 provides representative post-study photographs of the bundle inlet and outlet faces.

Table 6 summarizes animal hemodynamics at baseline (prior to cannulation) and at the end of the study. Heart rate was not affected by the device ($p > 0.05$) during any of the trials. MAP statistically decreased ($p < 0.05$) in Trial 2 (89 ± 5 mmHg to 64 ± 10 mmHg) and increased in Trial 3 (52 ± 6 mmHg to 58 ± 4 mmHg). CVP statistically decreased ($p < 0.05$) in Trial 4 (11 ± 2 mmHg to 7 ± 1 mmHg) to the average CVP of this series of studies. With the exception of cannula-related bruising described above for Trial 2, no device-related damage to the heart or lungs was observed upon necropsy.

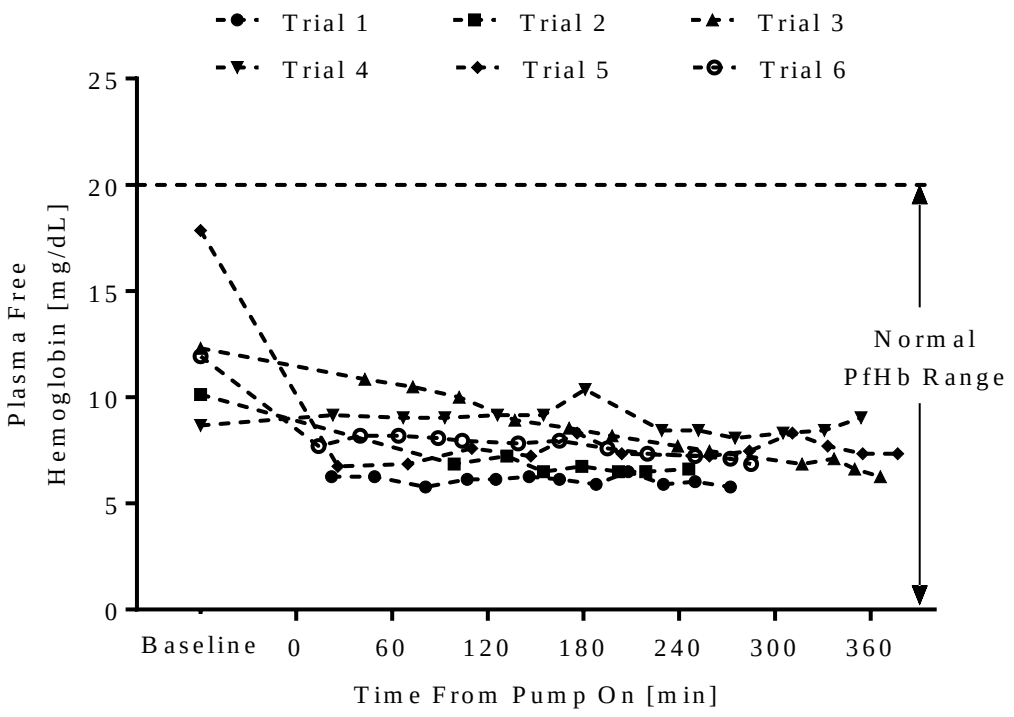

Figure 14 In Vivo Plasma-Free Hemoglobin Generated by the P-PAL

Table 6 Baseline and Final Animal Hemodynamics

	MAP [mmHg]		CVP [mmHg]		Heart Rate [beats/min]		PAP [mmHg]	
Trial No.	Baseline	Final	Baseline	Final	Baseline	Final	Baseline	Final
1	65 ± 5	54 ± 1.0	9 ± 2	9 ± 1	95 ± 13	88 ± 2	--	--
2	89 ± 5	64 ± 10*	8 ± 1	5 ± 1	81 ± 5	80 ± 1	17	18 ± 1
3	52 ± 6	58 ± 4*	6 ± 2	4 ± 1	94 ± 4	97 ± 2	18	21 ± 2
4	62 ± 14	53 ± 5	11 ± 2	7 ± 1*	93 ± 5	95 ± 8	11	11 ± 1
5	68 ± 15	49 ± 6	7 ± 2	5 ± 1	89 ± 15	102 ± 5	14	17 ± 1
6	61 ± 21	41 ± 1	5 ± 4	10 ± 1	92 ± 19	95 ± 1	12	15 ± 2

*$p<0.05$, considered significant between baseline and final values

5.4 Discussion

MV and ECMO are the primary treatment options for pediatric patients with lung failure. These treatments, however, greatly restrict patient mobility and MV can further lung injury. The ability to mobilize ECMO patients and increase their participation in physical therapy pre-transplant has been shown to improve post-transplant outcomes.[71,72,75] The P-PAL is specifically designed as a wearable, long-term respiratory assist device. The integration of the pump and oxygenator into a highly compact unit creates a less complex circuit to allow simplified, in-hospital patient ambulation. Previous in vitro work has demonstrated sufficient pumping, gas exchange, and hemolysis performance.[84] The present study used a healthy ovine model to evaluate the acute in vivo performance of the P-PAL as well as develop an optimal implantation strategy. Results demonstrated successful performance of the P-PAL in an acute support setting and established the surgical and implantation techniques needed for chronic, recovery studies.

Current pediatric ECMO devices are multicomponent systems connected via lengths of tubing. These complex and cumbersome circuits require highly trained teams during patient ambulation and the risk of device or circuit malfunction is elevated. Thus, current research efforts have shifted toward the development of compact respiratory support systems that could be worn paracorporeally and enable patient mobility. The University of Maryland is developing the Pediatric Pump Lung (PediPL) as an ambulatory ECMO device.[82,137] The PediPL integrates a centrifugal pump utilizing a magnetically levitated impeller with an annular HFM bundle. The PediPL has exhibited positive in vitro and in vivo results but has not progressed to clinical use as of yet. These efforts highlight the need for ambulatory respiratory support devices and the importance of the continued development necessary for their safe and effective use in patients.

The P-PAL demonstrated consistent oxygenation and pumping performance in an acute support setting. Blood flow limitation due to venous cannula inlet occlusion during Trial 2 led to a modified cannula placement technique via a right thoracotomy. In all subsequent trials, the P-PAL was able to generate the full range of targeted blood flow rates (1 – 2.5 L/min). The P-PAL device used during Trial 4 developed diffuse intra-bundle thrombus during the study duration. The thrombus formation resulted in progressive bundle resistance increase and oxygen transfer decrease during support. This was an isolated occurrence and is suspected to have originated from inadequate device priming prior to the implant. Previous computational work has predicted spatially uniform blood flow through the P-PAL HFM bundle[84] and all other trials in the current work resulted in an HFM bundle remarkably free of thrombus. With the exception of Trial 4, the P-PAL achieved full blood oxygen saturation at all evaluated blood flow rates. In vivo oxygen transfer rates were limited by low hemoglobin concentrations and thus are not representative of the full oxygenation capability of the device. The intraoperative anemia observed in these acute studies is not uncommon and likely attributable to hemodilution and perioperative red blood cell sequestration. A return to more normal hemoglobin concentrations in the days following surgery is expected during longer-term P-PAL studies. As expected, there was no discernible difference in device performance between the two slightly different P-PAL design iterations used in this study. The evolution of the design was driven by a goal to attain a lighter device (P-ModELAS was 436 g lighter) that was easier to prime.

P-PAL support was generally well tolerated and exhibited minimal effects on normal physiological function. Although statistically significant changes in MAP and CVP occurred in some trials, no consistent or concerning trends were observed. Hemolysis was low during P-PAL support with plasma free hemoglobin concentrations remaining generally constant throughout

support and well below 20 mg/dL. Outside of one incident of slight bruising at the right atrium attributed to cannula suction, the native heart and lungs were free of gross abnormalities resulting from the device at the time of necropsy.

Surgical and cannulation methods were refined throughout this series of acute studies and led to an optimized implantation strategy to be used during longer-term recovery studies. Changing from a left to right thoracotomy allowed for better placement of the cannula into the main wall of the right atrium. The later trials using this approach (Trial 3 – 6) were free of complications arising from cannula suction within the right atrium. The cannulas used in Trials 5 and 6 enabled even further increased venous drainage and will ease tunneling of the cannulas during future chronic studies. Based on this series of acute studies, the cannulation strategy for upcoming long-term recovery studies will utilize a right thoracotomy to place a 22 Fr right angle venous cannula into the RA and an 18 Fr arterial cannula into the PA.

Although the Avalon DLC has popularized peripheral cannulation in adult ECMO patients, pediatric patients present unique challenges which may benefit from a central cannulation. A central cannulation is often preferred in pediatric patients due to concerns with patient cooperation, availability of appropriate cannula sizes and blood recirculation between the cannula inlet and outlet. Maeda et al. have recently published two cases where long-term pediatric ECMO patients initially cannulated peripherally required recannulation centrally.[80]

5.5 Conclusion

The P-PAL is a compact, integrated pump-lung designed for ambulatory respiratory support in children. Acute in vivo evaluation of the devices confirmed the sufficient gas transfer,

pumping and hemolysis performance demonstrated during benchtop studies. Additionally, acute respiratory support with the P-PAL using the final implant strategy showed no adverse effects on animal hemodynamics or the native cardiopulmonary system. Future work includes 7- and 30-day sheep studies to further characterize the performance and hemocompatibility of the P-ModELAS and its long-term effect on the cardiopulmonary system.

6.0 Chronic In Vivo Performance of the Pediatric ModELAS

Platelet activation studies were conducted by Sang-Ho Ye, Ph.D.

6.1 Introduction

ECMO and mechanical ventilation are used to bridge respiratory failure patients to lung transplant. Pediatric lung transplant recipients, however typically wait 1 – 6 months for a transplant after being listed.[63] During this waiting period, ECMO patients who participate in physical therapy, including ambulating within the ICU, have improved post-transplant outcomes.[72,75] Cannulation in these patients should therefore accommodate long-term, ambulatory support.

Arterio-venous and veno-venous ECMO cannulation strategies have both been employed in pediatric patients. The use of dual lumen cannulas is becoming popular in the adult ECMO population and is generally considered less invasive as it requires cannulation of a single vein. In pediatric ECMO patients, however, a central cannulation is often preferred over dual lumen cannulation at the neck.[80] This preference is due to patient cooperation, blood recirculation, and limited availability of appropriate dual lumen cannula sizes. Based on pediatric ECMO cases reported to the ELSO registry between 1998 and 2011, there is not a significant difference in survival to discharge between patients receiving multisite VV-cannulation and single site, dual lumen cannulation.[138]

To accommodate long-term support of potentially ambulatory patients, the P-ModELAS has been designed to be connected to the vasculature via the RA and PA. This cannulation strategy

is surgically more invasive than single site DLC cannulation, however it best meets the needs for ambulatory, pediatric ECMO. Previous work has demonstrated that the P-ModELAS meets design specifications in vitro,[84] and has shown that the device can be connected to sheep for up to 6 hours without complication.[121] The next step in the advancement of the P-ModELAS is to develop methods for recovering the animal post-thoracotomy. The objective of this series of 7-day studies was to establish post-operative anticoagulation management methods for animals following P-ModELAS implantation. Study success criteria was based on cessation of the chest tube output, animal survival and device free of thrombus. These 7-day studies represent the next step towards 30-day in vivo evaluation of the P-ModELAS.

6.2 Methods

6.2.1 7-Day In Vivo Testing

The P-ModELAS was evaluated for 7 days in juvenile Dorper or Hampshire sheep (n=3, 23.8 – 26.5 kg). These studies were completed at the McGowan Institute's Center for Preclinical Studies under a protocol approved by the University of Pittsburgh's Institutional Animal Care and Use Committee.

Anesthesia was induced via a subcutaneous injection of atropine (0.25 mg/kg) followed by an intravenous infusion of ketamine (4.0 mg/kg). Inhaled isoflurane was used to maintain anesthesia during the surgical procedure. A venous line was placed in the left jugular vein and an arterial line was placed in the left carotid artery via a surgical cut down. These lines were sutured

to the vessel and tunneled underneath the skin for additional securement. A baseline ACT blood sample was drawn from the arterial line prior to any heparin administration.

A right thoracotomy allowed access to the RA and PA. Prior to cannula placement a 150 IU/kg heparin bolus was given to increase the ACT to at least 300 seconds (ACT-II, Medtronic, Minneapolis, MN). When necessary additional 1000 IU heparin boluses were administered to increase the ACT to 300 s. A 22 Fr venous cannula (Medtronic DLP Single Stage (#69322)) was sutured into the RA and an 18 Fr arterial cannula (Medtronic EOPA (#77518)) was sutured into the PA. The cannulas were tunneled underneath the skin and connected to a primed device (1 IU/mL heparin in normal saline) and extracorporeal blood flow initiated. A chest tube was placed in the thoracic cavity and connected to a Pleur-Evac system.

Extracorporeal blood flow was started at 2 – 2.5 L/min. The pure oxygen sweep gas flow rate was initially set to 4 L/min. The chest was closed and the animals were recovered in the ICU. The animals remained in a stanchion for the duration of the study. The P-ModELAS was placed in a modified backpack, and secured to the left side of the animal via backpack straps. Tension cables were used to relieve the animal of a portion of the device weight. Nicardipine (0.5 mcg/kg/min initial rate) was titrated to maintain a MAP of 85 – 90 mmHg, an analgesic (1 mg/kg flunixin meglumine as needed) and an antibiotic (0.25 mg/kg cefazolin daily) were also administered.

Blood was drawn for pfHb, platelet activation, complete blood count and a blood chemistry panel. Baseline blood samples were drawn on pre-operative days 5 and 1. Post-operative blood work was scheduled for 4 post-operative days. The blood sampling schedule was altered if the hematocrit was below 18% to maintain animal welfare. Methods for pfHb and platelet activation measurements have been previously described in detail.[69,123] Complete blood counts and blood

chemistry panels were completed by an external laboratory (IDEXX Laboratories, Inc, Westbrook, ME). Chest tube output was measured hourly. Blood flow rate, motor torque, device RPM and animal hemodynamics (heart rate, MAP, CVP) were recorded hourly. Device inlet and outlet blood gas samples were taken to measure the oxygenation rate of the device daily unless low hematocrit required altering the schedule. The inlet blood gas parameters were used as the input parameters to a previously developed and validated mass transfer model to attain a predicted oxygenation rates.[84]

6.2.1.1 Post-Operative Anticoagulation

During Trial 1, the post-operative heparin infusion was immediately started and titrated to achieve an ACT target of 1.5 – 2 times the baseline ACT. The ACT was maintained via a continuous heparin infusion through the animal's venous line. The ACT was measured every 4 hours. During Trial 2, heparin was not administered post-operatively until the chest tube output rate had plateaued and transitioned to serous fluid. The continuous heparin infusion was then initiated at a rate of 15 IU/kg/hr and increased at this rate until the ACT reached 1.5 – 2 times the baseline value. During Trial 3, an initial post-operative continuous heparin infusion of 25 IU/kg/hr was started and held at this rate until the chest tube output stabilized and transitioned to serous fluid. The heparin infusion rate was then increased step-wise until the 1.5 – 2 times baseline ACT target was achieved. During Trials 2 and 3 ACT was not measured until the heparin infusion was started in Trial 2, or increased in Trial 3, to prevent anemia due to blood sampling. ACT was then measured every 4 – 6 hours unless low HCT required altering the schedule.

6.2.2 Statistical Analysis

Data is represented as the mean ± standard deviation. The reported mean represents the average of each trial's averaged data during the specified time range. Data was binned into groups of pre- and post-operative days in order for there to be a sufficient number of measurements to permit statistical analysis. This was required due to skipped or postponed blood sampling due to low hematocrit and the early termination of Trial 1.

Motor torque, extracorporeal blood flow rate, and the oxygenation rate had an unequal number of samples within each POD grouping due to the early termination of Trial 1. As a result these parameters were statistically analyzed using a mixed linear model ANOVA and utilized the restricted maximum likelihood estimation method.[125] Parameters which violated the assumption of normality based on the Kolmogorov-Smirnov Test for Normality were normalized prior to statistical evaluation.[126] All other parameters were evaluated using a repeated measures ANOVA with Bonferroni post-hoc analysis. Statistical analysis was completed using SPSS software (IBM, Armonk, NY). Differences were considered significant at $p < 0.05$.

6.3 Results

All animals were successfully recovered and stood post-implant. Trials 2 and 3 were electively terminated at the scheduled end of study on POD 7. Trial 1 required a blood transfusion on POD 3 due to anemia and early termination on POD 4 due to dyspnea and pain non-responsive to analgesia. Trial 3 required a device exchange within the first 3 hours of the study.

Table 7 provides the daily averages of animal hemodynamics and device parameters. The P-ModELAS was operated at impeller speeds between 1328 and 1508 RPM. Blood flow rate ranged from 1.9 ± 0.6 L/min to 2.4 L/min. Animal hemodynamics remained stable throughout the study. The oxygenation rate ranged from 95.5 mL/min to 105.3 mL/min, and did not significantly change over the course of the study ($p = 0.255$) (Figure 15). Blood exited the device at oxygen saturations ranging from 68.1% to 100% and inlet saturations ranged from 13.9% to 71.9%. The in vivo data was within 10% of the oxygenation rate predicted by the mass transfer model.

Table 7 Device and Hemodynamic Parameters

Parameter	**POD 0 - 1**	**POD 2 - 3**	**POD 4 -5**	**POD 6 -7[b]**
MAP [mmHg]	81 ± 3	80 ± 1	83 ± 6	80
CVP[a] [mmHg]	6	6	8	8
Heart Rate [BPM]	128 ± 19	147 ± 15	167 ± 22	165
Blood Flow Rate [L/min]	2 ± 0	2 ± 0	2 ± 1	2
Motor Torque [mN-m]	15 ± 4	13 ± 3	13 ± 3	14
Device Speed [RPM]	1499 ± 243	1379 ± 179	1328 ± 187	1328

[a]CVP not measured during Trial 1 (n=2); [b] Includes data for Trials 2 and 3 only (n=2)

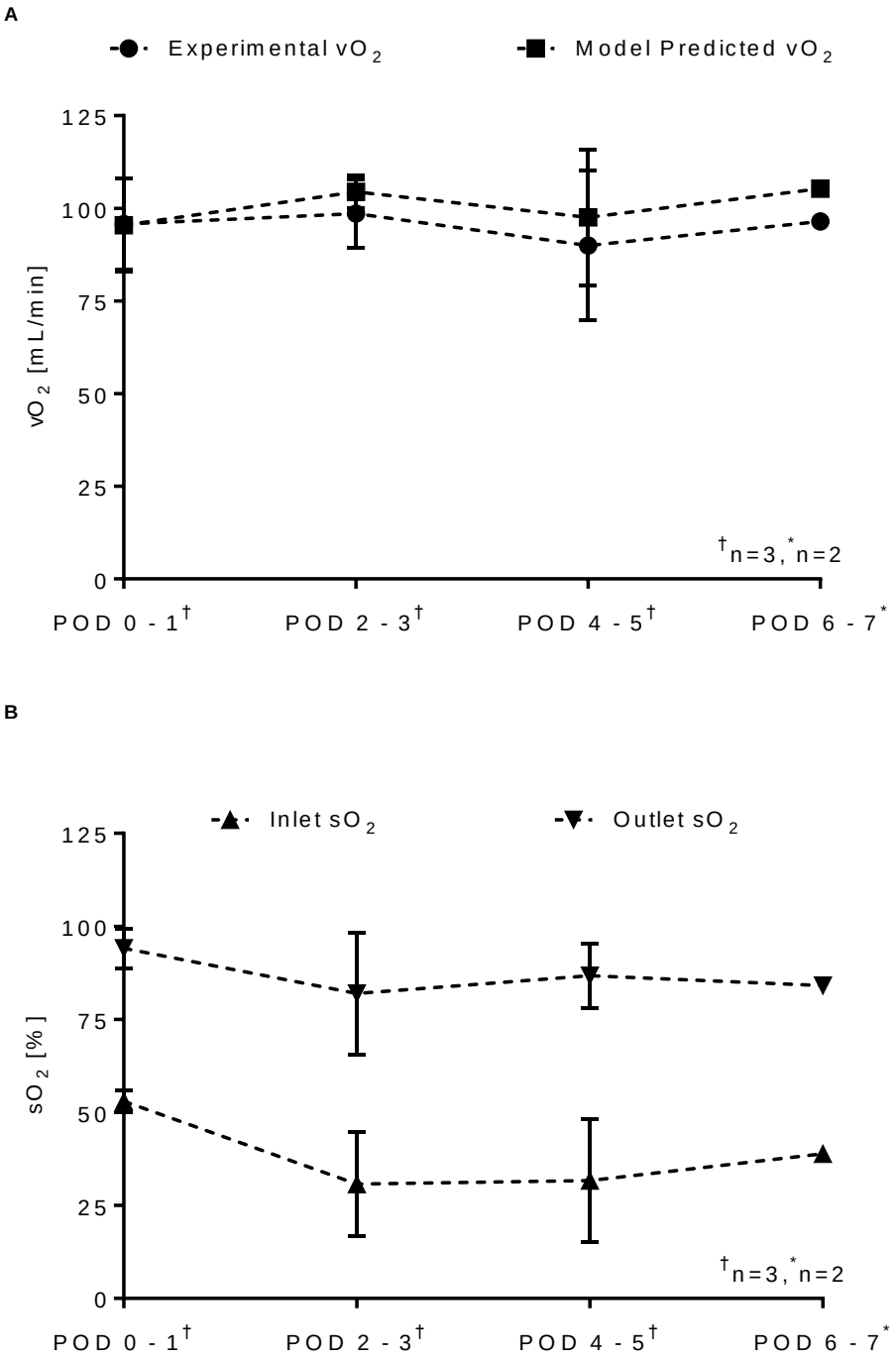

Figure 15 In Vivo Gas Transfer

(A) Average experimental and predicted oxygenation rate over the course of the study. (B) Device inlet and outlet blood oxygenation saturations

Post-operative average in vivo hemolysis was below 20 mg/dL (Table 8). There was no statistical increase from baseline (POD 0) hemolysis ($p = 0.052$). CD62P positive platelets remained below 22.6%, and those stimulated with platelet activating factor (PAF) showed increased activity of at least 74%. Platelet concentration was analyzed microscopically and ranged from 295 – 1048 K/µL. Liver (ALT and AST) and kidney (creatinine and BUN) biomarkers remained within the normal range for sheep and did not statistically change over the course of the study. The HFM bundle was free of thrombus after Trials 1 & 3, and contained a thrombus occluding ~30% of the bundle in Trial 2. Small thrombi were adhered to the bottom pivot of the impeller in all trials. All other aspects of the devices were free of thrombus.

Table 8 Hemodynamic and End Organ Parameters

Parameter	**Pre-Operative**	**POD 0 - 3[a]**	**POD 4 - 7[b]**
Hematocrit [%]	36 ± 2	24 ± 3*	21 ± 7
Platelet Count [K/µL]	711 ± 188	376 ± 22	845 ± 655
CD62-P [%]	5.2 ± 2.6	5.4 ± 1.9	17.2 ± 7.8
PAF Activated [%]	88.0 ± 2.9	74.5 ± 7.7	88.3 ± 3.0
WBC [k/µL]	8.2 ± 1.6	6.2 ± 2.3	16.9 ± 3.1
PfHb [mg/dL]	26.2 ± 8.0	13.9 ± 0.7	15.6 ± 3.2
ALT [U/L]	9 ± 7	8 ± 6	9 ± 9
AST [U/L]	88 ± 23	97 ± 35	77 ± 13
Creatine Kinase [U/L]	146 ± 46	1324 ± 625	140 ± 71
Blood Urea Nitrogen [mg/dL]	11 ± 2	11 ± 1	24 ± 23
Creatinine [mg/dL]	1 ± 0	1 ± 0	1 ± 1

[a] n=5; [b] n=4; *$p < 0.05$

The average total chest tube output was 1.1 ± 0.1 L. The chest tube output transitioned from blood to serous fluid on POD 1, and the output rate plateaued on POD 3 during all trials (Figure 16). A heparin pump malfunction on POD 1 of Trial 1 resulted in the ACT increasing to greater than 4 times the baseline value. Subsequently, 595 mL of fluid, primarily blood, was drained from the chest tube and an ACT of 1.5 times the baseline ACT was targeted for the remainder of the Trial 1 to prevent further bleeding. Trial 1 output transitioned back to serous fluid again on POD 3. During Trial 2, heparin was started 28 hours post-operatively and was within the 1.5 – 2 times baseline ACT range on POD 4. Increases in the heparin rate of Trial 3 were made starting on POD 3 and the ACT reached the targeted 1.5 – 2 times baseline ACT range on POD 5.

During the necropsy of Trial 1, approximately 1200 mL of blood was removed from the thoracic cavity. No source of the bleeding was identified. Adhesions were noted between the heart and sternal area and between the right lung and the heart. The right lung positioning was more dorsal than normal and showed diffuse atelectasis. Histopathological analysis of the lungs contained moderate to severe areas of hemorrhage, fibrin deposition and interstitial pneumonia. Both kidneys contained small infarcts and both medulla areas were hemorrhagic. Atelectasis of the right lung was present in Trials 2 and 3 and can be attributed to surgical manipulation. Upon the necropsy of Trial 3, widespread fungal growth was identified throughout the thoracic cavity and 150 mL of sero-hemorrhagic and purulent fluid was removed from the chest. This was likely the result of contamination during the device exchange. All other end organs were normal.

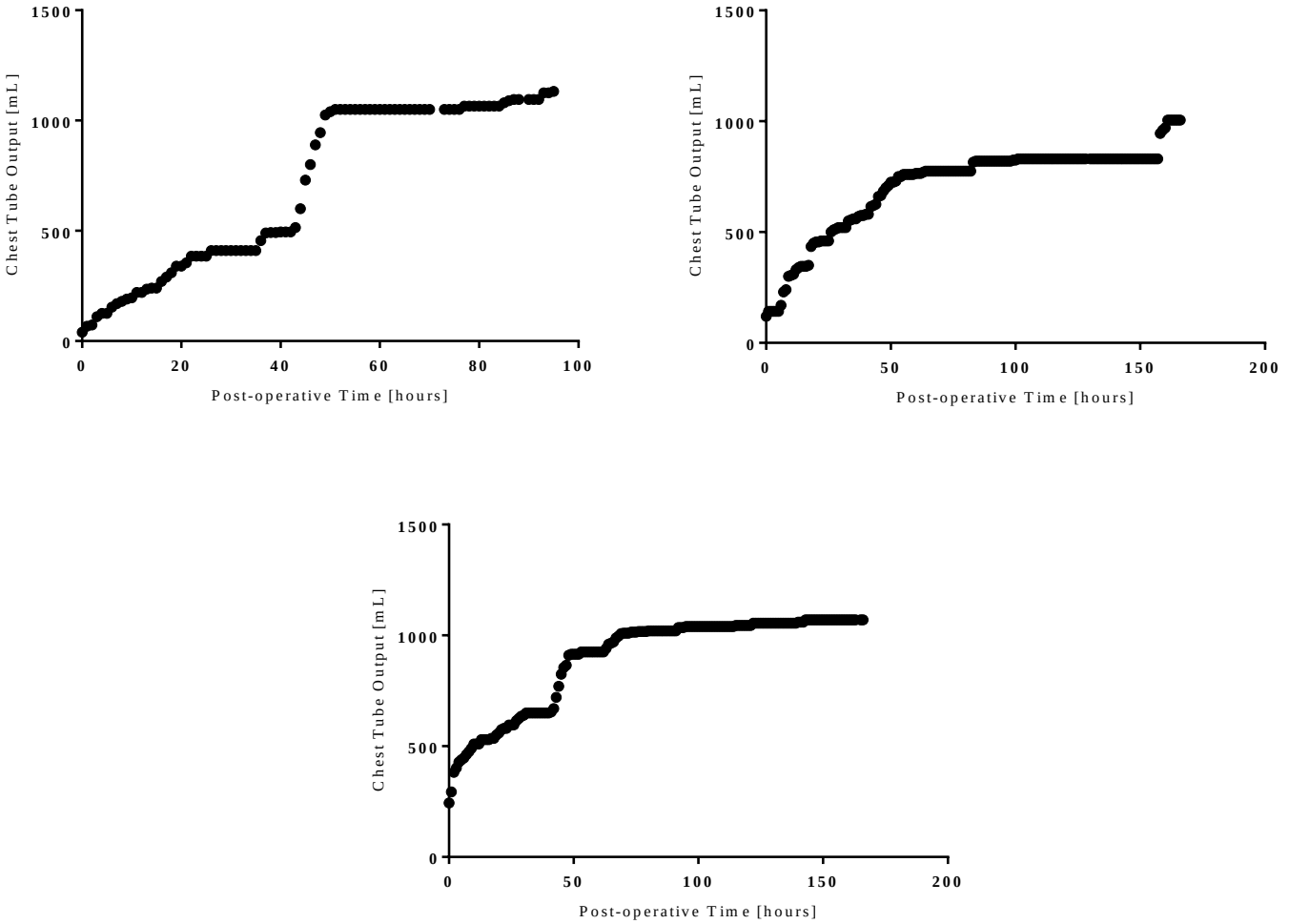

Figure 16 Cumulative Chest Output Over Course of Study

Cumulative chest tube ouput for Trial 1 (*top left*), Trial 2 (*top right*) and Trial 3 (*bottom*). Initial output measurement was taken post-operatively in the ICU after the animal stood

6.4 Discussion

Mechanical ventilation and current ECMO devices used to support pediatric lung failure patients restrict patient mobility. Evidence demonstrating improved post-transplant outcomes for patients whom participated in active physical rehabilitation, including ambulation, is increasing.[72,75,139] The P-ModELAS is being developed to address the need for an ECMO device which allows patient ambulation. In this study, the P-ModELAS was evaluated in awake sheep for 7 days with the primary objective to develop a suitable post-operative anticoagulation strategy. All animals survived the surgery, and two of the animals survived the entire study duration. The post-operative anticoagulation strategy was refined through this series of studies.

The Pediatric ModELAS was generally well tolerated by the animals. There was not a substantial change in animal hemodynamics or platelet function over time ($p > 0.05$). Post-operative plasma free hemoglobin did not exceed 20 mg/dL and was well below the threshold of 40 – 50 mg/dL.[114,127,128] Elevated pre-operative pfHb measurements are the result of samples being drawn via a venous puncture. Trial 2 required a device exchange within the first 3 post-operative hours due to high bundle resistance and decreasing extracorporeal blood flow rate. Air was observed in the bundle inlet plenum when extracorporeal blood flow was initiated in the operating room. Air in this location at the initiation of extracorporeal support is a result of incomplete priming of the pumping compartment or the inflow cannula and tubing. This was an isolated incident and additional measures were taken during Trial 3 to ensure the circuit was completely de-aired. The small thrombi which formed at the bottom pivot-bearing were not associated with increases in motor torque or pfHb. Subsequent ModELAS impeller design iterations have incorporated washout holes to increase blood velocity at the pivot-bearing, and exchanged the ceramic pivot for a smoother surfaced zirconium pivot. Both of these design changes were

implemented in the $ECCO_2R$ 7-day studies, reported in Chapter 4, and bottom pivot-bearing thrombus did not normally occur. Future P-ModELAS in vivo studies will include these design modifications and similar improvements are expected since the $ECCO_2R$ and P-ModELAS utilize identical pumps operated at similar RPM.

The average in vivo oxygenation rate was 95.1 ± 3.7 mL/min. The model predicted oxygenation rates within 10% of those measured during the in vivo experiments. Thus, changes in the measured oxygenation rate were likely caused by changes in the hemoglobin concentration and O_2 saturation of the inlet blood. The comparison to the model aids in distinguishing between lowered gas transfer rates due to bundle thrombus and an expected decrease in vO_2 resulting from non-standard venous inlet blood conditions. The major caveat though is in a perfusion limited regime, where the blood exits the device fully saturated, early or small intra-bundle thrombi would not be detectable based solely on vO_2. In future in vivo studies, the vCO_2 will also be measured to evaluate the patency of the HFM bundle. Carbon dioxide removal rate is the most sensitive indicator of early bundle thrombus[111] and work described in Chapter 3 of this thesis has provided a means to account for changes in vCO_2 due to changes in hematocrit.

The surgical invasiveness of the thoracotomy increases the risk of post-operative bleeding compared to the DLC cannulation strategy employed with the other ModELAS configurations. The anticoagulation strategy of the P-ModELAS must balance the need for coagulation at the surgical incisions with the extracorporeal circuit's anticoagulation requirement. All of the trials had approximately 1 L of chest tube output over the course of the study and output plateaued by POD 3. The first trial utilized a relatively aggressive anticoagulation strategy immediately post-operatively. This study was prematurely terminated due to dyspnea, likely resulting from the hemothorax. Subsequent studies used low or minimal heparin post-operatively until the chest tube

output rate stabilized and did not require early termination. The P-ModELAS tolerated this timeframe of low heparin well as demonstrated by devices generally free of thrombus. The explanted device from Trial 2 did have thrombus within the bundle, however bundle resistance did not increase and gas transfer did not decrease over the course of the study. Thus, it is likely that thrombus formed as the device was being removed from the animal post-study. In Trial 3, the ACT was increased to greater than 300 s prior to removing the device to prevent thrombus formation as the device is being removed. The addition of vCO_2 measurements during future in vivo studies will also improve the identification of intra-device thrombus during the study.

Other research groups have faced similar preclinical challenges when cannulating via a thoracotomy. Wang and Zwischenberger secure the cannulas into the RA and PA then 12 – 24 hrs later splice in the OxyRVAD device and anticoagulation restarted. This waiting period was done to allow the reversal of systemic anticoagulation and the chest incisions to begin to heal. One of the five OxyRVAD animals required early termination due to bleeding complicatoins.[140] Although the nature of animal studies sometimes require methodologies that may not be employed clinically a respiratory device that requires a 12 – 24 hour waiting period also delays respiratory support to the patient. The methodology used during these 7-day P-ModELAS studies is more challenging from a device perspective, however it is also a more clinically realistic approach.

The low number of trials and the use of different anticoagulation protocols during each trial is a limitation of these studies. Only 2 trials survived the entirety of the study and all three trials required postponed or skipped blood sampling. Specific conclusions regarding the hemocompatibility and performance of the device therefore should be made cautiously. Repeated trials using the recovery methodology of Trial 3 were not completed due to results from concurrent adult ModELAS 30-day studies and the platform nature of the ModELAS. An improved impeller

design has been implemented into the adult respiratory support ModELAS to mitigate thrombus formation at the bottom pivot-bearing and is currently being evaluated in 30-day adult ModELAS in vivo studies. Since all three ModELAS respiratory assist applications utilize an identical pump, improvements made to the adult device can be applied to the pediatric application as well. Additionally, from our experience transitioning from 5-day to 30-day adult in vivo studies, there will likely be unforeseen challenges during 30-day P-ModELAS studies. Thus, the decision was made to forego additional 7-day testing and transition to 30-day P-ModELAS studies once the successful 30-day adult ModELAS studies have been completed.

6.5 Conclusion

The P- ModELAS is a compact, integrated artificial pump-lung, and was connected to sheep for 7-days (n=3). One study required early termination, and one study required a device exchange within the first 3 hours of the study. The central goal of these studies was to develop the anticoagulation protocol during the first 48 – 72 post-operative hours. Future long-term studies will have an initial post-operative heparin infusion of 25 IU/kg/hr and it will be increased at this rate once the chest tube output rate has plateaued, as was done in Trial 3. Upcoming chronic 30-day ovine studies will build upon these 7-day studies and further evaluate performance and hemocompatibility of the P-ModELAS.

7.0 In Vitro Thrombus Formation

Platelet activation measurements were conducted by Sang-Ho Ye, PhD and CFD analysis was completed by Greg Burgreen, PhD.

7.1 Introduction

Thrombus formation within an artificial lung continues to be an important clinical issue. One report attributes 20% of ECMO device exchanges to acute or suspected thrombi.[130] To reduce intradevice thrombus formation, researchers have focused primarily on improving the biocompatibility of the blood contacting surface and eliminating blood stagnation zones. Improvements to material biocompatibility range from thromboresistant surface coatings to reducing the surface roughness of blood contacting surfaces.[28,141] Stagnation zones can be challenging to identify and eliminate. Extracorporeal devices such as the Hemolung RAS and the TandemHeart ventricular assist device utilize a continuous saline flush to clear blood from the pivot and pump thereby preventing thrombus formation.[142,143] A saline flush however is not suitable for the long-term device goals of the ModELAS due to the required additional port and infection risk. Alternatively, washout holes have been incorporated into impellers to circumvent the need for a saline flush by providing a flow path to drive fluid from the pivot-bearing back into the main blood flow pathway.[144,145]

The 30-day in vivo evaluation of the adult ModELAS full respiratory device resulted in all (n = 4) of the first-generation impeller devices containing significant thrombus at the bottom pivot-

bearing. This thrombus resulted in elevated plasma free hemoglobin, elevated motor torque and in one instance motor failure.[146] A second-generation impeller was designed with zirconium pivots and washout holes in an effort to improve thrombogenicity and washing at the bottom pivot-bearing. The zirconium pivot surface is an order of magnitude smoother than the ceramic pivots used in the first-generation impeller.

The challenge however is evaluating and comparing the thrombogenicity of these design modifications within the ModELAS. The gold standard comparison is in vivo comparisons of the modifications however, this approach is cost prohibitive. Recently, in an effort to mitigate cost, multiple groups have published methods to evaluate thrombus formation in vitro.[147,148] These methods, however, have typically been limited to evaluating thrombus formation via simple flow through a catheter or over a biomaterial. The ability to compare thrombogenicity of design changes in full devices in vitro would enable more rapid and efficient evaluation of design modifications.

In this chapter, methods are developed to evaluate the effect of pivot material surface roughness and impeller washout holes on the thrombogenicity of the ModELAS impeller. Thrombogenicity comparisons were based upon the thrombus dry weight and surface area at the bottom pivot. Platelet activation studies evaluated the effect of blood flow through the washout holes. The results of this work aim to not only evaluate the thrombogenicity of these design changes but also develop an in vitro testbed capable of examining the thrombogenicity of future ModELAS design iterations.

7.2 Methods

7.2.1 Impeller Description

Vertical cross sections of the baseline (no washout hole) impeller and the washout hole impeller are shown in Figure 17. The impeller vanes, pivot locations and the coupling magnet locations are identical in both impellers. The washout hole impeller contains 6 equidistant holes leading from the bottom pivot to one of the six impeller vanes. The holes are 0.8 mm in diameter and angled at 24°. The angled washout holes draw blood from underneath the impeller back into the main blood flow channels of the impeller and were optimized using computational fluid dynamics. The angled design maintains the hydrodynamic and magnetic forces on the impeller.[144] The sole difference between the ceramic and zironcium pivot impellers is the pivot material.

Figure 17 Cross Section of Impeller

Cross sections of the no washout hole impeller (left) and the washout hole impeller (right). Arrows indicate blood flow through the washout holes.

7.2.2 In Vitro Circuit

Ovine blood was purchased from Lampire Biologics (Pipersville, PA) and anticoagulated with acid citrated dextrose formula A. The blood was completely recalcified (3 g/L $CaCl_2$) and heparinized (3.5 U/mL) and treated with L-glutamine (2 mmol/L) and gentamicin (2.5 mL/L) to

preserve red blood cell integrity and prevent infection.[148] The heparin concentration was determined via a previously described static pretest.[147] Each test loop consisted of a 600-mL compliant reservoir submerged in a 37 °C water bath, and a modified ECCO$_2$R ModELAS device. Resistance of the HFM bundle and 15.5 Fr ALung dual lumen catheter were predicted by Blake-Kozey equation[149] and Hagan-Poiseuille equation, respectively. These resistances were simulated in the in vitro circuit by a 1/8 inch blood flow path where the HFM bundle normally resides and 5/16 inch tubing within the circuit. The cannula and fiber bundle were removed from the circuit to prevent thrombus formation in either of these locations. Thrombus does not consistently form in either the tubing or in the fiber bundle based on data from our in vivo studies with this device.

The control impeller device and the test impeller device were run in parallel with blood from the same animal (indicated by blood group 1 and blood group 2) to eliminate any influence hematologic variability between animals may have on the experiment. The device RPM was set to achieve a blood flow rate of 500 mL/min, and was not adjusted. Blood flow rate was recorded every 30 minutes. Activated clotting time (ACT), pfHb and hemoglobin concentration were measured every 1.5 hrs. At the completion of the study each device was disconnected from the circuit, passively flushed with phosphate buffered saline and disassembled. Each blood contacting surface of the device was photographed with a ruler for scale. The top and bottom of the impeller were identically photographed after each repetition of the experiment.

7.2.3 Image Processing and Heat Map Generation

The images of the impeller were imported into ImageJ. The scale of the image was set based on the ruler within the photograph and the images were cropped to a square the width of the impeller. If necessary, the image was scaled to exactly 3424 x 3424 pixels (1023 pixels/inch). The

color threshold was adjusted to a hue of 16 to 253, a brightness of 1 to 14 and passed saturations between 83 and 255. The thrombi were subsequently selected using the ImageJ wand tool. The area of the thrombi was then calculated via the ImageJ measure function. ImageJ software was then used to create a mask of the thrombi selection. The masks of each repeated trial were then layered into a single stacked image and exported to MATLAB.

The MATLAB program analyzed each layer of the stacked image on a pixel-by-pixel basis to determine the number of layers which contained thrombus at each pixel. Identical pixel locations on each layer were then averaged, the layered average. Thus, if 3 of the 5 trials contained thrombus within a certain pixel the layered average would be 0.6. The impeller image was then divided into concentric bins each spaced 15 pixels (equivalent to 0.015 inch) radially apart. The color of each bin represents the average of all the layered averages within that bin. The pivot was excluded from this analysis.

7.2.4 Platelet Activation

Platelet activation was evaluated in zirconium pivot impellers with and without washout holes. The recirculation loop was identical to the previously described loop. The circuits were primed with a 1% bovine serum albumin (BSA) solution and the solution was recirculated for at least 20 minutes. Excess BSA solution was drained from the circuit and 125 mL of ovine blood (ACD-A 1:9) from a donor sheep filled the circuit. Ovine blood was purchased either from Lampire Biologics and used 24 hours after being drawn (referred to as 24-hour old blood), or from a local sheep farm and used within 3 hours of being drawn (referred to as fresh blood). The RPM of the

device was increased until the blood flow rate was 0.5 L/min. Blood was allowed to recirculate for 1 hour.

A 3-mL blood sample was drawn from the blood donor bag and placed in an S-Monovette tube (SARSTEDT AG & Co, Germany) for baseline PAF activation measurements. Blood samples were drawn from each of the circuits and placed in an S-Monovette tube at 0 min, 15 min, 30 min and 60 min to measure CD62P expression. At the 1-hour time point an additional 3 mL sample was drawn from each loop to measure end of study PAF activation. PAF stimulated samples were used to evaluate the functionality of the circulating platelets. Details of the flow cytometry methods used to measure CD62P expression have been previously described.[123,124]

7.2.5 Statistical Analysis

Data are reported as the mean ± standard deviation. Statistical analysis was completed in SPSS (IBM, Armonk, NY). A student t-test was conducted to evaluate statistical significance of thrombi mass and surface area. A repeated measures ANOVA was completed to compare and determine the statistical significance of the platelet activation data. Comparisons were significant at $p < 0.05$.

7.3 Results

The thrombus mass and surface area formed on the ceramic-no washout hole impeller was greater than that formed on the zirconium-no washout hole impeller ($p = 0.03$ and $p = 0.02$,

respectively) (Table 9). The addition of washout holes to a zirconium pivot impeller did not affect the mass or surface area of thrombus formed ($p = 0.28$ and $p = 0.34$, respectively) (Table 9).

Heat maps of the bottom face of the impeller were generated to depict the frequency of thrombus formation at different concentric regions (Figure 18). Thrombus primarily occurred at the pivot and with decreasing frequency as one moves radially outward toward the edge of the impeller for all pivot and washout hole combinations. The ceramic pivot resulted in thrombus formation within 0.028 inches of the pivot in 100% of the trials. The maximum frequency of thrombus formation for all zirconium pivot impellers without washout holes was 40% and with washout holes 32%. These maximums occurred within 0.028 inches of the pivot. The zirconium pivot-washout hole impeller had thrombus that extended to a maximum radial distance of 0.059 inches.

Table 9 Thrombus Mass and Surface Area

	Blood Group 1		**Blood Group 2**	
	Ceramic Pivot *No Washout Holes*[+]	**Zirconium Pivot** *No Washout Holes*[+]	**Zirconium Pivot** *No Washout Holes*[‡]	**Zirconium Pivot** *Washout Holes*[‡]
Thrombus Mass [mg]	8.9 ± 6.2[*]	2.6 ± 1.9[*]	0.9 ± 1.6	2.7 ± 4.6
Thrombus Surface Area [cm^2]	1.72 ± 1.1[†]	0.4 ± 0.3[†]	0.2 ± 0.3	0.4 ± 0.6

[*],[†] Statistically significant ($p < 0.05$) compared to other pivot material;
[+]n=5, [‡] n=3

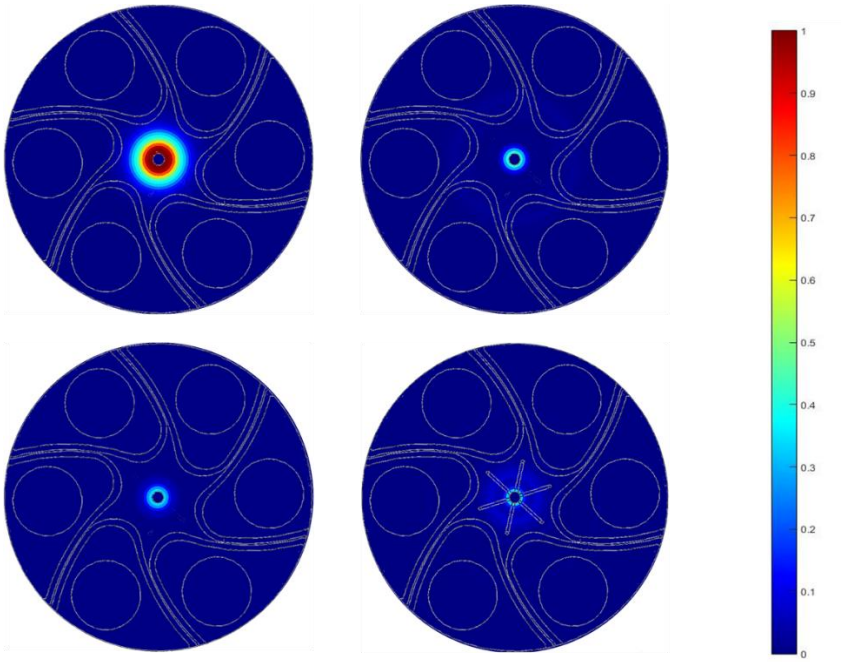

Figure 18 Heat Map Indicating Thrombus Location at Bottom Pivot

Ceramic pivot without washout hole impeller (top left), zirconium pivot without washout holes (top right), zirconium pivot without washout holes (bottom left), and zirconium with washout holes (bottom right). White lines indicate vanes, magnet location and washout holes.

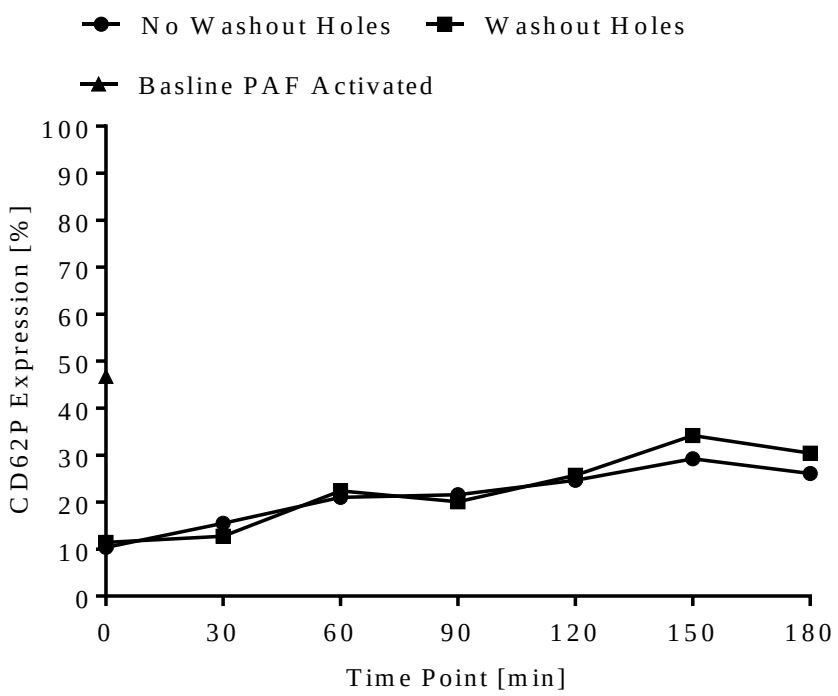

Figure 19 CD62P Expression -- 24 Hour Old Ovine Blood

24-hour old ovine blood initially anticoagulated with ACD-A, then recalcified and heparinized just prior to being placed in the circuit. Baseline CD62P expression of PAF activated platelets was measured prior to blood being added to the circuit. (n=2)

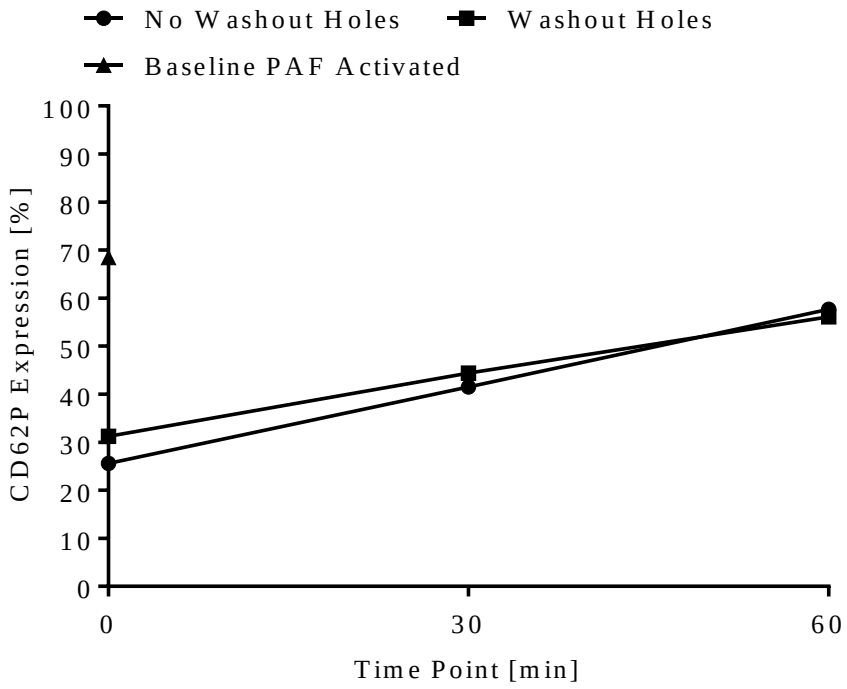

Figure 20 CD62P -- Fresh Ovine Blood

Fresh (less than 4 hour post-draw) ovine blood initially anticoagulated with ACD-A, then recalcified and heparinized just prior to being placed in the circuit. Baseline CD62P expression of PAF activated platelets was measured prior to blood being added to the circuit. (n=2)

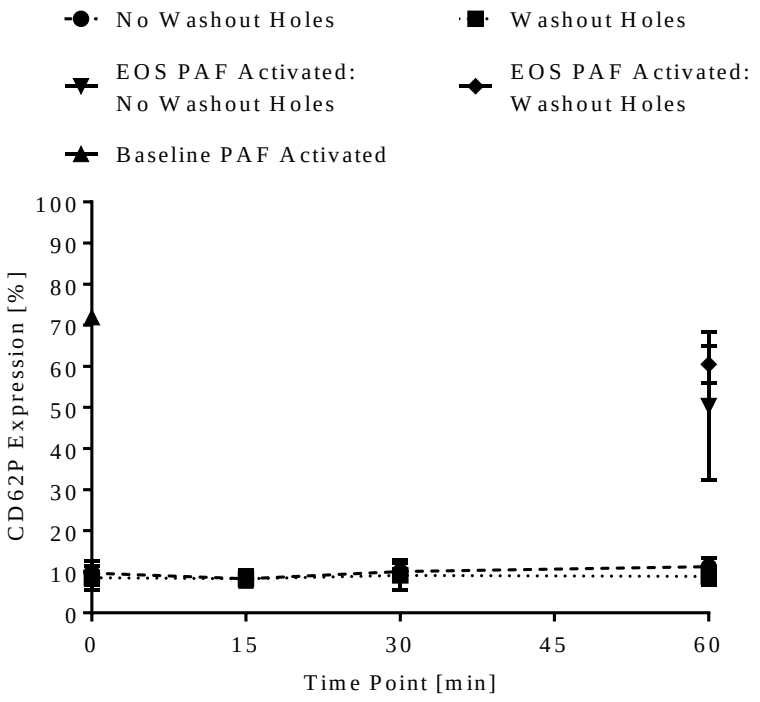

Figure 21 CD62P Expression -- Fresh Ovine Blood

Fresh (less than 4 hour post-draw) ovine blood anticoagulated with ACD-A and evaluated without recalcification. Baseline CD62P expression of PAF activated platelets was measured prior to blood being added to the circuit. End of study (EOS) PAF activated platelet samples were drawn from the circuit at the end of study. (n=3)

Figures 19 - 21 provides the percentage of platelets expressing CD62P, an indicator of platelet activation. Blood used 24 hours after collection (ACD-A added at collection, complete recalcification with $CaCl_2$ and heparin added just prior to start of study) showed low baseline CD62P expression (46.8%) when a PAF was added (Figure 19). Ovine blood collected and used within 4 hours (ACD-A added at collection, complete recalcification with $CaCl_2$ and heparin added just prior to start of study) showed acceptable PAF activated CD62P expression (68.5%) however over 50% of the platelets had become activated within the first 30 minutes of the study (Figure

20). Ovine blood collected and used within 4 hours (ACD-A added at collection, no recalcification) had acceptable baseline PAF activated CD62P expression (71.9%) (Figure 21). CD62P expression was not substantially different between the washout hole device and the no washout hole device ($p = 0.574$). Platelet activation did not increase over the course of the study ($p = 0.155$).

7.4 Discussion

Thrombus formation within the first generation ModELAS pump has been a consistent issue in vivo and resulted in increased hemolysis and motor torque. The second generation ModELAS pump includes zirconium pivots, which are smoother surfaced, and washout holes within the impeller in order to prevent this thrombus formation. In vitro hemolysis testing and CFD analysis has previously been the extent of testing done prior to in vivo evaluation. This however, can be costly. This chapter discusses the initial development and results of an in vitro protocol to evaluate the thrombogenicity of ModELAS impeller designs. Multiple sources of ovine blood, and anticoagulation regimes were evaluated for platelet activation and thrombus formation. This study demonstrated significantly less thrombus formation on the zirconium pivots, but no significant effect of the washout holes. The washout holes, however did not affect platelet activation.

Full device, in vitro thrombogenicity and platelet activation testing is challenging. The largest challenge is properly attaining and anticoagulating the donor blood in order to maintain platelet functionality ex vivo. The present study evaluated 24-hour old and same day ovine blood as well as complete recalcification with $CaCl_2$ and no recalcification. The same day ovine blood consistently showed baseline PAF activation similar to that seen during in vivo experiments

(Chapter 4) whereas blood stored for 24 hours show diminished platelet functionality. The literature also recommends that blood is used within 4 hours of being drawn for thrombogenicity testing.[150] The drawback to fresh ovine blood is the availability of donor sheep, the cost of maintaining in-house donor animals, and the volume and frequency of blood draws. Despite the availability of fresh ovine blood for the present work, restrictions to the volume and frequency of blood draws resulted in the thrombus formation and platelet activation studies needing to be completed separately. In the present study, only 250 mL of fresh ovine blood was able to be procured per day which equates to 125 mL per recirculation circuit. The total sample volume required for the platelet activation measurements (15 mL) depleted the blood reservoir and the blood was unable to be recirculated after 1 hour. Thrombus formation circuits required additional volume to permit blood sampling and maintain adequate reservoir volume for recirculation, therefore the experiments were separated and 24-hr old blood was used in the thrombus formation experiments. Jamiolkowski, et al. have shown 24-hr old blood is viable for thrombus formation testing.[147]

A two-fold approach, zirconium pivots and addition of washout holes, was taken in order to decrease the pivot surface roughness and increase fluid washing at the bottom pivot, respectively. Linnewaber et al. demonstrated a 38.5% decrease in platelet adhesion when whole blood was exposed to surfaces with a surface roughness of 0.05 μm compared to 0.2 – 0.4 μm.[141] Increased surface roughness of catheters has also been correlated to an increase in thromboembolic complications in human and animal models.[151,152] In the present study a change from a ceramic to zirconium pivot (representing a 98.5% decrease in surface roughness) substantially decreased the surface area and mass of the thrombus formed at the bottom pivot-bearing.

The experimental design, however does not allow one to differentiate the possibility of zirconium being inherently more anti-thrombotic than ceramic, independent of surface roughness. Previous studies, however, have evaluated surface roughness as an independent factor influencing thrombus formation. Catheters extruded from a single batch of polyvinylchloride resin at varying temperatures (temperature variations result in changes to the surface roughness) showed that greater surface roughness resulted in greater thrombus formation and concluded this may be due to better adhesion of the thrombus to the biomaterial.[153] Tsunoda, et al. also showed that cellulose HFM with rougher surfaces had higher platelet adhesion and concluded that surface roughness may dictate flow conditions at the surface which in turn affects thrombogenicity.[154] Both of these explanations indicate that greater surface roughness, independent of the material, results in increased thrombus formation. Thus, regardless of the inherent thrombogenicity of ceramic and zirconium, the smoother surface of the zirconium pivot is likely a contributing factor to decreased thrombus formation.

Blood flow stasis is one contributor to thrombosis based on Virchow's triad, thus washout holes were added to the impeller design to drive blood from underneath the impeller back into the main, high flow, impeller vanes. The addition of washout holes to the zirconium pivot impeller, however, did not further improve thrombus formation at the bottom pivot. One reason for this may be ingestion of upstream thrombus by the pump. Small thrombi, which may form at the pre-pump tubing connectors or within the reservoir bag, can dislodge and be ingested by the pump. Due to the size of the washout holes, it is likely that any thrombi drawn into the washout holes will occlude the hole. Once blood flow through the washout holes is occluded, the washout hole impeller essentially becomes the no washout hole impeller as blood no longer has a pathway from the bottom surface of the impeller back into the main blood flow channels. Although thrombus

originating with the blood reservoir in not a challenge in the ModELAS in vivo setting, thrombus formation at tubing connectors is a well-known clinical challenge.[155] Thus further washout hole design improvements are required to improve the ability of the washout holes to handle ingested thrombus.

One potential complication of the washout holes is shear induced platelet activation resulting from blood flow through the small diameter washout holes. Exposure to the supraphysiological shear stresses present within blood pumps can result in irreversible platelet activation and aggregation without exogenous agonists.[156] This chronic platelet activation can in turn increase the risk of adverse, thromboembolic complications.[157] Typical human arteries have a shear stress of 1.4 – 6.1 Pa,[158–160] and several studies have demonstrated that shear stresses of 10 – 50 Pa are sufficient to cause platelet activation.[161,162] CFD analysis predicted typical shear stresses within the washout holes to be 13 – 50 Pa, and thus sufficient for platelet activation. The present in vitro data, however, did not show a statistical increase in platelet activation due to the washout holes. This is probably due to noise, or activation, from the rest of the system. Designing a test fixture to isolate blood flow through the washout holes would allow one to determine whether or not the washout holes activate platelets. However, this determination would be binary, and does not provide insight as to the potential clinical relevance of the platelet activation. Interestingly, 30-day in vivo data utilizing the zirconium pivot-washout hole impeller did not show a clinically relevant increase in platelet activation (CD62P expression less than 10%).[163] Thus the washout holes may in fact be activating platelets, however the platelet activation contribution from the washout is not substantial in comparison to the platelet activation resulting from blood flow through the pump. Ultimately, a design which creates clinically relevant platelet activation in vivo

needs to be evaluated using the in vitro protocol presented within this chapter to determine the sensitivity of this in vitro activation assay.

Although limited comparisons to in vivo studies show general agreement with these in vitro results there are several limitations and aspects of this study which may be improved upon. The implementation of additional blood inclusion criteria, beyond platelet activation, would likely further reduce variability between repeated trials. For example, one group used thrombus surface coverage of PTFE and Latex material incorporated into the circuit to ensure consistent coagulability of the donor blood.[147] The sensitivity of these in vitro thrombogenicity studies is also unclear based upon the current results. The test is sensitive enough to differentiate between the surface roughness of different materials (ceramic vs zirconium), however it may not have the sensitivity to elucidate subtle difference, such as between washout holes and no washout holes. At present, there is not ModELAS in vivo data corresponding to the zirconium-no washout hole condition to confirm the in vitro no washout hole results. However, in vivo data does not indicate any adverse effects of including the washout holes.[163]

There is no accepted standard protocol for in vitro thrombogenicity testing. Multiple groups have evaluated in vitro thrombogenicity however there is significant methodological variability amongst groups. Literature has reported temperature ranges from room temperature to 37 °C, study durations have been reported 15 minutes[164] to 48 hours[148] and blood sourced from a fresh donor[165] to blood that is 24 hr post draw.[147] These studies however have been primarily limited to correlating thrombogenicity to the quantity of adhered platelets. The FDA is also actively pursuing methods to evaluate in vitro medical device thrombogenicity, however the testing has been limited to flow over biomaterial samples.[147,166] The creation of a standardized protocol would decrease

variability between research groups and improve the predictive power of an in vitro thrombogenicity test.

7.5 Conclusions

In conclusion, these studies demonstrated reduced thrombus formation on zirconium pivots compared to ceramic. Washout holes did not further improve thrombus formation, nor did the holes increase platelet activation. This in vitro test, however may not be sensitive enough to illuminate the effects of the washout holes. In terms of practical design, based on these studies, there is no drawback to incorporating the washout holes and zirconium pivots into the ModELAS. This work represents the initial steps in creating an in vitro thrombogenicity protocol for evaluation of ModELAS design changes, but further refinement of the in vitro protocol is needed to increase the sensitivity of this test.

8.0 Summary and Conclusion

Mechanical ventilation has typically been the primary treatment for patients with acute or chronic respiratory failure. Less invasive, lung protective mechanical ventilation techniques have improved the treatment of patients. The lower tidal volumes, however can be ineffective at removing CO_2 and necessitate returning to invasive mechanical ventilation. In patients with hypercapnic respiratory failure, the additional CO_2 removal provided by extracorporeal CO_2 removal ($ECCO_2R$) devices has been shown to allow extubation, prevent intubation, or permit lung-protective ventilation. For patients with end-stage lung disease awaiting a lung transplant, ECMO can provide full respiratory support and an alternative to mechanical ventilation. These systems, however, are still complex and often limit patient mobility or require sedation. Commercial devices designed specifically for the needs of children are even more limited due to the small patient population. The Modular Extracorporeal Lung Assist System (ModELAS) developed in this dissertation addresses the need for a compact, wearable artificial lung device while, through the platform nature of this technology, also leverages the adult $ECCO_2R$ market in an effort to bring the pediatric device to market. The objective of this dissertation was to develop the low-flow $ECCO_2R$ and pediatric full respiratory support applications of the ModELAS.

The ModELAS is a highly compact, wearable platform technology capable of providing full respiratory support for children and adults as well as low-flow $ECCO_2R$. A mathematical model was developed to define the bundle geometry required to meet the targeted 35 – 50% CO_2 removal rate. In vitro testing validated the model prediction and demonstrated the low-flow $ECCO_2R$ ModELAS is capable of removing 92 mL CO_2/min, under normocapnic conditions, at a blood flow rate of 500 mL/min with minimal hemolysis (in vitro TIH: 0.08 g/100min & NIH:

0.158 g/100L). Given this data, the $ECCO_2R$ device was evaluated in 7-day in vivo studies. These studies demonstrated consistent gas transfer performance with only isolated device related events. Anemia occurred during several in vivo trials and led to an in vitro investigation of the relationship between hematocrit and CO_2 removal. These studies demonstrated a linear decrease in vCO_2 as hematocrit decreases and a need to take hematocrit into account when interpreting changes in CO_2 removal.

The pediatric ModELAS was evaluated in acute and chronic animal studies. The acute studies evaluated the in vivo performance of the device and developed the cannulation strategy. The results demonstrated successful acute performance which supported in vitro data. Chronic, 7-day studies utilized the cannulation strategies developed during the acute studies. The primary goal of the 7-day studies was to find a post-surgical anticoagulation and recovery strategy which balanced the device's need for anticoagulation and the need for coagulation at the surgical site. Although only 3 studies were completed, the final animal recovered well and this post-surgical strategy will be implemented during upcoming 30-day studies. Additional repetitions were not completed due to experience with the adult ModELAS 30-day studies which demonstrated thrombus formation within the pump.

Animal studies, however, are an expensive and time intensive means of determining if and where thrombus forms within a device. An in vitro thrombogenicity test was developed to evaluate the effect of impeller design modifications on thrombus formation. Results showed that the zirconium pivot significantly reduced thrombus surface area at the bottom pivot, however no significant effect was demonstrated by the addition of washout holes. Platelet activation caused by the washout holes was inconclusive due to noise generated by the circuit.

ModELAS evaluation and design optimization is on-going. Further improvements to the impeller washout hole design have been made and are currently being evaluated in 30-day in vivo studies with the adult full respiratory support ModELAS. The improved impeller design will be used during future 30-day, in vivo pediatric ModELAS studies. The laboratory is also developing a tip-to-tip thromboresistant coating[133] which may allow reductions in the required systemic anticoagulation. Further improvements to the thrombogenicity study protocol, including blood inclusion criteria, may increase the power of the in vitro thrombogenicity results.

8.1 Future Visions

Artificial lungs will likely follow the path of artificial hearts. As the technology progresses patients will move from intensive care units to step-down units and eventually be discharged home on destination therapy devices. For this to become a reality, the pump and HFM bundle will need to be compact, power and oxygen supplies portable and a controller with smart feedback all while accounting for human factors. The ModELAS technology is not there, yet, but provides the primary design for which further product development will build from.

Thrombus formation within the ModELAS pump must be addressed in order for long-term (1 – 3 months) artificial lung support with this device to be realized. Again, research from ventricular assist technology can be translated to artificial lungs. The impeller washout holes currently incorporated into the ModELAS were based upon designs used in ventricular assist devices and have improved the pump performance. Completion of 30-day in vivo studies will demonstrate if these design modifications have solved the thrombus formation issue or if additional changes are required. Ultimately, transitioning from a pivot-bearing impeller to a magnetically

levitated impeller may be required for long-term support. Intrabundle thrombus has not been a consistent issue during ModELAS animal studies completed at present, however the HFM bundle does represent a significant non-biologic surface and HFM bundle biocompatibility may be a challenge after several months of support. The application of a biocompatible surface coating would improve long-term device performance and in a future, outpatient setting potentially prevent thrombus formation due to patient compliance with anticoagulation medicines.

The CO_2 removal mathematical model presented within this dissertation can be further built-upon in order to improve the accuracy of the gas transfer prediction across the full range of ModELAS blood flow rates. The current model treats the oxygenation and CO_2 removal occurring within the bundle as separate entities. The oxygen saturation however affects the CO_2 content of blood and the CO_2 diffusivity, and changes along the length of the HFM bundle. This relation, the Haldane Effect, can be taken into account by coupling CO_2 and O_2 transfer models. This dissertation has also demonstrated the need to include the hematocrit as an input parameter. These two modifications would likely further improve the predictive capabilities of the model, especially at higher blood flow rates.

Clinical interest in $ECCO_2R$ has grown due to positive clinical data and will likely continue to grow with positive outcomes from on-going pivotal clinical trials. This will likely further increase industry interest and drive innovative $ECCO_2R$ device designs focused on additional reductions in invasiveness, circuit complexity and advancing ideas explored in academia. Low HCT environments may present the prime application of carbonic anhydrase immobilized fibers due to less competition with native carbonic anhydrase. Specifically in systems, such as the ProLung[167] (Estor S.P.A., Milano, Italy; formerly the Hemodec DECAPsmart), which recirculate plasma through the HFM bundle. Work from this dissertation suggests that, since the hematocrit

is only locally decreased through the oxygenator, the CO_2 carrying capacity of the blood would not be altered. This, in combination with reduced native carbonic anhydrase competition, may result in enhancements that make developing stable, carbonic anhydrase coatings worthwhile.

Industry interest in commercializing a pediatric device will also be a challenge due to the small patient population. This has been the case for innovation in, and market variety of, pediatric ventricular assist devices. The solution may be to couple the pediatric application to a second larger market. For this approach to truly work, however devices will need to be designed with this goal in mind so that the device is optimized for each application. The Xenios AG's iLA Activve product line provides a range of similarly designed oxygenators for partial CO_2 removal, and pediatric and adult ECMO. The ModELAS design takes a similar approach, but has optimized fiber bundle geometries for each application and has created a compact pump-lung system. The in vivo work in this dissertation will be continued to evaluate the in vivo performance of the pediatric application over 30-days.

Bibliography

1. Kochanek K, Murphy S, Xu J, Arias E: Deaths: Final data for 2017 *Natl Vital Stat Rep* 68: 1–76, 2019

2. Slutsky A, Ranieri V: Ventilator-induced lung injury *N Engl J Med* 369: 2126–2136, 2013

3. Mathers CD, Loncar D: Projections of global mortality and burden of disease from 2002 to 2030 *PLoS Med* 3: e442, 2006

4. Wier L, Elixhauser A, Pfuntner A, Au D: Overview of hospitalizations among patients with COPD, 2008 *Agency Healthc Res Qual* Statistical Brief #106, 2011

5. Barnes PJ: Chronic obstructive pulmonary disease *N Engl J Med* 343: 269–280, 2000

6. American Lung Association: *State of lung disease in diverse communities*, 2010.

7. Stoller JK: Acute exacerbations of chronic obstructive pulmonary disease *N Engl J Med* 346: 988–994, 2002

8. Connors A Jr, Daswon N, Thomas C, et al.: Outcomes following acute exacerbation of severe chronic obstructive lung disease. The SUPPORT investigators (Study to Understand Prognoses and Preferences for Outcomes and Risks of Treatments) *Am J Respir Crit Care Med* 154: 959–967, 1996

9. American Lung Association: Lung Health & Diseases: Learn About ARDS *http://www.lung.org/lung-health-and-diseases/lung-disease-lookup/ards/learn-about-ards.html*, 2017

10. Ware LB: Pathophysiology of acute lung injury and the acute respiratory distress syndrome *Semin Respir Crit Care Med* 27: 337–349, 2006

11. Sweeney R, McAuley D: Acute respiratory distress syndrome *The Lancet* 388: 2416–2430, 2016

12. Thompson BT, Chambers RC, Liu KD: Acute respiratory distress syndrome *N Engl J Med* 377: 562–572, 2017

13. Rosenberg AA, Haft JW, Bartlett R, et al.: Prolonged duration ECMO for ARDS: futility, native lung recovery, or transplantation? *ASAIO J* 59: 642–650, 201AD

14. Tobin MJ, Laghi F, Brochard L: Role of the respiratory muscles in acute respiratory failure of COPD: lessons from weaning failure *J Appl Physiol* 107: 962–970, 2009

15. Esteban A, Alía I, Ibañez J, Benito S, Tobin MJ: Modes of mechanical ventilation and weaning. A national survey of Spanish hospitals. The Spanish Lung Failure Collaborative Group *Chest* 106: 1188–1193, 1994

16. Nava S, Rubini F, Zanotti E, et al.: Survival and prediction of successful ventilator weaning in COPD patients requiring mechanical ventilation for more than 21 days *Eur Respr J* 7: 1645–1652, 1994

17. Terragni P, Del Sorbo L, Mascia L, et al.: Tidal volume lower than 6 ml/kg enhances lung protection *Anesthesiology* 111: 826–835, 2009

18. Bein T, Weber-Carstens S, Goldmann A, et al.: Lower tidal volume strategy (~3 ml/kg) combined with extracorporeal CO_2 removal versus 'conventional' protective ventilation (6 ml/kg) in severe ARDS *Intensive Care Med* 39: 847–856, 2013

19. Plant PK, Owen JL, Elliott MW: Early use of non-invasive ventilation for acute exacerbations of chronic obstructive pulmonary disease on general respiratory wards: a multicentre randomised controlled trial *Lancet Lond Engl* 355: 1931–1935, 2000

20. Brochard L, Mancebo J, Wysocki M, et al.: Noninvasive ventilation for acute exacerbations of chronic obstructive pulmonary disease *N Engl J Med* 333: 817–822, 1995

21. Calverley PMA: Respiratory failure in chronic obstructive pulmonary disease *Eur Respir J* 22: 26s–30s, 2003

22. Budweiser S, Jörres RA, Pfeifer M: Treatment of respiratory failure in COPD *Int J Chron Obstruct Pulmon Dis* 3: 605–618, 2008

23. Chandra D, Stamm JA, Taylor B, et al.: Outcomes of noninvasive ventilation for acute exacerbations of chronic obstructive pulmonary disease in the United States, 1998-2008 *Am J Respir Crit Care Med* 185: 152–159, 2012

24. Morelli A, Del Sorbo L, Pesenti A, Ranieri V, Fan E: Extracorporeal carbon dioxide removal ($ECCO_2R$) in patients with acute respiratory failure *Intensive Care Med* 43: 519–530, 2017

25. Lund L, Federspiel W: Removing extra CO_2 in COPDpatients *Curr Respir Care Rep* 2: 131–138, 2013

26. Arthurs G, Sudhakar M: Carbon dioxide transport *Crit Care Pain* 5: 207–210, 2005

27. Kolobow T, Gattinoni L, White D, Pierce J, Iapichino G: The Carbon Dioxide Membrane Lung (CML): A new concept *ASAIO J* 23: 17–21, 1977

28. Federspiel W, Henchir K: Lung, Artificial: Basic principles and current applications *Encycl Biomater Biomed Eng* 9: 910–921, 2008

29. MacLaren G, Butt W, Best D, Donath S: Central extracorporeal membrane oxygenation for refractory pediatric septic shock: *Pediatr Crit Care Med* 12: 133–136, 2011

30. Baker A, Richardson D, Craig G: Extracorporeal carbon dioxide removal ($ECCO_2R$) in respiratory failure: an overview, and where next? *J Intensive Care Soc* 13: 232–237, 2012

31. Novalung A Xenios Company: iLA activve system platform custom-tailored extrapulmonary lung support, 2015

32. Zimmerman M, Bein T, Arlt M, et al.: Pumpless extracorporeal interventional lung assist in patients with acute respiratory distress syndrome: a prospective pilot study *Crit Care* 13: R10, 2009

33. Kolobow T, Gattinoni L, Tomlinson TA, Pierce JE: Control of breathing using an extracorporeal membrane lung *Anesthesiology* 46: 138–141, 1977

34. Morris A, Wallace C, Menlove R, et al.: Randomized clinical trial of pressure-controlled inverse ratio ventilation and extracorporeal CO_2 removal for adult respiratory distress syndrome *Am J Respir Crit Care Med* 149: 295–305, 1994

35. Ruberto F, Pugliese F, D'Alio A, et al.: Extracorporeal removal CO_2 using a venovenous, low-flow system (Decapsmart) in a lung transplanted patient: A case report *Transplant Proc* 41: 1412–1414, 2009

36. Terragni P, Birocco A, Faggiano C, Ranieri V: Extracorporeal CO_2 removal *Contrib Nephrol* 165: 185–196, 2010

37. ALung Technologies, Inc: "Low-flow" versus "mid-flow" extracorporeal CO_2 removal: A review of clinical performance and device efficiency, 2015

38. ALung Technologies, Inc: How activmix technology enhances CO_2 removal in the Hemolung RAS, 2015

39. ALung Technologies, Inc: Hemolung RAS: the first fully-integrated respiratory dialysis system, 2012

40. Bonin F, Sommerwerck U, Lund L, Teschler H: Avoidance of intubation during acute exacerbation of chronic obstructive pulmonary disease for a lung transplant candidate using extracorporeal carbon dioxide removal with the Hemolung *J Thorac Cardiovasc Surg* 145: e43–e44, 2013

41. Burki N, Mani R, Herth F, et al.: A novel extracorporeal CO_2 removal system: results of a pilot study of hypercapnic respiratory failure in patients with COPD *Chest* 143: 678–686, 2013

42. Mani RK, Schmidt W, Lund LW, Herth FJF: Respiratory dialysis for avoidance of intubation in acute exacerbation of COPD *ASAIO J* 59: 675–678, 2013

43. Sklar MC, Beloncle F, Katsios CM, Brochard L, Friedrich JO: Extracorporeal carbon dioxide removal in patients with chronic obstructive pulmonary disease: a systematic review *Intensive Care Med* 41: 1752–1762, 2015

44. Trahanas J, Lynch W, Bartlett R: Extracorporeal support for chronic obstructive pulmonary disease: a bright future *J Intensive Care Med* 32: 411–420, 2017

45. Akkanti B, Rajagopal K, Patel K, et al.: Low-flow extracorporeal carbon dioxide removal using the Hemolung Respiratory Dialysis System® to facilitate lung-protective mechanical ventilation in acute respiratory distress syndrome *J Extracorpor Technol* 49: 112–114, 2017

46. Parilla F, Bergesio L, Aguirre-Bermeo H, et al.: Ultra-low tidal volumes and extracorporeal carbon dioxide removal (Hemolung® RAS) in ards patients. a clinical feasibility study *Intensive Care Med Exp* 3: A7, 2015

47. Batchinsky A, Jordan B, Regn D, et al.: Respiratory dialysis: Reduction in dependence on mechanical ventilation by venovenous extracorporeal CO_2 removal *Crit Care Med* 39: 1382–1387, 2011

48. Fanelli V, Ranieri M, Mancebo J, et al.: Feasibility and safety of low-flow extracorporeal carbon dioxide removal to facilitate ultra-protective ventilation in patients with moderate acute respiratory distress syndrome *Crit Care* 20: 1–7, 2016

49. Braune S, Sieweke A, Brettner F, et al.: The feasibility and safety of extracorporeal carbon dioxide removal to avoid intubation in patients with COPD unresponsive to noninvasive ventilation for acute hypercapnic respiratory failure (ECLAIR study): multicentre case–control study *Intensive Care Med* 42: 1437–1444, 2016

50. Godet T, Combes A, Zogheib E, et al.: Novel CO_2 removal device driven by a renal-replacement system without hemofilter. A first step experimental validation *Anaesth Crit Care Pain Med* 34: 135–140, 2015

51. Schmidt M, Jaber S, Zogheib E, Godet T, Capellier G, Combes A: Feasibility and safety of low-flow extracorporeal CO_2 removal managed with a renal replacement platform to enhance lung-protective ventilation of patients with mild-to-moderate ARDS *Crit Care* 22: 122, 2018

52. Peperstraete H, Eloot S, Depuydt P, De Somer F, Roosens C, Hoste E: Low flow extracorporeal CO_2 removal in ARDS patients: A prospective short-term crossover pilot study *BMC Anesthesiol* 17: 155, 2017

53. Eloot S, Peperstraete H, De Somer F, Hoste E: Assessment of the optimal operating parameters during extracorporeal CO_2 removal with the Abylcap® System *Int J Artif Organs* 39: 580–585, 2017

54. Kalbhenn J, Neuffer N, Zieger B, Schmutz A: Is extracorporeal CO_2-removal really "safe" and "less" invasive? Observation of blood injury and coagulation impairment during $ECCO_2R$ *ASAIO J* 63: 666–671, 2017

55. Mathers CD, Boerma T, Ma Fat D: Global and regional causes of death *Br Med Bull* 92: 7–32, 2009

56. Cystic Fibrosis Foundation: Diagnosed With Cystic Fibrosis, 2019

57. Charman SC, Sharples LD, McNeil KD, Wallwork J: Assessment of survival benefit after lung transplantation by patient diagnosis *J Heart Lung Transplant* 21: 226–232, 2002

58. Ivy DD, Abman SH, Barst RJ, et al.: Pediatric pulmonary hypertension *J Am Coll Cardiol* 62: D117–D126, 2013

59. Ivy D: Pulmonary hypertension in children *Cardiol Clin* 34: 451–472, 2016

60. Barst RJ, McGoon MD, Elliott CG, Foreman AJ, Miller DP, Ivy DD: Survival in childhood pulmonary arterial hypertension: Insights from the registry to evaluate early and long-term pulmonary arterial hypertension disease management *Circulation* 125: 113–122, 2012

61. Goldstein BS, Sweet SC, Mao J, Huddleston CB, Grady RM: Lung transplantation in children with idiopathic pulmonary arterial hypertension: An 18-year experience *J Heart Lung Transplant* 30: 1148–1152, 2011

62. Kirkby S, Hayes D: Pediatric lung transplantation: indications and outcomes *J Thorac Dis* 6: 1024–1031, 2014

63. Valapour M, Paulson K, Smith J: OPTN/SRTR 2011 annual data report: lung *Am J Transplant* 13: 149–177, 2013

64. Elizur A, Sweet SC, Huddleston CB, et al.: Pre-transplant mechanical ventilation increases short-term morbidity and mortality in pediatric patients with cystic fibrosis *J Heart Lung Transplant* 26: 127–131, 2007

65. Maul TM, Nelson JS, Wearden PD: Paracorporeal lung devices: Thinking outside the box *Front Pediatr* 6, 2018

66. Maquet Getinge Group: Quadrox-i Neonatal & Pediatric, 2015

67. Taylor K, Holtby H: Emergency interventional lung assist for pulmonary hypertension: *Anesth Analg* 109: 382–385, 2009

68. Gazit AZ, Sweet SC, Grady RM, Huddleston CB: First experience with a paracorporeal artificial lung in a small child with pulmonary hypertension *J Thorac Cardiovasc Surg* 141: e48–e50, 2011

69. Jeffries R, Lund L, Frankowski B, Federspiel W: An extracorporeal carbon dioxide removal device operating at hemodialysis blood flowrates *Intensive Care Med Exp* 5: 2–12, 2017

70. Puri V, Epstein D, Paithel S: Extracorporeal membrane oxygenation in pediatric lung transplantation *J Thorac Cardiovasc Surg* 140: 427–432, 2010

71. Lehr CJ, Zaas DW, Cheifetz IM, Turner DA: Ambulatory extracorporeal membrane oxygenation as a bridge to lung transplantation *Chest* 147: 1213–1218, 2015

72. Turner D, Rehder K, Bonadonna D, et al.: Ambulatory ECMO as a bridge to lung transplant in a previously well pediatric patient with ARDS *Pediatrics* 134: e583-585, 2014

73. Schmidt F, Sasse M, Boehne M, et al.: Concept of "awake venovenous extracorporeal membrane oxygenation" in pediatric patients awaiting lung transplantation *Pediatr Transplant* 17: 224–230, 2013

74. Hayes D, Lloyd E, Yates A, McConnell P, Galantowicz M, Preston T: Pediatric ambulatory ECMO *Lung* 192: 1005–1005, 2014

75. Rehder KJ, Turner DA, Hartwig MG, et al.: Active rehabilitation during extracorporeal membrane oxygenation as a bridge to lung transplantation *Respir Care* 58: 1291–1298, 2013

76. Hayes D, Kukreja J, Tobias JD, Ballard HO, Hoopes CW: Ambulatory venovenous extracorporeal respiratory support as a bridge for cystic fibrosis patients to emergent lung transplantation *J Cyst Fibros Off J Eur Cyst Fibros Soc* 11: 40–45, 2012

77. Mangi AA, Mason DP, Yun JJ, Murthy SC, Pettersson GB: Bridge to lung transplantation using short-term ambulatory extracorporeal membrane oxygenation *J Thorac Cardiovasc Surg* 140: 713–715, 2010

78. Olsson KM, Simon A, Strueber M, et al.: Extracorporeal membrane oxygenation in nonintubated patients as bridge to lung transplantation *Am J Transplant* 10: 2173–2178, 2010

79. Garcia JP, Iacono A, Kon ZN, Griffith BP: Ambulatory extracorporeal membrane oxygenation: a new approach for bridge-to-lung transplantation *J Thorac Cardiovasc Surg* 139: e137-139, 2010

80. Maeda K, Ryan K, Conrad. CK, Yarlagadda V. VV: An alternative cannulation approach for veno-venous extracorporeal membrane oxygenatioin in children for long-term ambulatory support *J Thorac Cardiovasc Surg* 156: e13–e14, 2018

81. Thompson AJ, Buchan S, Carr B, et al.: Low-resistance, concentric-gated pediatric artificial lung for end-stage lung failure *ASAIO J*: 1, 2019

82. Liu Y, Sanchez P, Wei X, et al.: Effects of cardiopulmonary support with a novel pediatric pump-lung in a 30-day ovine animal model *Artif Organs* 39: 989–997, 2015

83. Madhani S, Frankowski B, Burgreen G, et al.: In vitro and in vivo evaluation of a novel integrated wearable artificial lung *J Heart Lung Transplant* 36: 806–811, 2017

84. Orizondo RA, May AG, Madhani SP, et al.: In vitro characterization of the Pittsburgh Pediatric Ambulatory Lung device *ASAIO J* 64: 806–811, 2018

85. Iqbal CW, Wall J, Harrison MR: Challenges and climate of business environment and resources to support pediatric device development *Semin Pediatr Surg* 24: 107–111, 2015

86. Ulrich L, Joseph F, Lewis D, Koenig R: FDA's pediatric device consortia: National program fosters pediatric medical device development *Pediatrics* 131: 981–985, 2013

87. US Food and Drug Administration: *Report to Congress: FY 2016 Premarket Approval of Pediatric Use of Devices*, 2017.

88. Thiagarajan RR, Barbaro RP, Rycus PT, et al.: Extracorporeal Life Support Organization registry international report 2016 *ASAIO J* 63: 60–67, 2017

89. Ricard J-D, Dreyfuss D, Saumon G: Ventilator-induced lung injury *Eur Respir J* 22: 2s–9s, 2003

90. Abrams D, Brenner K, Burkart K, et al.: Pilot study of extracorporeal carbon dioxide removal to facilitate extubation and ambulation in exacerbations of chronic obstructive pulmonary disease *Ann Am Thorac Soc* 10: 307–314, 2013

91. Kluge S, Braune S, Engel M, et al.: Avoiding invasive mechanical ventilation by extracorporeal carbon dioxide removal in patients failing noninvasive ventilation *Intensive Care Med* 38: 1632–1639, 2012

92. Karagiannidis C, Brodie D, Strassmann S, et al.: Extracorporeal membrane oxygenation: evolving epidemiology and mortality *Intensive Care Med* 42: 889–896, 2016

93. Arazawa D, Kimmel J, Federspiel W: Kinetics of CO_2 exchange with carbonic anhydrase immobilized on fiber membranes in artificial lungs *J Mater Sci Mater Med* 26: 1–8, 2015

94. Zanella A, Castagna L, Salerno D, et al.: Respiratory electrodialysis: A novel, highly efficient extracorporeal CO_2 removal technique *Am J Respir Crit Care Med* 192: 719–726, 2015

95. Zanella A, Mangili P, Giani M, et al.: Extracorporeal carbon dioxide removal through ventilation of acidified dialysate: An experimental study *J Heart Lung Trans* 33: 536–541, 2014

96. Abrams D, Roncon-Albuquerque R, Brodie D: What's new in extracorporeal carbon dioxide removal for COPD? *Intensive Care Med* 41: 906–908, 2015

97. Funakubo A, Taga I, McGillicuddy J, Fukui Y, Hirschl R, Bartlett R: Flow vectorial analysis in an artificial implantable lung *ASAIO J* 49: 383–387, 2003

98. Madhani S, Frankowski B, Federspiel W: Fiber bundle design for an integrated wearable artificial lung *ASAIO J* 63: 631–636, 2017

99. Svitek RG, Federspiel WJ: A mathematical model to predict CO_2 removal in hollow fiber membrane oxygenators *Ann Biomed Eng* 36: 992–1003, 2008

100. Hines A, Maddox R: *Mass transfer: fundamentals and applications* Englewood Cliffs, NJ: Prentice Hall, 1985.

101. ANSI/AAMI/ISO 7199:2009 -- cardiovascular implants and artificial organs -- blood-gas exchangers (oxygenators):, 2009

102. Svitek R, Frankowski B, Federspiel W: Evaluation of a pumping assist lung that uses a rotating fiber bundle *ASAIO J* 51: 773–78, 2007

103. Medtronic: Medtronic minimax plus, instructions for use, 2008

104. Svitek R, Smith D, Magovern J: In vitro evaluation of the tandem heart pediatric centrifugal pump *ASAIO J* 53: 747–753, 2007

105. Medtronic: Find your ideal cannulae, 2017

106. Combes A, Pesenti A, Ranieri V: Is extracorporeal circulation the future of acute respiratory distress syndrome management? *Am J Respir Crit Care Med* 195: 1161–1170, 2017

107. Maquet Getinge Group: Pump assisted lung protection cardiohelp system, 2010

108. Maquet Getinge Group: HLS Set Advanced: Integration meets innovation, 2015

109. Seiler F, Trudzinski F, Hennemann T, et al.: The Homburg Lung: Efficacy and safety of a minimal-invasive pump-driven device for veno-venous extracorporeal carbon dioxide removal *ASAIO J* 63: 659–665, 2017

110. Wang D, Lick S, Campbell K, et al.: Development of ambulatory arterio-venous carbon dioxide removal ($AVCO_2R$): The downsized gas exchanger prototype for ambulation removes enough CO_2 with low blood resistance *ASAIO J* 51: 385–389, 2005

111. Kaesler A, Hesselmann F, Zander MO, et al.: Technical indicators to evaluate the degree of large clot formation inside the membrane fiber bundle of an oxygenator in an in vitro setup *Artif Organs* 43: 159–166, 2019

112. May AG, Jeffries RG, Frankowski BJ, Burgreen GW, Federspiel WJ: Bench validation of a compact low-flow CO_2 removal device *Intensive Care Med Exp* 6, 2018

113. Federspiel W, Hattler B: Sweep gas flowrate and CO_2 exchange in artificial lungs *Artif Organs* 20: 1050–1052, 1996

114. Wearden PD, Federspiel WJ, Morley SW, et al.: Respiratory dialysis with an active-mixing extracorporeal carbon dioxide removal system in a chronic sheep study *Intensive Care Med* 38: 1705–1711, 2012

115. Barr DP, Peters JP: The carbon dioxide absorption curve and carbon dioxide tension of the blood in severe anemia *J Biol Chem* 45: 571–592, 1921

116. Bidani A, Crandall ED: Analysis of the effects of hematocrit on pulmonary CO_2 transfer *J Appl Physiol* 53: 413–418, 1982

117. Deem S, Alberts MK, Bishop MJ, Bidani A, Swenson ER: CO_2 transport in normovolemic anemia: complete compensation and stability of blood CO_2 tensions *J Appl Physiol* 83: 240–246, 1997

118. Blumgart H, Altschule M: Clinical significance of cardiac and respiratory adjustments in chronic anemia *Blood* 3: 329–348, 1948

119. Salathé EP, Fayad R, Schaffer SW: Mathematical analysis of carbon dioxide transport by blood *Math Biosci* 57: 109–153, 1981

120. ARDSNetwork: Ventilation with lower ridal volumes as compared with traditional tidal volume for acute lung injury and the acute respiratory distress syndrome *N Engl J Med* 342: 1301–1308, 2000

121. May AG, Orizondo RA, Frankowski BJ, Wearden PD, Federspiel WJ: Acute in vivo evaluation of the Pittsburgh Pediatric Ambulatory Lung *ASAIO J* 65: 395–400, 2018

122. Madhani S, Frankowski B, YE S, et al.: In vivo 5 day animal studies of a compact, wearable pumping artificial lung *ASAIO J* 65: 94–100, 2017

123. Johnson CA, Wearden PD, Kocyildirim E, et al.: Platelet activation in ovines undergoing sham surgery or implant of the second generation PediaFlow pediatric ventricular assist device *Artif Organs* 35: 602–613, 2011

124. Johnson Jr. C, Snyder T, Woolley J, Wagner W: Flow cytometric assays for quantifying activated ovine platelets *Artif Organs* 32: 136–145, 2008

125. Duricki DA, Soleman S, Moon LDF: Analysis of longitudinal data from animals with Missing values using SPSS *Nat Protoc* 11: 1112–1129, 2016

126. Templeton GF: A two-step approach for transforming continuous variables to normal: implications and recommendations for IS research *Commun Assoc Inf Syst* 28: 41–58, 2011

127. Extracorporeal Life Support Organization: *ELSO Guidelines for Cardiopulmonary Extracorporeal Life Support*. 5th ed. Ann Arbor, MI, 2017.

128. Omar HR, Mirsaeidi M, Socias S, et al.: Plasma free hemoglobin is an independent predictor of mortality among patients on extracorporeal membrane oxygenation support *PLoS ONE* 10: e0124034, 2015

129. Dornia C, Philipp A, Bauer S, et al.: Analysis of thrombotic deposits in extracorporeal membrane oxygenators by multidetector computed tomography *ASAIO J* 60: 652–656, 2014

130. Lubnow M, Philipp A, Foltan M, et al.: Technical complications during veno-venous extracorporeal membrane oxygenation and their relevance predicting a system-exchange--retrospective analysis of 265 cases *PLoS ONE* 9: e112316, 2014

131. Starling RC, Moazami N, Silvestry SC, et al.: Unexpected abrupt increase in left ventricular assist device thrombosis *N Engl J Med* 370: 33–40, 2014

132. Uriel N, Han J, Morrison KA, et al.: Device thrombosis in HeartMate II continuous-flow left ventricular assist devices: A multifactorial phenomenon *J Heart Lung Transplant* 33: 51–59, 2014

133. Malkin A, Ye S, Lee E, et al.: Development of zwitterionic sulfobetaine block copolymer conjugationstrategies for reduced platelet deposition in respiratory assist devices *J Biomed Mater Res B Appl Biomater* 106: 2681–2692, 2018

134. Barbaro RP, Paden ML, Guner YS, et al.: Pediatric extracorporeal life support organization registry international report 2016: *ASAIO J* 63: 456–463, 2017

135. Barrett CS, Jaggers JJ, Cook EF, et al.: Pediatric ECMO outcomes: comparison of centrifugal versus roller blood pumps using propensity score matching *ASAIO J* 59: 145–151, 2013

136. Gulack B, Hirji S, Hartwig M: Bridge to lung transplantation and rescue post-transplant: the expanding role of extracorporeal membrane oxygenation *J Thorac Dis* 6: 1070–7079, 2014

137. Wu Z, Gellman B, Zhang T, Taskin M, Dasse K, Griffith B: Computational Fluid Dynamics and Experimental Characterization of the Pediatric Pump-Lung *Cardiovasc Eng Technol* 2: 276–287, 2011

138. Zamora IJ, Shekerdemian L, Fallon SC, et al.: Outcomes comparing dual-lumen to multisite venovenous ECMO in the pediatric population: The Extracorporeal Life Support Registry experience *J Pediatr Surg* 49: 1452–1457, 2014

139. Fuehner T, Kuehn C, Hadem J, et al.: Extracorporeal membrane oxygenation in awake patients as bridge to lung transplantation *Am J Respir Crit Care Med* 185: 763–768, 2012

140. Wang D, Lick S, Zhou X, Liu X, Benkowski R, Zwischenberger J: Ambulatory oxygenator right ventricular assist device for total right heart and respiratory support *Ann Thorac Surg* 84: 1699–1703, 2007

141. Linneweber J, Dohmen PM, Kerzscher U, Affeld K, Nosé Y, Konertz W: The effect of surface roughness on activation of the coagulation system and platelet adhesion in rotary blood pumps *Artif Organs* 31: 345–351, 2007

142. Kar B, Adkins LE, Civitello AB, et al.: Clinical experience with the TandemHeart percutaneous ventricular assist device *Tex Heart Inst J* 33: 111–115, 2006

143. ALung Technologies, Inc: Hemolung RAS: Training Workbook (HL-PL-0036_RH)

144. Arvand A, Hahn N, Hormes M, Akdis M, Martin M, Reul H: Comparison of hydraulic and hemolytic properties of different impeller designs of an implantable rotary blood pump by computational fluid dynamics *Artif Organs* 28: 892–898, 2004

145. Nishida M, Yamane T, Maruyama O, Sankai Y, Tsutsui T: Computational fluid dynamics analysis of the flow around the pivot bearing of the centrifugal ventricular assist device *JSME Int J Ser C* 49: 837–851, 2006

146. Orizondo R, May A, Frankowski B, et al.: Pittsburgh paracorporeal ambulatory assist lung, 2019

147. Jamiolkowski M, Hartung M, Malinauskas R, Lu Q: An in vitro blood flow loop system for evaluating the thrombogenicity of medical devices and biomaterials *ASAIO J*, 2019

148. Hastings S, Deshpande S, Wagoner S, Maher K, Ku D: Thrombosis in centrifugal pumps: location and composition in clinical and in vitro circuits *Int J Artif Organs* 39: 200–204, 2016

149. Pacella H, Eash H, Frankowski B, Federspiel W: Darcy permeability of hollow fiber bundles used in blood oxygenation devices *J Membr Sci* 382: 238–242, 2011

150. Braune S, Walter M, Schulze F, Lendlein A, Jung F: Changes in platelet morphology and function during 24 hours of storage *Clin Hemorheol Microcirc* 58: 159–170, 2014

151. Wilner GD, Casarella WJ, Baier R, Fenoglio CM: Thrombogenicity of angiographic catheters. *Circ Res* 43: 424–428, 1978

152. Libsack CV, Kollmeyer KR: Role of catheter surface morphology on intravascular thrombosis of plastic catheters *J Biomed Mater Res* 13: 459–466, 1979

153. Hecker JF, Edwards RO: Effects of roughness on the thrombogenicity of a plastic *J Biomed Mater Res* 15: 1–7, 1981

154. Tsunoda N, Kokubo K, Sakai K, Fukuda M, Miyazaki M, Hiyoshi T: Surface roughness of cellulose hollow fiber dialysis membranes and platelet adhesion *ASAIO J* 45: 418–423, 1999

155. Hastings S, Ku D, Wagoner S, Maher K, Deshpande S: Sources of circuit thrombosis in pediatric extracorporeal membrane oxygenation *ASAIO J* 63: 86–92, 2017

156. Hellums JD, Peterson DM, Stathopoulos NA, Moake JL, Giorgio TD: Studies on the Mechanisms of Shear-Induced Platelet Activation, in: Hartmann A, Kuschinsky W (eds) *Cerebral Ischemia and Hemorheology*. Berlin, Heidelberg: Springer Berlin Heidelberg, 1987, pp. 80–89.

157. Travis BR, Marzec UM, Ellis JT, et al.: The sensitivity of indicators of thrombosis initiation to a bileaflet prosthesis leakage stimulus *J Heart Valve Dis* 10: 228–238, 2001

158. Kroll MH, Hellums JD, McIntire LV, Schafer AI, Moake JL: Platelets and shear stress *Blood* 88: 1525–1541, 1996

159. Kaufmann TAS, Linde T, Cuenca-Navalon E, et al.: Transient, three-dimensional flow field simulation through a mechanical, trileaflet heart valve prosthesis *ASAIO J* 57: 278–282, 2011

160. Chua LP, Ong KS, Yu CMS, Zhou T: Leakage flow rate and wall shear stress distributions in a biocentrifugal ventricular assist device *ASAIO J* 50: 530–536, 2004

161. Feng S, Lu X, Reséndiz JC, Kroll MH: Pathological shear stress directly regulates platelet alphaIIbbeta3 signaling *Am J Physiol Cell Physiol* 291: C1346-1354, 2006

162. Fallon AM, Marzec UM, Hanson SR, Yoganathan AP: Thrombin formation in vitro in response to shear-induced activation of platelets *Thromb Res* 121: 397–406, 2007

163. Orizondo R, May A, Frankowski B, et al.: 30-day sheep studies of a wearable pumping artificial lung, 2019

164. Nguyen KT, Su S-H, Sheng A, et al.: In vitro hemocompatibility studies of drug-loaded poly-(L-lactic acid) fibers *Biomaterials* 24: 5191–5201, 2003

165. Grove K, Deline SM, Schatz TF, Howard SE, Porter D, Smith ME: Thrombogenicity testing of medical devices in a minimally heparinized ovine blood loop *J Med Devices* 11: 021008, 2017

166. Lu Q, Hofferbert BV, Koo G, Malinauskas RA: In vitro shear stress-induced platelet activation: Sensitivity of human and bovine blood *Artif Organs* 37: 894–903, 2013

167. Ruberto F, Bergantino B, Testa MC, et al.: Low-flow veno-venous extracorporeal CO_2 removal: first clinical experience in lung transplant recipients *Int J Artif Organs* 37: 911–917, 2014